NTNU
Norwegian University of
Science and Technology

Topo-Bathymetric LiDAR for Hydraulic Modeling

Evaluation of LiDAR Data From Two Rivers

Ingrid Sundsbø Alne

Civil and Environmental Engineering
Submission date: June 2016
Supervisor: Knut Alfredsen, IVM
Co-supervisor: Morten Stickler, Statkraft

Norwegian University of Science and Technology
Department of Hydraulic and Environmental Engineering

NTNU
NORGES TEKNISK NATURVITENSKAPLIGE UNIVERSITIET
Institutt for Vann- og miljøteknikk

Masteroppgåve i vassdragsteknikk

Kandidat: **Ingrid Alne**

Tema: **Bruk av LIDAR-data for hydraulisk modellering.**

1. Bakgrunn

Hydraulisk modellering er eit verkty som er brukt i svært mange samanhengar innan vassdragsteknikk der ein treng å finne vannstander, hastigheter, bølgeforplantning, vannstandsvariasjon og mange andre hydrauliske variable. For å få gode resultat treng ein å lage ein god beskrivelse av geometrien i vassdraget, noko som kan før med seg omfattande datainnsamling. Eit alternativ er å skanne vassdraget og terrenget rundt ved hjelp av grøn laser som trenger gjennom vassflata og måler geometrien under vatn. Dette gir potensiale for å samle store datamengder på kort tid. Hausten 2015 har Statkraft og Eco fått samla inn data for tre vassdrag i Norden. I denne oppgåva skal ferdig prosesserte data for Ljungan i Sverige og Hallingdalselva i Norge brukast i hydraulisk modellering og i ei vurdering av kvalitet på data frå måling med laser.

2. Arbeidsoppgåver

Oppgåva vil ha følgjande hovuddelar:

1. Data for dei to elven skal vurderast med tanke på innsamla geometri under vatn. Utifrå dette skal metodar for korreksjon utarbeidast, og desse skal sidan vurderast utifrå modellen.
    a. Det skal gjerast ei vurdering av datakvalitet i dei to datasetta. Spesielt viktig vert det å identifisere profil med manglande data, og korleis dette varierer mellom elvene og internt i kvar elv.
    b. Det skal målast inn tverrprofil for kontroll i både Ljungan og Hallingdal. Talet på profil og kvar målingane skal gjerast må baserast på profildata ein får frå dei prosesserte laserdatasetta.
    c. Med utgangspunkt i laserdata og måledata skal det vurderast om ein kan lage korreksjonsrutiner for manglande data basert på terrengdata, form på måledata og andre variable som ein kan samle inn frå vassdraget. Rutinane skal testast på datasetta frå dei to elvene.

2. Den hydrauliske modellen HECRAS (1-dimensjonal) skal settast opp for Ljungan. Modellen skal kalibrerast mot målt nivå på vassflata som er henta frå laserdata. Med tanke på volum av data tilgjengeleg må det gjerast ei vurdering av talet på tverrprofil og plasseringa av desse.

a. Det skal køyrast ei dynamisk simulering av typisk regulert vassføring frå Viforsen kraftverk og til nedre ende av den oppmålte strekninga.
b. Det skal vidare køyrast ei statisk berekning av ei flomvassføring der ein kan utnytte den fulle bredda av tverrprofilen.

3. Det skal settast opp ein hydraulisk modell for Hallingdalselva på tilsvarande måte som for Ljungan. Det skal gjerast simuleringar for regulert vassføring (normalsituasjonen) og for flomvassføringar.

4. Basert på resultat frå punkt 1-3 skal det gjerast ei vurdering av hydraulisk modellering med grønlaser som inngangsdata i dei to elvene. Skilnader på datakvalitet, modelloppsett og modellresultat skal diskuterast.

3. Rettleiing, data og informasjon

Faglærar vert professor Knut Alfredsen ved institutt for vann- og miljøteknikk, NTNU. Morten Stickler ved Statkraft er ansvarleg for prosjektet i Statkraft, og vil fungere som medrettleiar. Kandidaten er elles ansvarleg for innsamling, kontroll og bruk av data. Hjelp frå ovannemnde eller andre må refererast i rapporten.

4. Rapport

Struktur og oppsett av rapporten er viktig. Gå utifrå at det målgruppa er teknisk personell på seniornivå. Rapporten skal innehalde eit samandrag som gir lesaren informasjon om bakgrunn, framgangsmåte og hovudresultata. Rapporten skal ha innhaldsliste og referanseliste. Referanselista skal vere formatert etter ein eksisterande standard.

Denne oppgåveteksta skal vere inkludert i rapporten.

Data som er samla inn skal dokumenterast og leverast på digital form.

Formatet på rapporten skal følgje standarden ved NTNU. Alle figurar, kart og bilete som er inkludert i rapporten skal vere av god kvalitet.

Kandidaten skal inkludere ei signert fråsegn som seier at arbeidet som er presentert er eins eige, og at alle bidrag frå andre kjelder er identifiserte gjennom referanser eller på andre måtar.

Frist for innlevering er 1. juli 2016.

Insitutt for vann og miljøteknikk, NTNU

Knut Alfredsen
Professor

ABSTRACT

Hydraulic modeling is a tool that is widely used for studying rivers to find water depth, velocity, wave propagation, water level variations and other hydraulic variables. To achieve accurate results it is often necessary to have a detailed description of the channel topography, which requires extensive data collection. Conventional methods for collecting data are time consuming if a high density is needed and often limited by accessibility or safety. Airborne Light Detection and Ranging (LiDAR) Bathymetry is a remote sensing technique for mapping shallow water bodies which is increasingly used for topo-bathymetric surveys. The purpose of this study was to evaluate Airborne LiDAR Bathymetry (ALB) as a tool for mapping Nordic rivers with different characteristics by comparing data from two rivers. LiDAR data from the deep, dark river Ljungan was compared to the LiDAR data from the clear, shallow river Storåne to evaluate the potential influence of environmental conditions on accuracy and range. The LiDAR data was used to set up a hydraulic model for each of the rivers and run steady and unsteady simulations in one dimension using HEC-RAS. Manual measurements were carried out in the two rivers to assess the vertical accuracy of the LiDAR data, which was found to be less than 4 cm in all areas and did not appear to be affected by physical characteristics or depth. The LiDAR recorded depths up to 3 meters in the dark river and 6 meters in the clear river but the data showed a significant reduction in point density when exceeding depths of 2.5 m and 3 m, respectively. The depth range was mainly limited by the water clarity, but dark substrate or vegetation on the bottom also appeared to influence the depth range. The limited depth range in Ljungan resulted in large areas with missing data and did not provide an accurate hydraulic model. To obtain an accurate model in a dark and deep river like Ljungan it would be necessary to conduct manual measurements or it may be possible to estimate a channel shape based on interpolation of the LiDAR points from the banks. This study found that ALB is an efficient method for mapping rivers with a high density over large areas and can provide accurate hydraulic models with a wide application.

SAMMENDRAG

Hydraulisk modellering er eit verkty som er brukt i svært mange samanhengar innan vassdragsteknikk der ein treng å finne vannstander, hastigheter, bølgeforplantning, vannstandsvariasjon og mange andre hydrauliske variable. For å få gode resultat trenger en å lage en god beskrivelse av geometrien i vassdraget, noe som ofte krever omfattende datainnsamling. Et alternativ er å skanne vassdraget og terrenget rundt ved hjelp av batymetrisk LiDAR (Light Detection and Ranging) som trenger gjennom vannflaten og kartlegger elvebunnen. Hensikten med denne studien var å evaluere flybåren laser skanning som et verktøy for å kartlegge nordiske elver med ulike egenskaper ved å sammenligne data fra to elver. LIDAR data fra den dype, mørke elven Ljungan ble sammenlignet med LIDAR data fra den klare, grunne elven Storåne for å vurdere mulig påvirkning av miljøforhold på nøyaktighet og rekkevidde. LiDAR data ble brukt til å sette opp en hydraulisk modell for hver av elvene og kjøre stasjonær flomsimulering og ustasjonær simulering av normal vannføring. Manuelle målinger ble utført i de to elvene for å vurdere nøyaktigheten av LiDARdataene, som ble funnet til å være under 4 cm på alle områder og virker derfor ikke som å være påvirket av fysiske egenskaper eller dybde. LiDAR registrerte punkter ned til 3 meters dyp i den mørke elva og 6 meter i den klare elven, men dataene viste en betydelig reduksjon i punkttetthet under henholsvis 2.5 m og 3 m dyp. Vannets farge syntes å ha størst innvirkning på dybderekkevidden, men mørkt substrat eller vegetasjon på elvebunnen påvirket også. Den begrensede rekkevidden i Ljungan resulterte i store områder med manglende data og ga ikke en nøyaktig hydraulisk modell. For å få en nøyaktig modell i en mørk og dyp elv som Ljungan vil det være nødvendig å utføre manuelle målinger, eller det kan være mulig å anslå geometrien til transekter basert på interpolasjon av LiDAR punkter fra de grunne områdene. Studien fant ALB til å være en effektiv metode for kartlegging elver med en høy tetthet over store områder og kan gi nøyaktige hydrauliske modeller med mange bruksområder.

PREFACE

This thesis is submitted as the final requirements of the Master's Degree in Hydraulic and Environmental Engineering at the Norwegian University of Science and Technology. The work has been supervised by Professor Knut Alfredsen and Morten Stickler from Statkraft. The field work has been carried out in compliance with Statkraft and E-CO Energi's safety regulations.

There has been a a great number of people that have helped and contributed to this thesis. It has been motivating to see people take interest in my work. First and foremost I would like to thank Knut Alfredsen. I appreciate your keen interest, good discussions and of course the technical support. Your short response time on email has been greatly appreciated. And last but not least for providing me with the R script that made the huge amount of LiDAR data manageable.

I would also like to thank Morten Stickler for your support and honest feedback throughout the semester. Your dedication to the project and salmon fishing has been motivating. Furthermore, I would like to thank PhD candidate Ana Adeva Bustos for assisting me in the field and for good company on long train rides. I would also like to thank Bjørn Otto Dønum at E-CO Energi for facilitating the field work in Hallingdal and providing me with necessary information. A great thanks to Angela Odelberg at Statkraft Sweden and everyone who contributed during the field work in Ljungan. And a thanks to the stakeholder group for taking interest and giving the project a genuine purpose. Lastly, I would like to thank Ramona Baran at AHM for answering technical questions I have had along the way.

I hereby declare that the work I have submitted is my own and the help from others has been acknowledged or referenced.

Trondheim, June 21 2016

Ingrid Sundsbø Alne

CONTENTS

1 INTRODUCTION 1
1.1 Background . . . 1
1.2 Objectives . . . 2
1.3 For the reader . . . 3

2 AIRBORNE LIDAR BATHYMETRY 5
2.1 ALB for Hydraulic Modeling . . . 5
2.2 LiDAR Systems . . . 6
2.3 Suppliers in the Nordic Market . . . 7

3 STUDY SITES AND METHODS 9
3.1 Study Sites . . . 9
3.2 Methods . . . 11
3.2.1 Data Basis and Handling . . . 11
3.2.2 Manual Measurements . . . 14
3.2.3 Hydraulic Modeling . . . 16
3.2.4 Validation of LiDAR Data . . . 18
3.2.5 Interpolation in Areas With Missing LiDAR Data . . . 21
3.2.6 Statistical Analysis . . . 22

4 RESULTS 23
4.1 Validation of LiDAR Data . . . 23
4.1.1 Ljungan . . . 23
4.1.2 Storåne . . . 29
4.2 Interpolation in Areas With Missing LiDAR Data . . . 36
4.3 Hydraulic Modeling . . . 41

5 DISCUSSION 45
5.1 Validation of LiDAR data . . . 45
5.2 Correction of Data in Areas with no LiDAR Range . . . 48
5.3 LiDAR for Hydraulic Modeling . . . 50

6 CONCLUSIONS 53
6.1 Recommendations for future work . . . 54

References 55

Appendices 59

LIST OF FIGURES

Figure 1 Overview of the study sites 9
Figure 2 Workflow ALB 11
Figure 3 Workflow for handling LiDAR data 11
Figure 4 LiDAR cross sections before and after classification 12
Figure 5 Cross section before and after point reduction 13
Figure 6 Overview of the manual measurements in Ljungan 15
Figure 7 Overview of the manual measurements in Storåne 15
Figure 8 The water edge line from the left and right banks in Ljungan 17
Figure 9 The water edge line from the left and right banks in Storåne 17
Figure 10 The location of the point groups in Storåne 20
Figure 11 One to one plots Ljungan 24
Figure 12 Elevation difference versus depth for point comparison in Ljungan . . 24
Figure 13 Error versus depth for point to point comparison Ljungan 25
Figure 14 Error distribution for the two groups in Ljungan 26
Figure 15 Residual raster deep glide Ljungan 27
Figure 16 Residual raster pool Ljungan 27
Figure 17 Extracted cross section from the DEMs in Ljungan 28
Figure 18 Extracted cross section from the DEMs in Ljungan 28
Figure 19 Extracted cross section from the DEMs in Ljungan 28
Figure 20 Measured Z versus LiDAR Z Storåne 30
Figure 21 Error versus depth for point to point comparison Storåne 31
Figure 22 Error versus depth for point to DEM comparison Storåne 32
Figure 23 Error distribution for the three groups in Storåne 34
Figure 24 Residual raster for the soft and hard bottom in Storåne 34
Figure 25 Residual raster from the deep glide in Storåne 34
Figure 26 Extracted cross section from the DEMs in Storåne 35
Figure 27 Extracted cross section from the DEMs in Storåne 35
Figure 28 Extracted cross section from the DEMs in Storåne 35
Figure 29 Residual raster from the corrected DEM in Ljungan 36
Figure 30 Cross sections from the corrected LiDAR DEM in Ljungan 37

Figure 31 Residual raster from the corrected DEM in Storåne 37
Figure 32 Cross sections from the corrected LiDAR DEM in Storåne 37
Figure 33 Polynomial interpolated cross section for Ljungan 38
Figure 34 Linear interpolated cross section for Ljungan 39
Figure 35 Linear interpolated cross section for Storåne 39
Figure 36 Linear interpolated cross section for Storåne 40
Figure 37 Steady flow simulations Ljungan 41
Figure 38 Water surface line Ljungan 41
Figure 39 Steady flow simulations Storåne 42
Figure 40 Water surface line Storåne 43
Figure 41 Unsteady flow profiles Ljungan 43
Figure 42 Surface elevation versus flow for Ljungan 44
Figure 43 Unsteady flow profiles Storåne 44
Figure 44 Surface elevation versus flow for Storåne 44

LIST OF TABLES

Table 1 Specifications of existing bathymetric LiDAR systems 7

Table 2 Characteristics of Ljungan and Storåne 10
Table 3 Summary of data captured from ALB for Ljungan and Storåne 11
Table 4 Data input and output for the hydraulic models of Ljungan and Storåne 13
Table 5 Data from the manual measurements in Ljungan and Storåne 16
Table 6 The flow scenarios run for Ljungan and Storåne 18
Table 7 Summary of the data basis for the comparison for Ljungan 20
Table 8 Summary of the data basis for the comparison in Storåne 21

Table 9 Height discrepancies between measured points and LiDAR points for Ljungan 24
Table 10 Height discrepancies between measured points and LiDAR DEM for Ljungan 25
Table 11 Height discrepancies between ADCP DEM and LiDAR DEM 26
Table 12 Point to point comparison Storåne 31
Table 13 Point to DEM comparison Storåne 33
Table 14 Height discrepancies between LiDAR DEM and ADCP DEM for Storåne 33

ACRONYMS

ADCP – Acoustic Doppler Current Profiler
AHM – Airborne Hydromapping
ALB – Airborne Laser Bathymetry
DTM – Digital Terrain Model
DEM – Digital Elevation Model
GPS – Global Positioning System
LiDAR – Light Detection and Ranging
NIR – Near Infrared
NGO – Non Governmental Organisations
NVE – Norges Vassdrags- og Energidirektorat
NTNU – Norwegian University of Science and Technology
PRF – Pulse Repetition Frequency
SONAR – Sound Navigation and Ranging
UTM – Universal Transverse Mercator
WFD – Water Framework Directive

1

INTRODUCTION

1.1 BACKGROUND

Greenhouse gas emissions due to human activities - particularly the burning of fossil fuels - has affected the global climate and increased the average temperature (IPCC, 2007). To reduce global warming and the effects of climate change it is essential to change from fossil fuels to renewable energy sources. Hydropower production is the most flexible and consistent of the renewable energy resources, meeting baseload requirements as well as peak demand (World Energy Council, 2016) and thus an important contributor in the future renewable energy scheme. Storage of water also serves the purpose of securing water for dry periods and mitigate flooding.

Increased rainfall intensity has emphasised the need for flood protection and flood risk assessment. Between 1998 and 2009, there were 213 major damaging floods in Europe causing some 1126 deaths and displacement of half a million people, in addition to economic losses of at least EUR 52 billion (European Environment Agency, 2011). The frequency of damaging floods are likely to increase in the future and it is therefore necessary to take action to reduce their likelihood and limit their impacts (The EU Floods Directive, 2015). The Floods Directive in coordination with the Water Framework Directive (WFD) require flood risk maps and management plans for all river basins and sub basins in Europe with significant potential risk of flooding (The EU Floods Directive, 2016). WFD focuses on integrated management of water resources to balance the multipurpose use of water bodies for hydropower, drinking water, agriculture, industry and recreation while ensuring a healthy ecosystem. Production of hydropower can lead to heavy modification of rivers and lakes and thus a central focus of the WFD.

With almost half of the total reservoir storage capacity in Europe, Norway can play an important role in the shift from fossil to renewable energy sources. Norway is a leading producer of renewable energy and 99 percent of the country's power consumption is covered by renewable energy sources (Statkraft, 2009). The measures from the WFD in Norway are implemented in coordination with the Norwegian Water Resources and Energy Directorate (NVE) who administrates the licenses to run hydropower plants. Current licenses for hydropower installations that are to be audited by 2022 have been evaluated by the NVE in a report by Halleraker et al. (2013) with consideration to environmental impacts and priority of reassessment. This report concerns regulated rivers and reaches where the societal benefits of potentially improved environmental conditions are considered to overrun the cost of reduced

renewable power production (Halleraker et al., 2013). Mitigation like minimum or environmental flow, reservoir restrictions and habitat improvement often leads to less production and thus an extra cost for the power producer. The benefit of such measures are often difficult to predict and it is therefore desirable to find the optimal balance between power production and ecosystem. A cost/benefit approach with an integrated model can help keep the production losses at a minimum while ensuring a healthy ecosystem. Adaptive management with an integrated approach is a tool for assessing rivers in a holistic way to account for all aspects and interests of the river by simulating the response from the ecosystem for different hydrological and hydraulic scenarios, further described in Maddock et al. (2013). Hydraulic modeling of rivers on a catchment scale rather than meso or micro scale requires extensive data collection to achieve accurate numerical models. On the basis of this, Norway's two largest hydropower producers, Statkraft and E-CO Energy, have applied a new holistic method for collecting data from three rivers where the balance between power production and ecosystem is challenged. Airborne Light Detection and Ranging (LiDAR) Bathymetry or Airborne Hydro Mapping is a remote sensing technique that collects detailed data from the river bed and nearby terrain over large areas in a short time.

The purpose of this study is to evaluate Airborne LiDAR Bathymetry (ALB) as a tool for mapping Nordic rivers with different characteristics to assess the limitations and possibilities of this method. The two rivers Ljungan and Storåne are cases where integrated modeling can help balance power production, ecosystem services and recreational use. Hydraulic modeling of Ljungan and Storåne can be used to model impacts of mitigations such as new or improved spawning areas, changes to the channel hydraulics or removal of weirs. A stakeholder group was established in Ljungan in 2010 to improve communication between different interest groups and consists of power producers, non-governmental organisations (NGOs) and the local county. The preliminary results of this study were presented at a stakeholder seminar in Sundsvall in May 2016 and the LiDAR data for Ljungan was applied for mapping depths in potential spawning areas.

1.2 OBJECTIVES

The intention of this study is to evaluate ALB as a tool for mapping Nordic rivers with a holistic approach. A comparative study of the two rivers Ljungan and Storåne was carried out focusing on how different characteristics influence LiDAR data quality. Processed LiDAR data obtained from the two rivers was evaluated based on the following objectives:

- Validate the accuracy of LiDAR data by manual measurements
- Evaluate the potential for a correctional method in areas with missing LiDAR data
- Create a hydraulic model in HEC-RAS based on LiDAR data to run a steady flood simulation and unsteady common flow simulation for the two rivers

This study is part of a collaborative project between Statkraft and E-CO Energi as the users, Norwegian University of Science and Technology (NTNU) as the research partner and Airborne Hydromapping (AHM) as the supplier. The evaluation was based on prosessed LiDAR data delivered as cross sections by AHM collected from two regulated rivers. The

LiDAR data was only used for one dimensional modeling using HEC-RAS. The flood simulations were conducted as tests and are not in high flood risk areas.

1.3 FOR THE READER

The first chapter is about ALB as a method with a description of the features of different systems and suppliers. Chapter 3 includes a brief description of the two study sites and the methods applied to achieve the objectives in this study. Chapter 4 displays the results from the accuracy assessment, the correctional interpolation method and the hydraulic simulations. Chapter 5 discusses the results and uncertainties from chapter 4 as well as the challenges and potential for ALB as a method. Chapter 6 has some concluding remarks as well as suggestions for further work.

2

AIRBORNE LIDAR BATHYMETRY

In recent years there has been extensive research and development of remote sensing techniques for mapping rivers and shallow water bodies. Airborne LiDAR Bathymetry (ALB) has proved to be a suitable tool for mapping rivers with a high density over large areas. Conventional methods for mapping bathymetry can provide accurate measurements but may only cover limited areas due to restricted accessibility and safety precautions (McKean et al., 2014). To develop accurate numerical hydraulic models it is essential to obtain a detailed and accurate data basis which requires efficient methods for data collection. The growing need for modeling and monitoring of water bodies coincides with the rapid development of shallow bathymetric LiDAR systems and an increasing number of suppliers. This chapter discusses conventional methods for collecting bathymetric data and ALB as a method for data collection, as well as the features of different shallow bathymetric systems and suppliers.

2.1 ALB FOR HYDRAULIC MODELING

Mapping underwater topography for coastal areas and inland water bodies is widely used for the purpose of studying flood risk, sediment transport, habitat mapping, hydraulics and environmental impacts. A conventional method for collecting bathymetric data from rivers is by wading with a differential GPS or total station to obtain cross sectional measurements from the river bed. This is restricted to shallow, wadable areas with low velocities and the accuracy dependens on GPS signal quality. Deep sections are often mapped by SONAR navigated by boat or kayak, but accessibility may be limited if strong currents or due to legal access. SONAR does not work in very shallow ($<$0.2 m) areas and thus a combination of both techniques would be required to obtain measurements from the entire riverbed. Flood risk maps are often created by combining topographic LiDAR data from the floodplains and river banks with cross sectional measurements of the wetted area obtained by GPS or SONAR (Mandlburger et al., 2015). Optical airborne remote sensing surveys can be used to map the water depth by radiance values gained from aerial images and creates a smooth surface which can be combined with topographic LiDAR data (Flener et al., 2013). This is only applicable for clear water and is highly dependent on specific weather conditions. ALB is an active remote sensing technique that allows for mapping of both terrain and underwater topography in shallow ($<$10 m) water bodies. The bathymetric LiDAR is similar to the topographic Near Infrared (NIR) LiDAR, but the NIR light is absorbed at the water surface whereas the green light propagates through the water column on to the river bed. A laser beam with known direction is emitted from the scanner and measures the time it takes for the back-scattered

beam to return. Direct georeferencing registers each returning beam and the peaks correspond to the location of a point on the ground, vegetation, water surface or river bed. In very shallow waters (< 0.2 m), only the river bed is detected. The high pulse repetition rate and low flying altitude create a three dimensional point cloud with a density of up to 20-50 point/m^2 (AHM, 2015). Georeferencing of the point cloud is done by fitting it to manually measured reference points from large objects visible from aerial images. ALB is a fast method for collecting data with a high density, covering rivers of 15 - 20 km in a few hours. The high level of detail results in a large amount of data, which requires extensive processing before it can be used. The post processing, described in detail in Hammeren et al. (2015), includes removal of false echoes, correction for the refraction of the water surface and classification of the points. Environmental conditions, weather and time of year can affect the result from ALB surveys and are thus important to consider during planning. The water conditions such as turbidity, suspended sediments and organic material will reduce the penetration depth by absorption or scattering of the laser beam. This also applies to dark vegetation and substrate as seen in a study done by Kartverket in 2014 (Kartverket, 2014). Densely vegetated areas or vegetation overhanging the river may challenge the LiDAR performance and the survey is thus often conducted in early autumn or spring.

2.2 LIDAR SYSTEMS

Bathymetric LiDAR systems can be divided into two categories; deep water systems with a low pulse repetition frequency (PRF) and shallow water systems with a high PRF. The development of deep water bathymetric LiDAR systems began in the 1960's and are known today as SHOALS by the US Army Corps of Engineers, LADS by the Royal Australian Navy and the Swedish HawkEye (Irish et al., 1999). These systems utilise high pulse energy to propagate through the water down to 50-60 m depths with a low PRF and high beam divergence, results in a low point density (0.2 pts/m^2) (Kinzel et al., 2013). The recently developed shallow water systems allow for high density (20 pts/m^2) scanning of the transition zone in coastal waters or underwater topography in rivers and shallow lakes with medium pulse energy for eye safety. This allows for topo-bathymetric surveys with a single system and is practical for flood mapping and morphodynamics as well as purely bathymetric surveys. The features of the shallow LiDAR systems can vary as they may have been built for different purposes. Table 1 provides an overview of the specifications for some of the existing bathymetric systems. There are a few systems that have integrated NIR (wavelength 1064 nm) channels and green (wavelength 532 nm) channels to detect the water surface and terrain with the NIR light and the green light for mapping underwater topography. This may improve the detection of the water surface in areas with a still and clear water surface, in which case the green laser beam may only reflect points from the river bed. Despite fewer returns, the water surface derived from the green wavelengths has been found to be within the accuracy of the topo-bathymetric scanner according to Mandlburger et al. (2013). Shallow bathymetric LiDAR systems with only green wavelengths are increasingly used for topo-bathymetric surveys, having the benefit of using a single system.

The depth range of the shallow LiDAR systems will depend on the water clarity, defined by the diffuse attenuation coefficient or Secchi depth. The maximum depth range is often stated as a factor of the Secchi depth, defined as the maximum depth the human eye can detect a specific

black and white disk. The depth range is often stated as 1.5 Secchi depth for the shallow systems but this applies to bright ground with a high reflectivity and will therefore be reduced with a dark river bed. The spatial resolution or point density from the LiDAR scan will vary depending on the PRF, as a higher PRF will send out more pulses and thus return more points. The beam divergence determines the laser beam footprint on the mapped surface which will influence the vertical accuracy and is therefore important to consider (Fernandez-Diaz et al., 2014). A small footprint is desired for a high resolution and will depend on the beam divergence and flying altitude. With a beam divergence of 1 mrad and flying altitude of 500 m, the footprint will be 0.5 m. The beam divergence is typically 0.5 mrad for topographic scanners and in the range of 0.7 to 3 mrad for bathymetric systems to allow for accurate scanning under water as well as of the terrain.

Table 1: Specifications of existing bathymetric LiDAR systems collected from AHAB (2014), AHAB (2015), Fernandez-Diaz et al. (2014), Shrestha et al. (2010), Optech NOVA (2016), Kinzel et al. (2013), Fugro LADS Corporation (2011), RIEGL (2016), Optech (2016)

System	λ **[nm]**	**Max depth [m]**	**Max PRF [kHz]**	**Beam divergence [mrad]**	**Flying altitude [m]**	**Point density [pts/m^2]**	**System weight [kg]**
Aquarius	532	12	70	1	300-600	0.2-5	83
CATS	532		8	2	500-1000		40
Leica Chiroptera	Topo:1064 Bathy:532	1.5 Secchi	500 35	0.5 3	1600 400-600	12 1.5	80
EEARL	532	25	10	0.5	300		114
Leica HawkEye III	T:1064 B:532	50	T: 500 D: 10 S: 35	2-12	1600 400-600	T: 12 D: 0.4 S: 1.5	170
LADS Mk3	532	2.5 Secchi	1.5		365-900		132
RIEGL VQ-880 G	532	1.5 Secchi	550	0.7-2	600	20	60
SHOALS 3000	T:1064 B:532	60	20 3	5	300-400		217
Optech Titan	T:1550 / 1064 B:532	1.5 Secchi	300	T: 0.35 B: 0.7	300-2000 300-600	T: $>$ 45 B: $>$ 15	116

2.3 SUPPLIERS IN THE NORDIC MARKET

There are commercial suppliers in Europe who provide topo-bathymetric surveys commonly using green LiDAR systems or integrated NIR and green systems. As discussed in Kinzel et al. (2013) and Hammeren et al. (2015), the accuracy of the final data is influenced by environmental conditions as well as the post processing software. It is therefore beneficial to have a turnkey supplier with a well developed software who can plan the flight after weather and environmental conditions. In Europe, one of the main turnkey suppliers of LiDAR data is

the Austrian company Airborne Hydromapping (AHM) who delivers high resolution data with the bathymetric system from RIEGL, VQ 880-G. AHM's post processing software, HydroVISH, is designed for large data handling and is under continuous development. Since their commencement in 2010, AHM has conducted surveys for Norwegian companies like Kartverket and Statkraft in Norway as well as European organisations. Terratec is a leading provider of LiDAR data in Norway and recently conducted ALB surveys for the NVE for the purpose of flood mapping. Terratec use the integrated LiDAR system Titan from Optech and have their own post processing software TerraPos. Leica Geosystems (previously Airborne Hydrography AB (AHAB)) provide ALB surveys using the deep water system HawkEye III and the shallow water system Chiroptera. Both systems include a NIR channel in addition to the green channel but the low point density (1.5 pts/m^2) may not be sufficient for some purposes. For studying shallow rivers with a high resolution and accuracy it is beneficial to choose a system with a high PRF and low beam divergence, such as the RIEGL VQ-880 G or the Optech Titan.

3

STUDY SITES AND METHODS

The vision of this study is to evaluate ALB as a holistic tool for mapping rivers of different characteristics and assess processed LiDAR data as a basis for hydraulic modeling. ALB surveys were performed on 15.4 km of Ljungan river in Sweden and 2.7 km of Storåne river in Norway, figure 1, during autumn 2015. A description of the study sites is given in this chapter as well as the methods used to achieve the objectives. The methods include an assessment of the applicability of the processed LiDAR data at each step from preparing data for application in the GIS tool ArcMap to setting up the hydraulic model with GeoRAS. The vertical accuracy of the LiDAR data was assessed by conducting manual measurements and comparing it to the LiDAR data. The hydraulic modeling was conducted with HEC-RAS running steady and unsteady flow simulations for the two rivers. Ljungan's physical characteristics prevented the LiDAR from mapping the deep sections and a potential correctional method for areas with missing LiDAR data was therefore investigated.

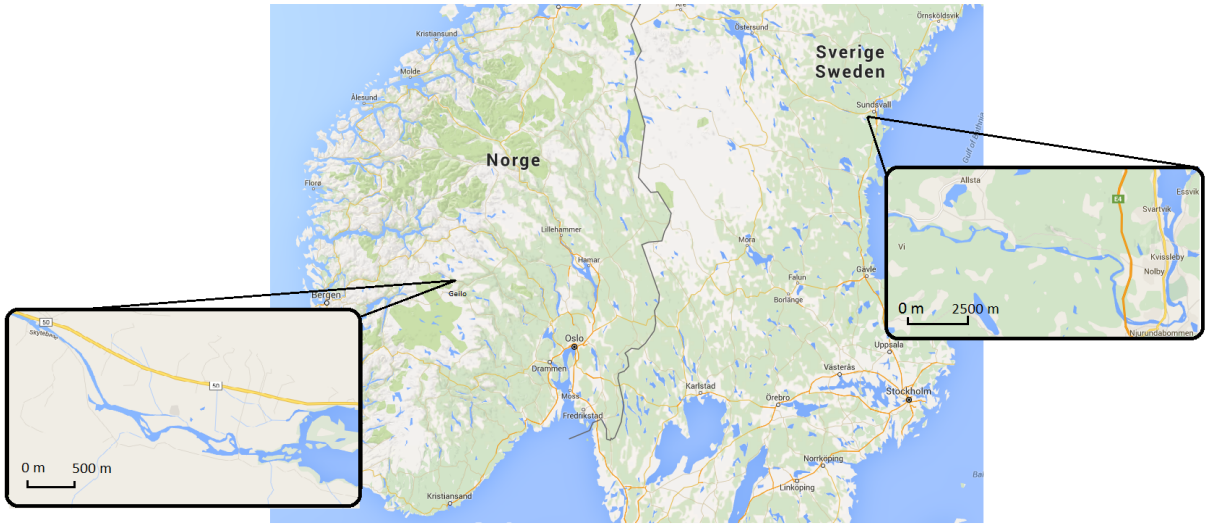

Figure 1: Overview of the study sites Ljungan (right) and Storåne (left)

3.1 STUDY SITES

Ljungan is a calm flowing, deep river with dark colour whereas Storåne is a shallow, clear mountain stream with turbulent waters. Both rivers are important for the local population in

terms of recreation and fisheries. The characteristics of the two rivers are summed up in table 2 and reflects the basis for the comparative study.

Table 2: Characteristics of Ljungan and Storåne (Bendiksby, 2013; Kristofers, 2014; B O Dønum, ECO-Energi (Pers. com. April 12 2016))

River	**I [%]**	**Length [km]**	**Mean flow [m^3/s]**	**Average depth [m]**	**Secchi depth [m]**	**Riffles / glides** [%]	**Median substrate size [cm]**
Ljungan	0.1	15.4	120	3	3.1*	10/90**	30**
Storåne	0.2	2.6	30.5	0.85		60/40**	10

* Secchi depth was measured downstream of the dam in Viforsen
** Qualitatively evaluated (M Stickler, Statkraft (pers. com. April 12 2016))

Ljungan

Ljungan originates on the Norwegian border and runs through the middle part of Sweden passing Härjedalen, Jämtland and Västernorrland (SMHI, 2002) before it reaches the Gulf of Bothnia (SMHI, 2003). Its total length is 399 km with a catchment area of 12851.1 km^2 (SMHI, 2002) and a total of 13 power plants, 5 of which are owned by Statkraft (Statkraft Sweden, 2015). Viforsen is the last power plant before the Gulf of Bothnia and is located about 13 km south of Sundsvall (62^o18'23"N, 17^o18'42"E; WGS 84). The study site at Ljungan is from the outlet of Viforsen power plant to 2.5 km before the Gulf of Bothnia (see figure 1). The discharge in this area depends entirely on the power production. The mesohabitat characteristics are mainly glide and deep pools but there are a few sections of riffle (Kristofers, 2014). The bank widths range from 40-280 meters and the banks are steep ($> 20\%$) in many areas. The river bed is dominated by dark substrate and vegetation and the water has a high content of organic material.

Storåne

Storåne is a part of the river Holselva which is located in Hol municipality in Buskerud county and is a part of E-CO Energi's regulation in the catchment. Storåne is 10.7 km long from its source in Lake Sudndalsfjorden to the outlet in Hovsfjorden (E-CO Energi, 2014). The study area is from the outlet of the power plant Hol 1 at Ruud (60^o37'35"N, 8^o10'55"E; WGS 84) to Hovsfjorden, shown in figure 1. The first 400 meters is a man made stone laid trapezoidal channel whereas the rest of the river has natural bends and formations with several side streams. The discharge depends on the production in Hol 1 in addition to the unregulated bypassed section, which catchment areas are 736 km^2 and 163 km^2 respectively (E-CO Energi, 2014). Storåne is a clear, relatively shallow (mean < 1 m) mountain stream with light coloured substrate and little vegetation. The mesohabitat varies between glide and riffle with some steep sections. The bank widths range from 10 - 150 meters and there are several sections where the river braids into smaller streams. The river bed mainly consists of cobbles with an increasing amount of gravel in the lower part (Bendiksby, 2013).

3.2 METHODS

The ALB survey was conducted by AHM with the RIEGL VQ-880 G and lasted 2-3 hours at each site. Table 3 shows a summary of the information from the ALB survey stated by the supplier. The methods described in the following sections are based on processed LiDAR data delivered by the supplier. Figure 2 shows the steps of an ALB survey from the flight to the final user product. Depending on the size of the scanned area, the post processing may take weeks or months.

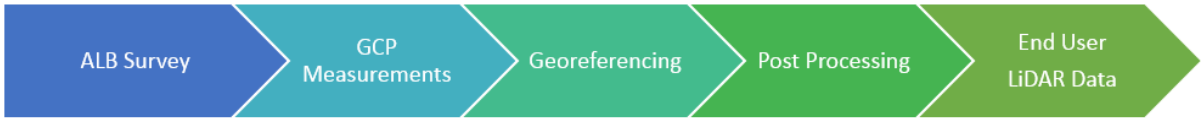

Figure 2: The process of ALB before the end user product. Measurements of the ground control points (GCP) are required to do by the customer

Table 3: Summary of data captured from the ALB survey of Ljungan and Storåne on September 2nd and October 3rd 2015, respectively

River	**Measured flow [m^3/s]**	**Max depth reached [m]**	**Accuracy (XY) [m]**	**Limiting factor**	**Weather**
Ljungan	58.9	2.8	0.07	Organic material, Dark bottom	Windy, Overcast
Storåne	31.72	6	0.06	Turbulence	Overcast

3.2.1 *Data Basis and Handling*

The LiDAR data was delivered as cross sections for every 5 meters along with a shapefile containing the water surface edge line from both rivers. The cross sections were delivered in text and PDF format. The text formatted cross sections contained UTM X, Y, Z coordinates which were used as the basis in the hydraulic model. The first delivery of cross sections contained points from the water surface and vegetation as well as the river bed and bank, figure 4a. To interpolate a Digital Elevation Model (DEM) of the river topography it is necessary to have points only from the river bed and ground to obtain an accurate hydraulic model. These cross sections were therefore not suitable for this purpose and required further processing. The second delivery contained cross sections where vegetation and water surface were removed and the remaining points were classified as river bed or bank points, figure 4b. These cross sections were the basis for setting up the hydraulic model. The steps described in the following section are shown in figure 3.

Figure 3: Workflow for handling LiDAR data

To create a DEM from the LiDAR data that could serve as the basis for the hydraulic model, the data first had to be imported to ArcGIS. ArcMap is commonly used for creating DEMs and the GeoRAS add-in enables to set up the hydraulic model directly for HEC-RAS. The large size of the files presented a challenge when trying to open multiple files in ArcMap which is not designed to handle such large amount of data. Each text file represented one cross section, whose size ranged from 80 kB to 1500 kB containing up to 40 000 points. To open multiple cross sections in ArcMap and interpolate a continuous DEM of the whole river, the size and thus the point density had to be reduced. The cross sections were processed through a script in the programming language R. The script picked out points with an interval calculated as the total number of points divided by 500 to ensure all the files were reduced in the same order. Cross sections from before and after the point reduction were plotted and compared in Matlab, figure 5, to ensure that the reduced cross sections did not loose the features of the original cross sections. The points remaining after the reduction were distributed throughout the cross sections but areas with a low density were most affected. The reduced cross sections were copied into a single file using Command Prompt and the command ”copy *.txt”. The file was then opened in ArcMap using the add XY data command.

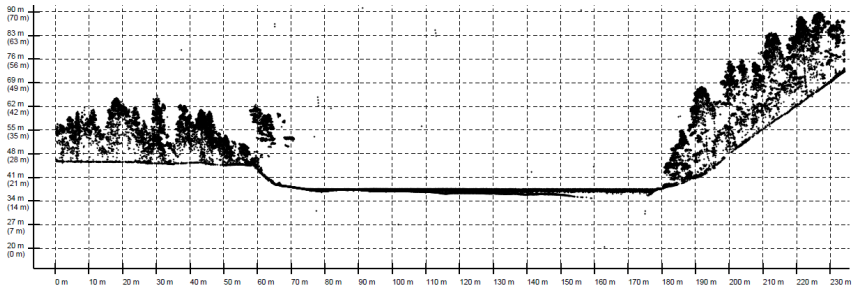

(a) Unclassified cross section

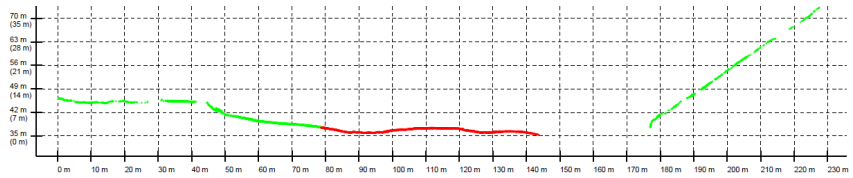

(b) Classified cross sections with river bed (red) and banks (green)

Figure 4: LiDAR cross section from Ljungan before (a) and after (b) classification. The missing part is outside the LiDAR range where no points were obtained

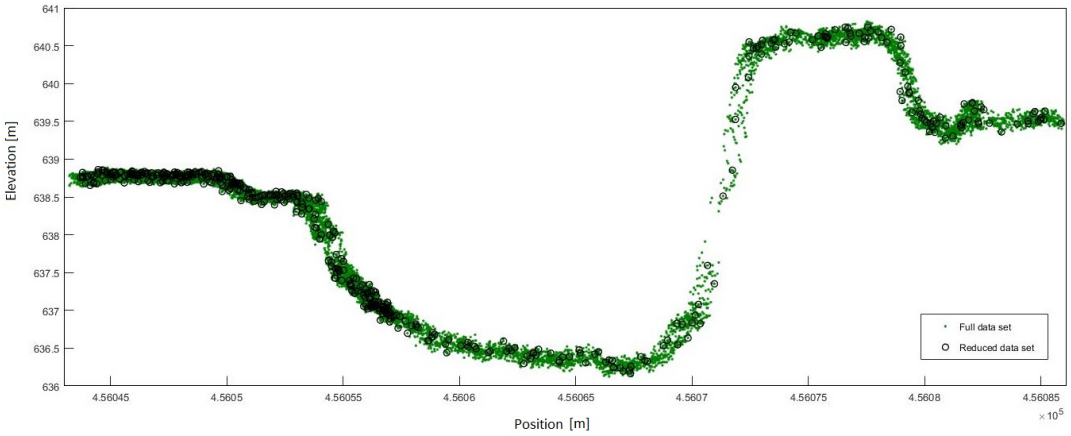

Figure 5: A cross section from Storåne with the reduced point density (black circles) and original LiDAR points (green). High density areas still have a large amount of points whereas low density areas show smaller sections with no points after the reduction

The DEM was created using the geostatistical interpolation method Kriging which is a common method for creating rasters from LiDAR data. This process could take up to several days, depending on the grid size and the size of the area. Because of this, only every fifth cross section was used from Ljungan whereas all the cross sections were used for Storåne. This was also why a larger grid size was chosen for Ljungan than for Storåne, table 4. Once a suitable DEM was created the hydraulic model could be set up using the installed GeoRAS Add-In. The DEM for Ljungan was converted to TIN format as GeoRAS require data in TIN or GRID format and the GRID format caused some problems in the initial set up. The model created for Storåne was done with GRID. Layers were created for the Stream Centerline, Bank Lines, XS Cut Lines and Flow Path Centerlines which all were assigned attributes in editor mode. The Stream Centerline was drawn in a continuous line from upstream to downstream following the main flow path of the river. The cross sections were drawn with location and spacing based on the geometry. The cross sections were placed right before and after riffles with increased spacing in straight calm sections and reduced spacing in areas with geometric variability. The bank lines were created using ”trace element” in editor mode to trace the water edge line. This was also done for the creation of right and left Flow Path Lines. After assigning attributes to the various layers the data was exported from ArcMap and opened in HEC-RAS. A summary of the input and output for the hydraulic models is stated in table 4 and the DEMs can be seen in Appendix B.

Table 4: Data input and output for the hydraulic models of Ljungan and Storåne

River	**LiDAR XS spacing [m]**	**LiDAR DEM grid size [m]**	**# GeoRAS XS**	**Mean spacing GeoRAS XS [m]**
Ljungan	25	2	96	135.7*
Storåne	5	1	60	43

*After manual correction with additional cross sections

3.2.2 *Manual Measurements*

The standard method for assessing the accuracy of LiDAR data is to compare point elevations between LiDAR points and manually measured points. Manual measurements were conducted over two days for both Ljungan and Storåne in April 2016 and resulted in 8018 and 8746 measured points, respectively. The measurements included points from the river bed and banks obtained by ADCP, differential GPS and total station. The measurements in Ljungan were only conducted with ADCP because of the depth, covering a limited area due to restricted accessibility and safety precautions. The conditions in Storåne allowed for measurements by ADCP in deep areas and differential GPS in wadeable areas. Ground points and water surface points were also measured with the GPS and total station in Storåne. Photos from the study sites can be seen in Appendix A.

Data points from the river bed were collected with a Sontek RiverSurveyor M9 Acoustic Doppler Profiler (ADCP) mounted on a Hydroboard. The XY coordinates are obtained from the attached GPS antenna whereas depth points are collected with the echosounder. The Z coordinate is obtained by measuring the water surface elevation. The supplier states that the M9 has a depth range of 0.2 m - 80 m and an accuracy of 1 % (Sontek, 2016), resulting in an accuracy of 0.01 - 0.1 m (depth 1-10 m) for the studied areas. The ADCP connects to a computer by Bluetooth signal and is set up and controlled in the software RiverSurveyor. The first thing required is a compass calibration to allow for movement due to surface waves. The transducer depth has to be measured and stated in RiverSurveyor, which is the distance from the water surface to the bottom of the ADCP sensor. The data was collected as multiple cross sectional and longitudinal profiles. A Leica Viva Differential GPS with an accuracy of 0.01-0.02 m in the XY direction and 0.015-0.03 m in the Z direction was used in wadeable areas. A total station, Topcon GTS-105, was used to measure bank points in an area with overhanging vegetation where the GPS did not get a signal.

The two areas studied in Ljungan, Viforsen and Allsta, shown in figure 6 were chosen based on accessibility and safety. The measurements in Viforsen were conducted directly downstream the power plant. The discharge was not consistent during the day and was therefore lower for the measurements conducted in the morning than those in the afternoon. The installed gauge downstream Viforsen measured discharge and water level every minute. The measurements in Allsta were conducted downstream the rapid Allstaforsen in a backwater pool. The navigation was influenced by currents and the range of the surveyed area was therefore limited.

The measurements in Storåne were conducted in the area downstream of the trapezoidal channel up until 200 m before the outlet as shown in figure 7. River bed, water surface and bank points were measured by the differential GPS in the lower part of the study area around Mørkaøyne, figure 7. Cross sectional measurements from the river bed were obtained in different mesohabitat areas. The ground points were measured on the open grassland on the island and on the river bank. The total station was set up at the bridge downstream Mørkaøyne to measure points from the banks, one of which had dense vegetation. The ADCP was used to measure a deep section directly downstream the bridge and was thus navigated from the bridge. The measurements at Ellingsøyne were obtained by pulling the ADCP back and forth across the channel. Two sections were measured here; one with a silt/clay river bed and one with

cobbles and boulders. Water surface measurements were obtained with the Differential GPS on the first day only.

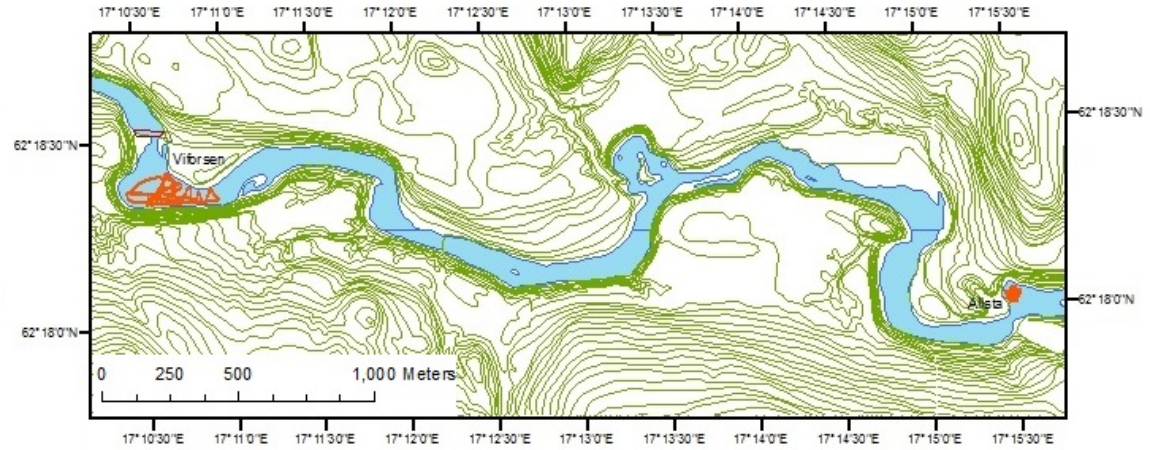

Figure 6: Overview of the measurements in Ljungan conducted at Viforsen on day 1 (left) and Allsta on day 2 (right) marked in red. The dam at Viforsen can be seen upstream of the study site. The flow direction is from left to right

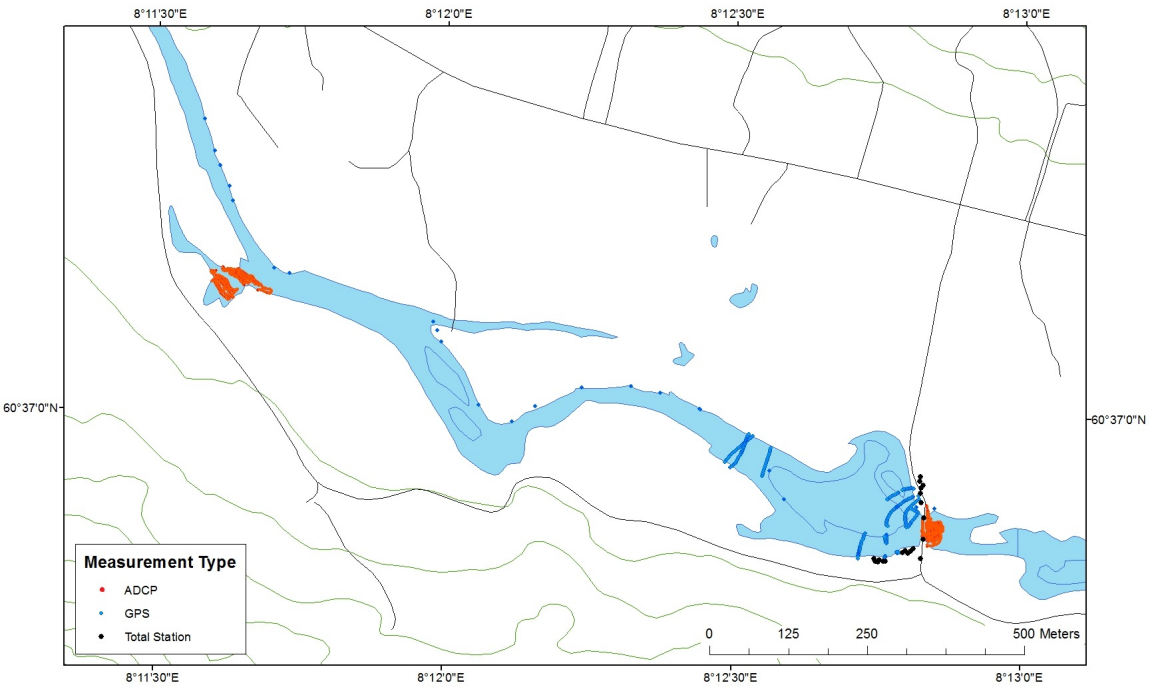

Figure 7: Overview of the manual measurements in Storåne coloured after measurement device with ADCP points (red), GPS points (blue) and total station (black). Ellingsøyne is the area on the left which was measured on day 1 and Mørkaøyne is the area to the right measured on day 2. The flow direction is from left to right

Table 5: Data from the manual measurements in Ljungan and Storåne

River	Study Site	Measured Flow [m^3/s]	Max Depth Reached [m]	Water Surface Elevation [m]	# Points
Ljungan	Viforsen	72.2 / 84.5	10.79	10.41 / 10.47	5887
	Allsta	86.3	6.43		2131
Storåne	Mørkaøyne	15.6	7.27	590.16	3879
	Ellingsøyne	27.8	3.46	593.81	4867

3.2.3 *Hydraulic Modeling*

HEC-RAS is a software developed by the US Army Corps of Engineers (USACE) at the Hydrological Research Center for one-dimensional and two dimensional hydraulic computations in natural rivers and channels. It is widely used to calculate steady and unsteady water surface profiles, sediment transport, water quality analysis and hydraulic design. (USACE, 2010) The computation of steady gradually varied flow solves the one-dimensional energy equation whereas the unsteady flow equation solver is adapted from Barkau's UNET model (1992) (USACE, 2010). HEC-RAS is commonly used in Norway for flood mapping and in areas where simple 1D models are feasible. Versions 5.0.0 and later 5.0.1 were used for the computations which allowed for the creation of a 2D grid for Storåne. This was not used for the simulations due to some problems with the set up. To run the simulations requires the following input; cross sections, Mannings n roughness coefficient for channel and banks, and upstream/downstream boundary conditions.

To open the file exported from GeoRAS a new project was started and the geometry file was added in Edit Geometric data by Import Geometry Data choosing GIS format. The Mannings n values were not added in GeoRAS like the other input and were therefore adjusted directly in Geometry Data under Tables. The initial calibration of the model was done by fitting the water surface elevation to the water surface edge line constructed by the supplier. As the bank points were extracted from the water surface edge line, these represented the water surface level on the day of the scan. A steady simulation with the flow value from the day of the scan was run with the downstream boundary condition set as the known water surface, which was the value of the bank points of the last cross section. There was a high variation between the left and the right bank line which made the calibration challenging, figure 8 and 9. A mean value between the left and right bank line was chosen in areas where the lines did not match unless one of the lines had a high, sudden peak in which case the most likely value was chosen. The simulated water surface was fitted to the bank lines by varying the roughness coefficient, Mannings n, to get the best fit. The initial values were set to reflect the roughness conditions in the river and was only varied for the channel and not the banks as the flow did not exceed the channel area. Two or three cross sections were changed at a time starting from downstream to upstream to account for the chosen sub critical flow regime. The Mannings n value was increased in areas where the water surface line was lower than the bank lines and decreased in the opposite case to fit the water surface line to the calibration lines. The final Mannings n values can be seen in Appendix D.

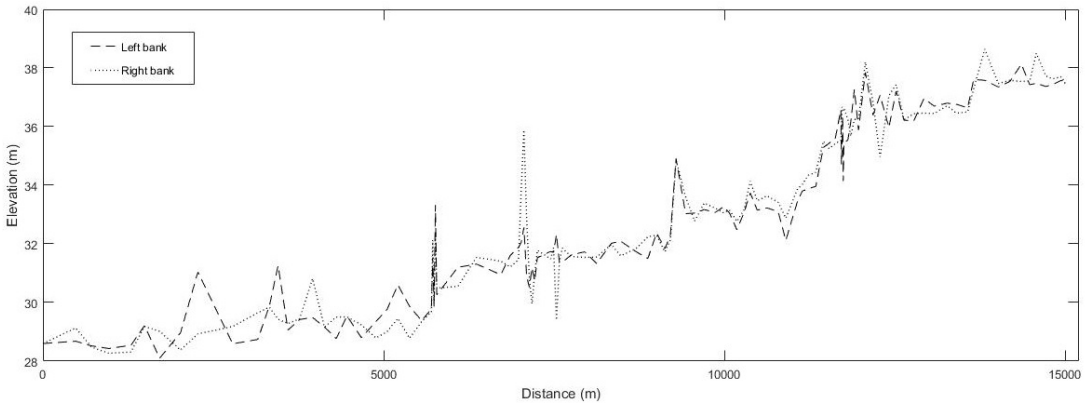

Figure 8: The water edge line from the left (dashed) and right (dotted) banks in Ljungan. The middle value of the two were used as the water surface elevation for the calibration

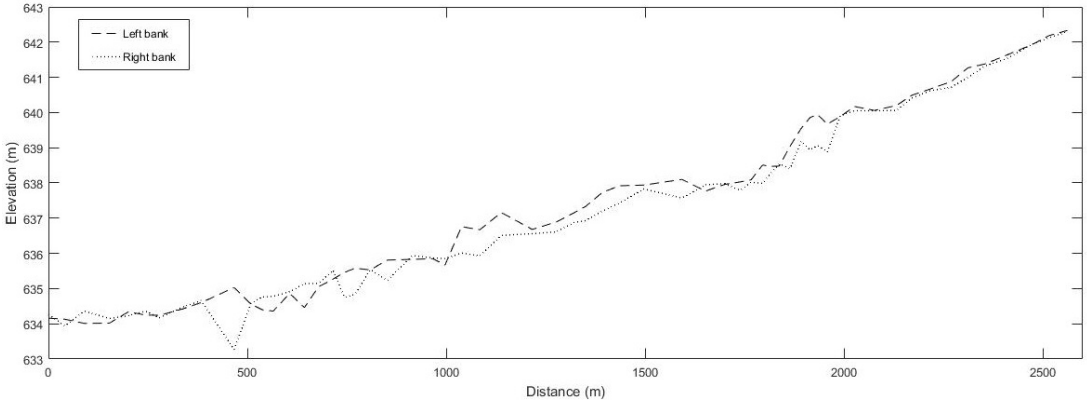

Figure 9: The water edge line from the left (dashed) and right (dotted) banks in Storåne. The middle value of the two were used as the water surface elevation for the calibration

The depth plot in RAS Mapper for Ljungan revealed some areas where the flow in the river was discontinuous between two cross sections. New cross sections were interpolated in HEC using Interpolation Tools and Interpolation Between 2 XS. The cross sections were then fitted to the underlying DEM in the Cross Section Editor. The simulation was run again with the same discontinuous flow and the cross sections were then manually adjusted using the Graphical Cross Section Editor. The DEM was inspected along with the LiDAR points for this area and revealed that there were no LiDAR points from the middle of the river which caused the interpolation to assume a flat river bed. Due to the extent of the areas of missing data it was not possible to obtain a reliable hydraulic model in Ljungan. The water surface profiles from the initial run were exported to ArcMap to create a depth plot for potential spawning areas. As the result from this would not be accurate in the deep sections, values from below 2.5 m were excluded from the plot and seen as not valid. Due to the low contingency in the profiles, the plot was not very accurate. It was also attempted to create a depth plot by interpolating the water surface edge line in ArcMap and subtracting LiDAR DEM from the constructed water surface to map the depths. As large floods will be less affected by inaccuracies in the channel topography, a steady flow simulation was conducted for a large flood and an unsteady simulation for a spring flood, using the Mannings values from the initial calibration. The

largest recorded flood in Ljungan was measured in the year 2000 to 1059 m^3/s (Kristofers, 2014) and was used for the steady flood simulation. The period for the unsteady simulation was from January 1st 2005 until July 22nd 2005, which was a year with normal discharge. The input hydrograph had a time step of 12 hours and the computation interval was set to 2 hours as recommended in the user manual, based on the time of rise of the peak wave divided by 20.

The hydraulic model for Storåne was calibrated for for the flow from the scan date int eh same wasy as Ljungan. It was also conducted another steady flow simulation with the flow on the day of the manual measurements, which was calibrated with the manually measured water surface points. The water surface measurements were only from one side of the river and did not include measurements from the lowermost part of the river. The downstream boundary condition was set as the normal depth using the river bed gradient. The steady flood simulation was run for the highest measured flow after the regulation at 217 m^3/s which was recorded in 1967 (E-CO Energi, 2014). The Mannings n values from the initial calibration were applied. The unsteady simulation was run for a period from January 1st 2010 until May 30th 2010. The input hydrograph had a time step of 24 hours and the calculated computational interval was set to 1 hour based on the same rule as Ljungan.

Table 6: The flow scenarios run for Ljungan and Storåne

River	**Simulation**	**Flow [m^3/s]**
Ljungan	Steady	58.9
	Steady	1059
	Unsteady	59 - 381
Storåne	Steady	15.5
	Steady	31.7
	Steady	217
	Unsteady	8.96 - 57.52

3.2.4 *Validation of LiDAR Data*

To evaluate the vertical accuracy of the LiDAR data a comparison was made to the manual measurements obtained from the ground survey described in section 3.2.2. The data was compared by measuring the elevation difference between the following:

- LiDAR point and measured point
- LiDAR DEM and measured point
- LiDAR DEM and measured DEM

The comparison of point elevation measurements is the standard method of accuracy assessment. As the DEM is the basis for the hydraulic model, the vertical accuracy and features of the DEM was also investigated. The data from the two study sites was categorised after mesohabitat characteristics in the measurement area to evaluate if there is a correlation between characteristics and LiDAR performance.

The point elevation comparison was done in ArcMap by using the geoprocessing tool Intersect which located overlapping points and created a new file with the attributes for each point. The attribute table was then exported and opened in Excel to calculate the difference between each measured Z value and LiDAR Z value. The error was calculated as mean, median and standard deviation. The Z values of the measured points were plotted against LiDAR Z values to see how well the values correlate. The error was also plotted against the depth to investigate whether there is a correlation between accuracy and depth. The DEM to point comparison was done in ArcMap using the geoprocessing tool Extract Values to Points which requires a raster and point features as input. The input raster was the LiDAR DEM created for the hydraulic model and the point features were the measured points. A new file with attributes from all the points was created and exported to Excel and processed in the same way as described for the point comparison. The DEM to DEM comparison was done in ArcMap with the geoprocessing tool Minus Raster which requires two input rasters and subtracts the Z values of the second raster from the Z value of the first. The output is a new raster with the vertical discrepancies between the two rasters. The measurement raster was created in areas with ADCP measurements as these covered larger areas that were feasible to interpolate. The input rasters were the LiDAR rasters created for the same areas. As these areas were quite small, a smaller grid size was used than the grid of the DEM for the entire river, table 7 and 8. As the interpolated area stretches further than the actual measurements there is a large deviation in the areas without measurements. To get a a comparison of the rasters in the overlapping areas only, the intersecting ADCP and LIDAR points were applied to extract the values of the minus raster in the areas where the points were overlapping. The mean and standard deviation for these values were calculated by ArcMap. The residual raster from the whole area was then used after excluding all values above the maximum error values found in the overlapping areas.

Ljungan

The comparison of the ADCP measurements from Ljungan and the LiDAR data first showed that the Z-values were not in the same height reference system. The ADCP data was measured in orthometric heights but the LiDAR data was delivered in ellipsoidal heights (GRS80). It was attempted to conduct orthorectification with ArcMap by creating a mosaic raster data set but this was unsuccessful. A manual correction of the ADCP Z-values was therefore necessary before the two data sets could be compared. This was done by adding a correctional factor to all the ADCP points calculated from the average vertical offset between the intersecting LiDAR and ADCP points. The data were added back into ArcMap after the correction to conduct the comparison. The correction factor was calculated from the intersecting points found in ArcMap with XY tolerance 0.07 m as the horizontal accuracy stated by the supplier, table 3. The ADCP Z value for Viforsen was then calculated for each point by the formula:

$$Z_{Corrected\,ADCP} = Z_{Orthometric\ Water\ Surface} + CorrectionalHeight - Z_{ADCP} - H_{Transducer}$$

There was not obtained any measurements of the water surface in Allsta. To construct a water surface level for this area the intersecting points from the ADCP and LiDAR were used to calculate a mean water surface level of 32.59 m after the correction. This was done by applying the following formula to each intersecting point:

$$Z_{WaterSurface} = Z_{LiDAR} + Depth_{ADCP} + H_{Transducer}$$

The data obtained from Ljungan were categorised as deep glide for the area in Viforsen and pool for the area in Allsta. A summary of the data basis for the comparison can be seen in table 7.

Table 7: Summary of the data basis for the comparison for Ljungan

Group	**# Points**	**Transducer depth [m]**	**Correction height [m]**	**LiDAR grid size [m x m]**	**ADCP grid size [m x m]**
Deep glide	5887	0.19	27.59	0.5	0.5
Pool	2131	0.15	27.59	0.5	0.5

Storåne

The manual measurements in Storåne were also collected in orthometric heights and had to be converted to ellipsoidal heights in the same way as Ljungan. The correctional height was first calculated as an average based on the intersecting points from the ADCP measurements. This later proved to be erroneous as the correctional factor had a variation of 0.15 m. Since the data were grouped after characteristics it was decided to calculate individual correctional factors based on the intersecting points from each group as shown in 8. The intersecting points were found using ArcMap with XY tolerance 0.06 m based on the horizontal accuracy stated by the supplier, table 3. It was decided not to create a new LiDAR raster surface with a smaller grid size in the deep glide in Storåne due to the low coverage of LiDAR points in this area. The transducer depth of the ADCP was 0.07 m for for all the measurements.

Figure 10: The location of the point categories from the manual measurements in Storåne ; Shallow glide: Dark blue ; Alluvial forest: Brown ; Riffle: Green ; Grassland: Pink ; Soft bottom: Light blue ; Hard bottom: Yellow ; Deep glide: Red

Table 8: Summary of the data basis for the comparison for Storåne

Group	**Device**	**# Points**	**Correction height [m]**	**LiDAR grid size [m x m]**	**ADCP grid size [m x m]**
Soft Bottom	ADCP	1838	44.14	0.25	0.25
Hard Bottom	ADCP	3029	44.16	0.25	0.25
Deep Glide	ADCP	3615	44.16	1	0.25
Shallow Glide	GPS	158	44.30		
Riffle	GPS	66	44.23		
Alluvial Forest	Total Station	11	44.24		
Grassland	GPS / Total Station	29	44.34		

3.2.5 *Interpolation in Areas With Missing LiDAR Data*

Due to the physical characteristics in Ljungan there were missing LiDAR data throughout the river. This caused a significant error in the interpolated DEM and the hydraulic model would need further correction before it could be applied. The ADCP measurements from the ground surveys were added to the LiDAR data in the deep areas to assess the necessary density of additional points for the interpolation to work correctly. This was later used as a basis for mapping areas in need of additional measurements with the purpose of collecting data with a kayak. It was also attempted to interpolate the LiDAR cross sections from the slope of the banks to evaluate if this could potentially be applied to rivers with missing data.

The manual measurements conducted in Ljungan and Storåne by ADCP were used to study how the kriging interpolation in ArcMap responds when adding points from the deep sections. This was done by Select Features in ArcMap to highlight the ADCP points from the deep sections and exporting them from the Attribute table. The exported ADCP points were added to the text file containing the LiDAR points. This was then imported back to ArcMap and the Kriging interpolation was repeated. For comparison, cross sections were extracted from the old and the new LiDAR DEM as well as the ADCP DEM using the 3D Analyst tool Interpolate Line and Surface Graph. The cross sections were exported and plotted with Sigmaplot.

In order to avoid manual measurements in areas with missing LiDAR data, it may be possible to estimate the cross section shape of a river based on observed topography and measurements obtained from the side banks. The width/depth ratio of the channel is valuable for describing cross section shape according to Rosgen (1996), who has developed methods for estimating representative cross sections for different stream types. Cross sections from the deep glides in Ljungan and Storåne were extracted to qualitatively evaluate the estimated channel shape based on interpolation of the LiDAR bank points. The LiDAR points were exported from ArcMap by identifying features and exporting selected features from the Attribute table. In order to separate the two channel banks the points were marked and exported separately. This allowed the points to be plotted separately in Excel and create a trend line from the points of each bank. The ADCP points were also plotted to evaluate how well the interpolated LiDAR

slope line matched with the actual cross section. The cross sections had a varying number of points and the method was therefore tested in areas with only a few river bank points and areas where there was good LiDAR range on both sides of the channel.

3.2.6 *Statistical Analysis*

The statistical analysis of the accuracy of the LiDAR data was calculated as mean, median and standard deviation which are commonly used in statistics. The mean and standard deviation include the outliers which was desirable in the accuracy evaluation. The median was included to account for a skewed distribution, in which case the mean may be misleading.

4

RESULTS

4.1 VALIDATION OF LIDAR DATA

The vertical accuracy assessments are summed up in tables for each of the three assessment types: point to point, measured point to LiDAR DEM and measured DEM to LiDAR DEM. The point comparison is illustrated with plots of the measured Z values against the LiDAR Z value. The vertical error is plotted against depth for both the point comparison and for the measured point to LiDAR DEM comparison. The point to LiDAR DEM comparison show high offsets in the areas with no LiDAR points. The DEM to DEM comparison shows values for the areas with overlapping LiDAR and ADCP points and the distribution is illustrated for each group. The residual raster plots show the elevation error between LiDAR raster minus ADCP raster in the areas with overlapping points in the vicinity.

4.1.1 *Ljungan*

The vertical discrepancies between manually measured points and LiDAR points for the two groups in Ljungan are shown in table 9. The deep glide show a higher deviation than the pool but also found more intersecting points for comparison as the measurements in the deep glide covered a larger area. Figure 11 shows the measured Z values compared to the LiDAR Z values which show well fitted regression lines with R^2 = 0.97 and 0.98. The LiDAR Z appears to be lower than the measured Z as the regression line is shifted below the one to one line. According to figure 12 the elevation error does not show an increase with depth and appears to have evenly distributed deviations. The deep glide, 12a, has a few outliers of 0.4 - 1 m from 1 to 3 meters depth and the deepest point observed is around 3 meters with an error of about 0.3 m. The pool, 12b, show a cluster of small errors at 3 m but nothing between 2.5 m and 3 m. The deep glide and pool both show a reduction in point density at about 2.5 meters depth.

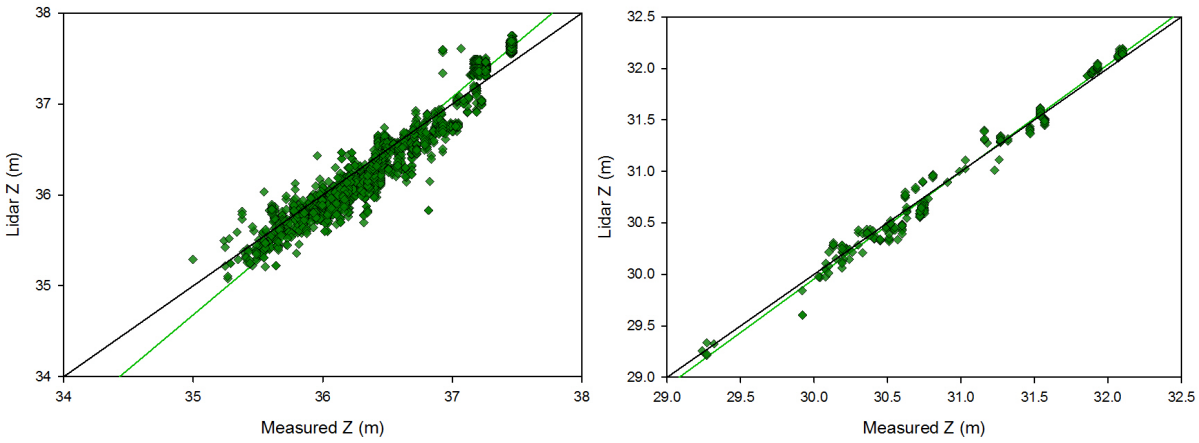

(a) Deep glide R^2=0.97 (b) Pool R^2=0.98

Figure 11: Measured Z values (x) and LiDAR Z values (y) with the calculated regression line (green) and 1:1 line (black) for Ljungan. The stated determination coefficient of the regression line, R^2, was calculated for both groups

Table 9: Height discrepancies between measured points and LiDAR points for Ljungan

Parameter	**Deep Glide**	**Pool**
Mean [m]	-0.04	0.00
Median [m]	-0.11	-0.02
Std. dev. [m]	-0.18	0.10
Max [m]	0.98	0.31
Min [m]	0.00	0.00
# Points	3685	254

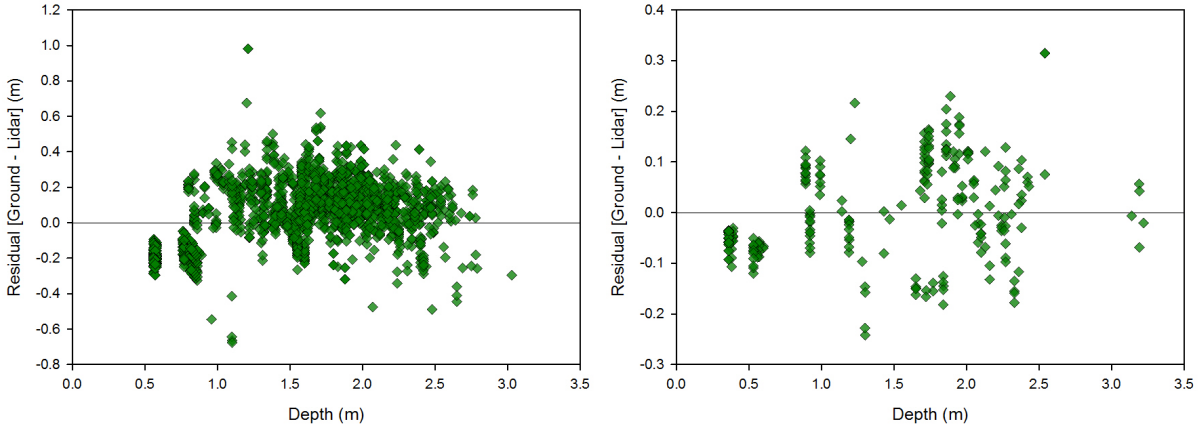

(a) Deep glide (b) Pool

Figure 12: Elevation difference between measured points and LiDAR points at various depths for the two groups in Ljungan

The elevation difference between measured points and the LiDAR DEM are shown in table 10. The high offsets illustrate the effect of large areas without LiDAR points and an interpolated DEM without any points from the deep sections. As the manual measurements registered depths down to 10.8 m and the LiDAR only reached down to 3 m there were large errors in the LiDAR DEM. This is illustrated in figure 13 where the error show a proportional increase with the depth. These results show that it is not sufficient to use interpolation if there are large sections of LiDAR data missing.

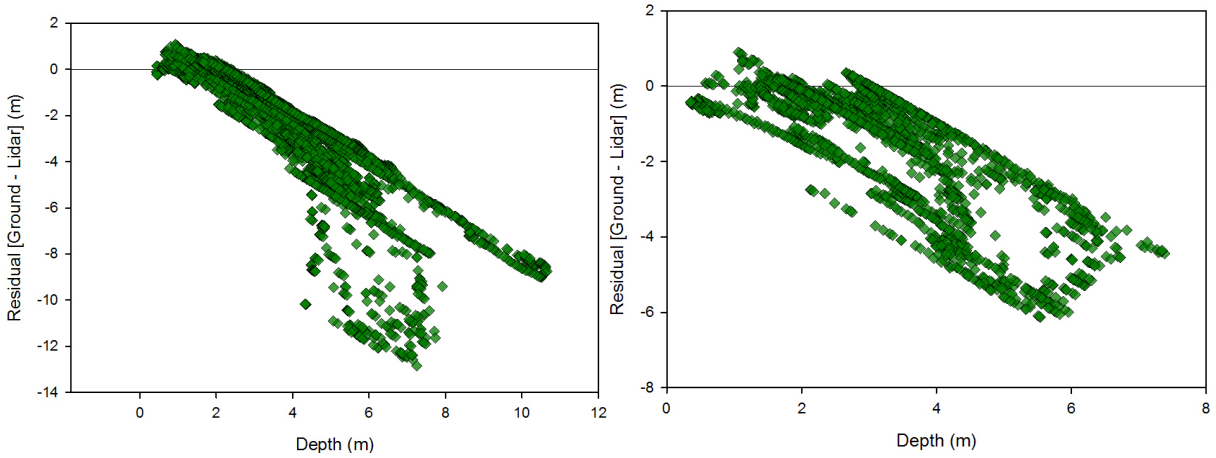

(a) Deep glide (b) Pool

Figure 13: Elevation difference between measured points and the LiDAR DEM at various depths for the two groups in Ljungan. The large offsets are due to the missing LiDAR points in the deep areas.

Table 10: Height discrepancies between measured points and LiDAR DEM for Ljungan

Parameter	**Deep glide**	**Pool**
Mean [m]	-1.93	-1.63
Median [m]	-0.94	-0.91
Std. dev. [m]	2.60	1.66
Max [m]	12.83	6.12
Min [m]	0.00	0.00
# Points	5886	2127

The discrepancies between the measured ADCP DEM and LiDAR DEM was calculated from the areas with overlapping data only to compare the rasters on a basis where there points from both measurement devices to evaluate how accurate the rasters are in the areas where there are LiDAR points obtained. The mean error, standard deviation and maximum error were obtained from ArcMap and are shown in table 11. The error distribution, figure 14, show a normal distribution around -0.1 m for the deep glide with a few outliers from 0.2 - 1.17 m whereas the pool show that all the rasters except one is within an offset of 0.2 m. The residual rasters are from the LiDAR DEM minus the ADCP DEM but excluded the values that are higher than the maximum and minimum of the overlapping rasters. This was done to evaluate the rasters in the

overlapping areas and not where there is large areas with missing data from either the LiDAR or the ADCP. These areas were evaluated in the point to DEM comparison. The raster comparison in figure 15 and 16 include the areas in the vicinity of the overlapping data which have errors lower than the maximum values in table 11. Due to the variable spacing between the manual measurements there are some larger areas with high errors but in the neighbourhood of the overlapping points there are errors in the range of 0 to 0.2 m. The light colour shows the smallest error with a range of 0.1 m and the darkest colours indicate higher errors. The exact location of the overlapping ADCP points and LiDAR points that were the basis for the DEMs can be seen in Appendix E. How the LiDAR range affects the interpolation can be seen in figure 17, 18 and 19 which show the extracted interpolated cross sections from the LiDAR DEM (green) and ADCP DEM (blue) in areas with various LiDAR range. The cross sections include a deep section with no LiDAR range in figure 17, a section with overlapping points in figure 18 and a section with partial LiDAR range with a steep drop where it gets to deep for the LiDAR, figure 19.

Table 11: Height discrepancies between ADCP DEM and LiDAR DEM for Ljungan. The large offsets are due to missing LiDAR points in the deep areas

Parameter	**Deep glide**	**Pool**
Mean [m]	-0.04	0.02
Std. dev. [m]	0.23	0.12
Max [m]	1.17	0.64

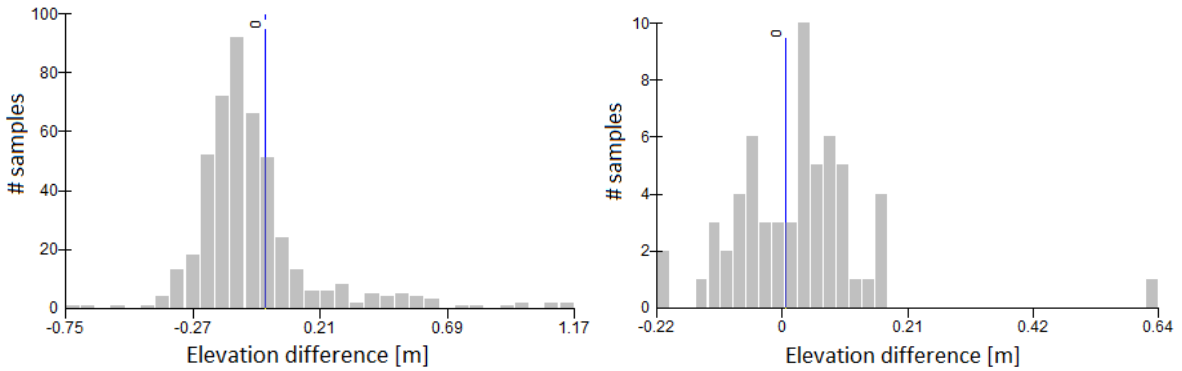

(a) Deep glide

(b) Pool

Figure 14: Error distribution for LiDAR DEM minus ADCP DEM in the areas with overlapping points for the two groups in Ljungan constructed by ArcMap

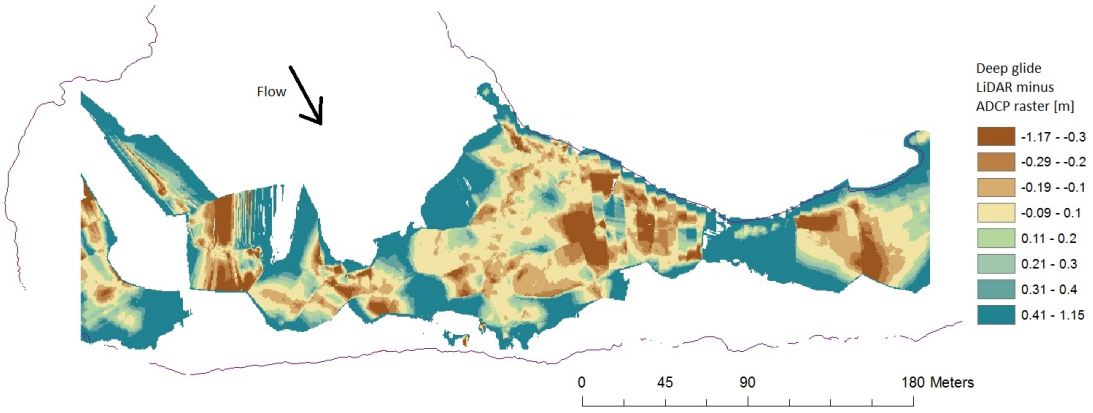

Figure 15: Residual rasters from LiDAR DEM minus ADCP DEM for the deep glide in Ljungan with 0.5 m grid size. The smallest errors are shown in the lightest colour whereas the darker colours show higher deviations. The large areas in blue are deep sections without overlapping points

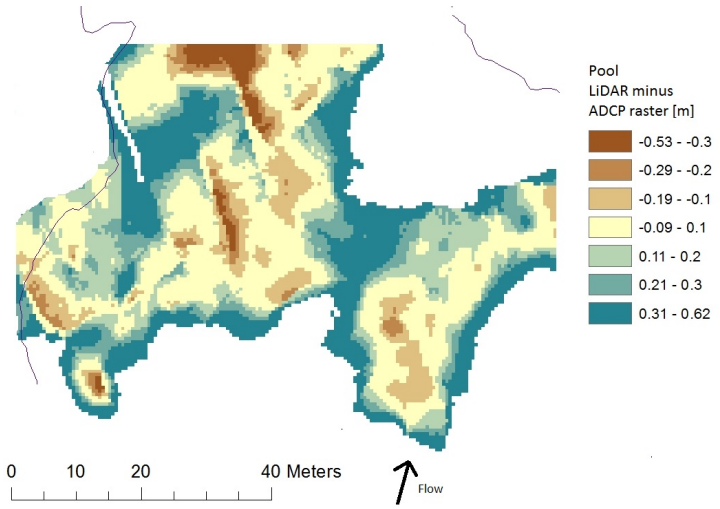

Figure 16: Residual rasters from LiDAR DEM minus ADCP DEM for the pool in Ljungan with 0.5 m grid size. The smallest errors are shown in the lightest colour whereas the darker colours show higher deviations. The large areas in blue are deep sections without overlapping points

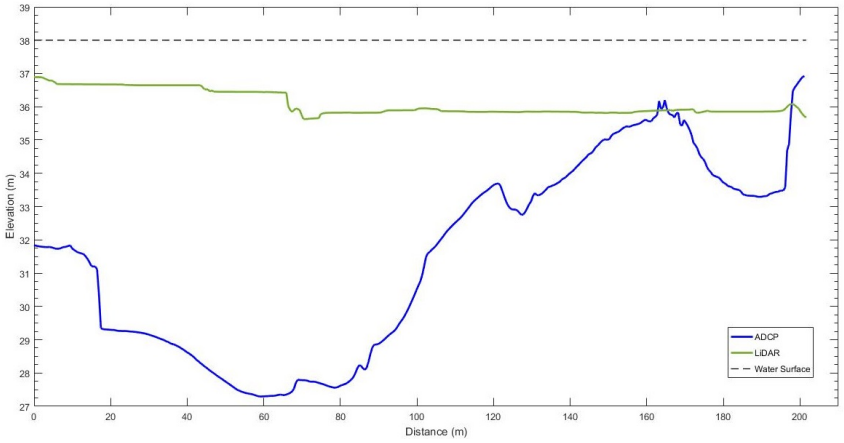

Figure 17: Extracted cross section from the LiDAR DEM (green) and the ADCP DEM (blue) in the deep glide in Ljungan in a deep area with no LiDAR range. The dashed line is the water surface

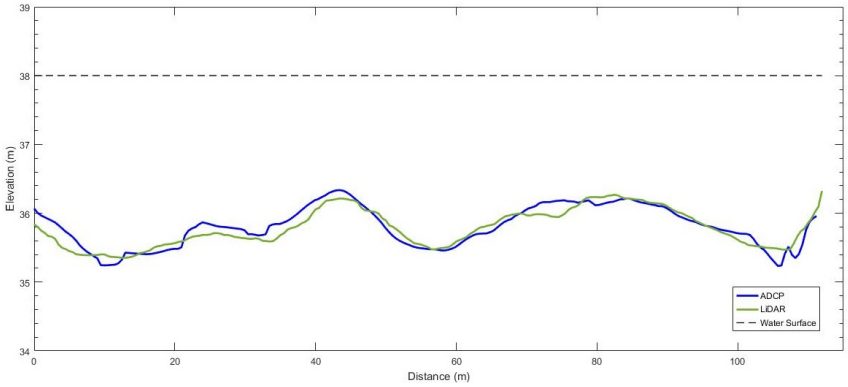

Figure 18: Extracted cross sections from the LiDAR DEM (green) and the ADCP DEM (blue) in the deep glide in Ljungan in a shallow area with full LiDAR range. The dashed line is the water surface

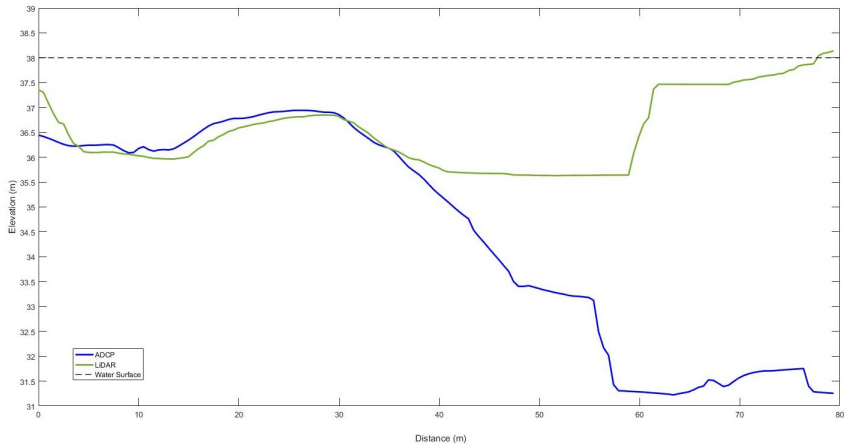

Figure 19: Extracted cross sections from the LiDAR DEM (green) and the ADCP DEM (blue) in the deep glide in Ljungan in an area with full LiDAR range in the shallow area and no LiDAR range in the deep section. The dashed line is the water surface

4.1.2 *Storåne*

The vertical discrepancies between the manually measured points and LiDAR points for the different groups in Storåne are shown in table 12. The vertical error was less than 4 cm for all the groups except the deep glide which had a high median compared to the others. Around 50 % of the measured points were found to intersect with LiDAR points for the river bed measurements except for the deep glide where only 18 % were compared due to the deep section without LiDAR points. Figure 20 shows the Z values for the measured points compared to the Z value of the LiDAR points with the calculated regression line (green) and the 1:1 line (black). The regression lines show a good fit with a determination coefficient of R^2 = 0.97-0.99 for all the groups except for the riffle (0.81) and deep glide (0.36). The regression line shows that the measured Z value is slightly over the LiDAR Z for the same 4 groups whereas the riffle and deep glide show a measured Z value lower than the LiDAR Z value. The small offsets (max = 0.19 m) in the riffle, figure 20e, was due to the few outliers that influence the points as there were only 38 intersecting points in this area. The deep glide, figure 20d has a large amount of outliers where the LiDAR Z value is about 1 - 2 m higher than the ADCP value. The elevation difference between the measured points and LiDAR points for the different groups compared to the depth can be seen in figure 21. The shallow glide has the highest error values at depths of 0.1 m to -0.1 m and has negative depths, meaning the LiDAR Z values are above the measured water surface. The water surface elevation may not have been in the exact spot of the measured points which may have caused this offset. The error from the hard and soft river bed does not imply any significant increase with depth but the hard bottom and deep glide both have a few errors in the magnitude of 1 m. There is a significant reduction of intersecting points when the depth exceeds 3 meters for the deep glide, figure 21d. The deepest intersecting point was at 5.1 m with only 5 intersecting points below 3.5 m depth, but the vertical accuracy is less than 10 cm for all of these points. The high errors in the deep glide of up to 1.85 m occur at a depth of 0.5 m up to 3 m. The points were located to be in two different areas which both had few LiDAR points but all of these had a high vertical offset. It was investigated whether these corresponded to the water surface but it appeared that in one area the points were below the water surface and in the other they were above the water surface. As these points did not correspond to neither the water surface nor the river bed they may have been caused by echoes or false returns, which were not removed by the supplier during the post processing. The hard bottom category also had errors of about 1 m in some areas but these had a lower Z value than the measured points. The investigation of these showed that two LiDAR points with the same XY coordinate had intersected one of the ADCP points where one LiDAR point showed an error of 1.15 m whereas the other showed an error of 0.10 m. This could be caused by either false bottom returns below the river bed or from sudden drops in the terrain that the ADCP did not pick up. The shallow glide, figure 21c, has the highest errors around 0 m depth and shows that there are several intersecting LiDAR points per ADCP point.

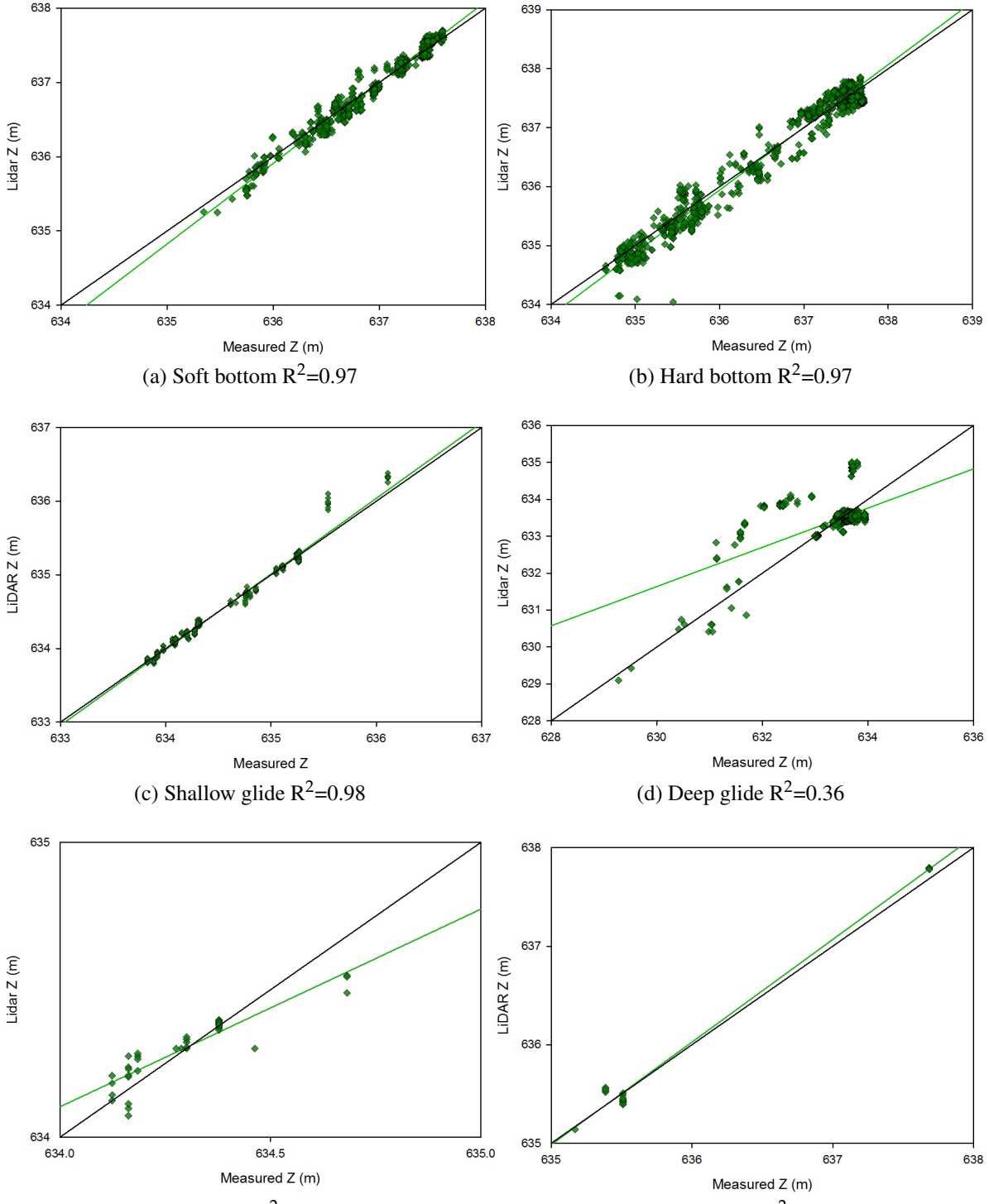

(a) Soft bottom R^2=0.97

(b) Hard bottom R^2=0.97

(c) Shallow glide R^2=0.98

(d) Deep glide R^2=0.36

(e) Riffle R^2=0.81

(f) Grassland R^2=0.99

Figure 20: Measured Z values (x) and LiDAR Z values (y) with the regression line (green) and the 1:1 line (black) for the different groups in Storåne. The stated determination coefficient, R^2, was calculated for each group

Table 12: Height discrepancies between measured points and LiDAR points for Storåne

Parameter	Riffle	Soft Bottom	Hard Bottom	Shallow Glide	Deep Glide	Grassland	Alluvial Forest
Mean [m]	-0.00	0.00	0.00	0.00	0.00	-0.02	-0.04
Median [m]	-0.01	0.00	-0.03	0.01	0.17	0.01	
Std. dev. [m]	0.07	0.09	0.19	0.09	0.53	0.10	0.02
Max [m]	0.19	0.36	1.40	0.56	1.86	0.18	0.05
Min [m]	0.00	0.00	0.00	0.00	0.00	0.00	0.02
# Points	38	949	1488	158	670	18	2

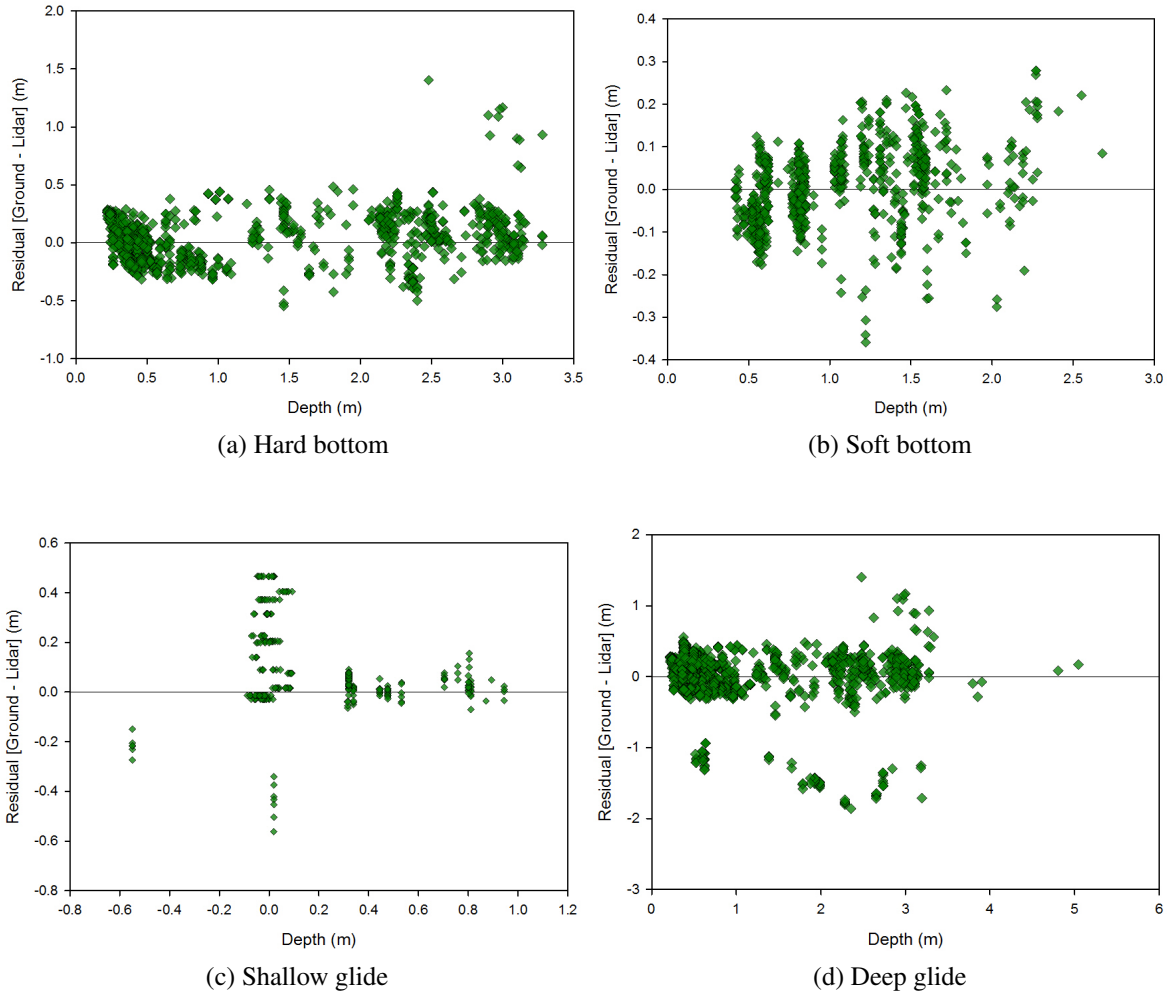

(a) Hard bottom

(b) Soft bottom

(c) Shallow glide

(d) Deep glide

Figure 21: Elevation difference between measured points and LiDAR points at various depths for each group in Storåne

The elevation difference between the measured points and the LiDAR DEM are shown in table 13. The mean and median errors are in the range of 0 to 0.12 m for all the groups except the deep glide. The effect of the missing LiDAR data in the deep glide caused the interpolated

DEM to be shallower than the actual depth, which was the same problem that occured in Ljungan. The maximum errors are in the range of 0.3 - 1.85 m for the groups which had full LiDAR range but the DEM still shows a high overall accuracy. The alluvial forest and grassland have the largest mean and median but are also the two groups with the fewest measurements. Figure 22 show the error for varying depths, which appears to be evenly distributed for all groups except for the deep glide. The error for the deep glide, figure 22d, increases proportionally with depth but the interpolation error is also high in the shallow areas. The hard bottom, figure 22a has a few outliers from 0.5 - 1 m which may be caused by the faulty points identified in the point comparison. The shallow glide, figure 22c shows negative depths with a few outliers of up to 0.9 m which could imply higher errors in the bank areas.

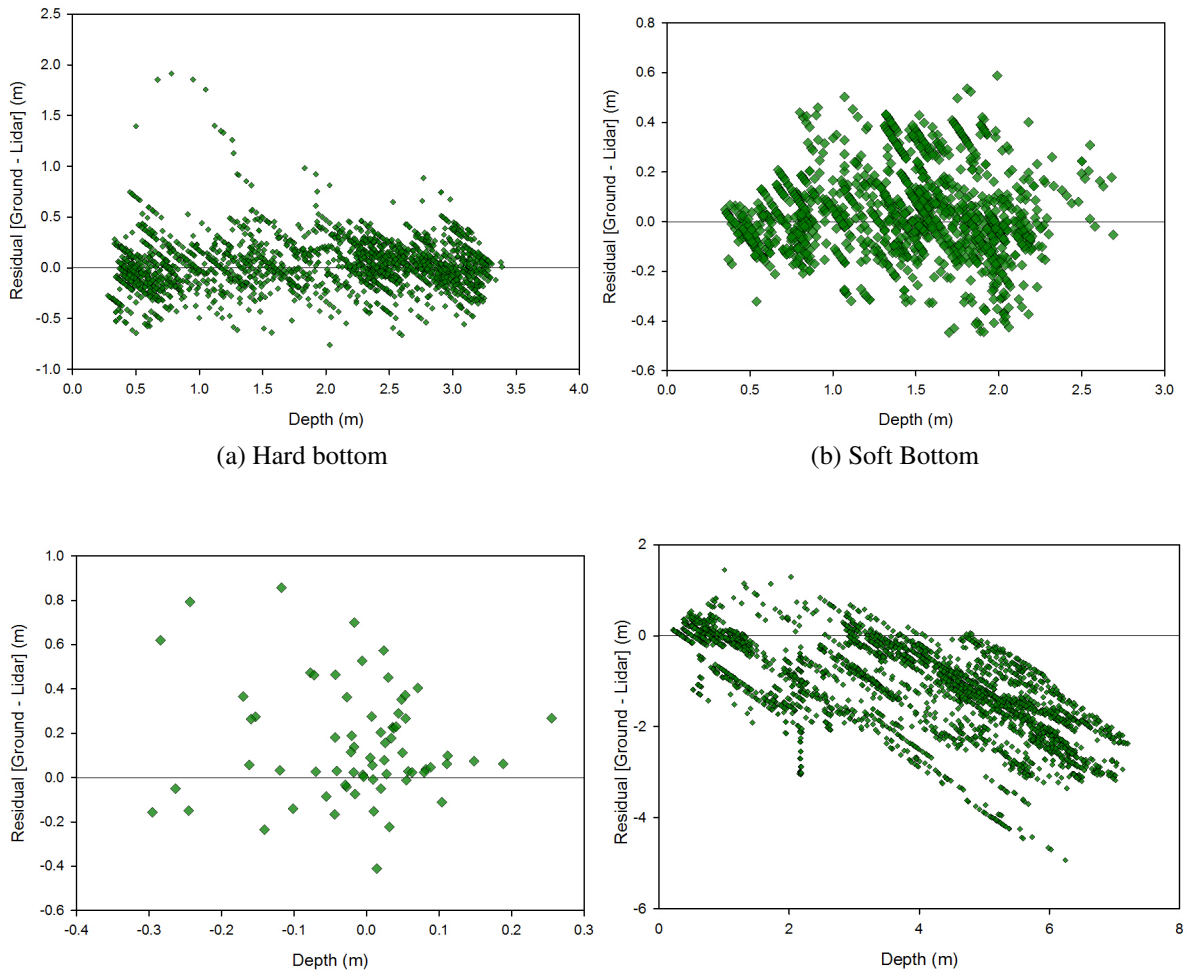

(a) Hard bottom

(b) Soft Bottom

(c) Shallow Glide

(d) Deep Glide

Figure 22: Elevation difference between measured points and LiDAR DEM at various depths for the groups in Storåne. The large offset in the deep glide (d) is due to missing LiDAR points in the deep areas

Table 13: Height discrepancies between measured points and the LiDAR DEM for Storåne

Parameter	Riffle	Soft Bottom	Hard Bottom	Shallow Glide	Deep Glide	Grassland	Alluvial Forest
Mean [m]	-0.03	0.07	0.03	-0.01	-1.51	-0.12	-0.07
Median [m]	-0.04	0.04	0.02	0.00	-1.43	-0.10	0.07
Std. dev. [m]	0.09	0.17	0.23	0.10	0.93	0.19	0.53
Max [m]	0.30	0.59	1.85	0.63	4.92	0.90	1.57
Min [m]	0.00	0.00	0.00	0.00	0.00	0.03	0.00
Points	66	1838	3029	158	3615	29	11

The discrepancies between the measured ADCP DEM and LiDAR DEM was calculated from the areas with overlapping data only to compare the rasters on a basis where there points from both measurement devices to evaluate how accurate the rasters are in the areas where there are LiDAR points obtained. The mean error, standard deviation and maximum error were obtained from ArcMap and are shown in table 14. The error between the rasters are low for both the soft and hard bottom whereas the deep glide shows the same high errors as for the previous comparisons. The error distribution for the three groups in figure 23, show that the soft bottom and hard bottom have distributions around 0.1 m and 0.2 m respectively, whereas the deep glide has a few outliers of up to 1.78 m. The residual rasters from the three groups, figure 24 and 25, include the areas that are in the close vicinity of the overlapping points and exclude errors higher than the ones measured from the overlapping rasters. The residual rasters from the soft and hard bottom are shown in figure 24, where the light areas show the smallest errors and the dark areas are the largest errors. The large areas with high errors are areas where there are no overlap of ADCP points and LiDAR points.The location of the ADCP points and LiDAR points can be seen in Appendix F. For the deep glide in figure 25 the large errors on the right side of the channel is where there were faulty LiDAR points as mentioned in the point comparison, which caused the erroneous interpolation. Cross sections from the LiDAR and ADCP DEMs were extracted from this section in the deep glide, figure 26 and 27 where the green line is the LiDAR DEM whereas the blue line is the ADCP DEM. A cross section from the middle section of the hard bottom raster can be seen in figure 28 which illustrates the possible sudden drops in the terrain.

Table 14: Height discrepancies between LiDAR DEM and ADCP DEM for Storåne. Only three of the groups contained enough points to create rasters. The large offsets in the deep glide is due to faulty LiDAR points

Parameter	Soft bottom	Hard bottom	Deep glide
Mean [m]	0.01	-0.01	0.47
Std. dev. [m]	0.12	0.20	0.69
Max [m]	0.41	0.90	1.78

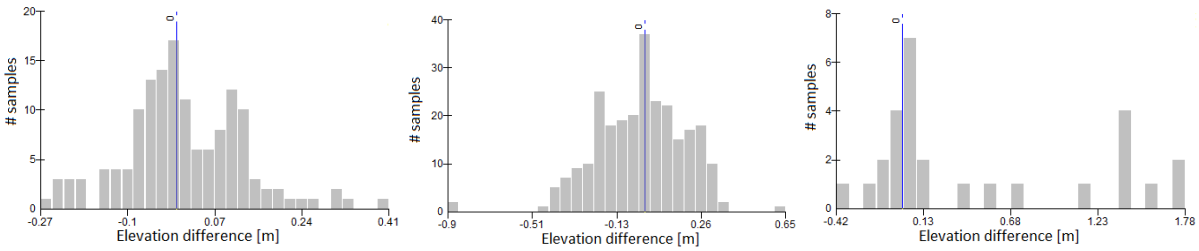

(a) Soft bottom (b) Hard bottom (c) Deep glide

Figure 23: Error distribution for LiDAR DEM minus ADCP DEM for the three groups in Storåne constructed by ArcMap

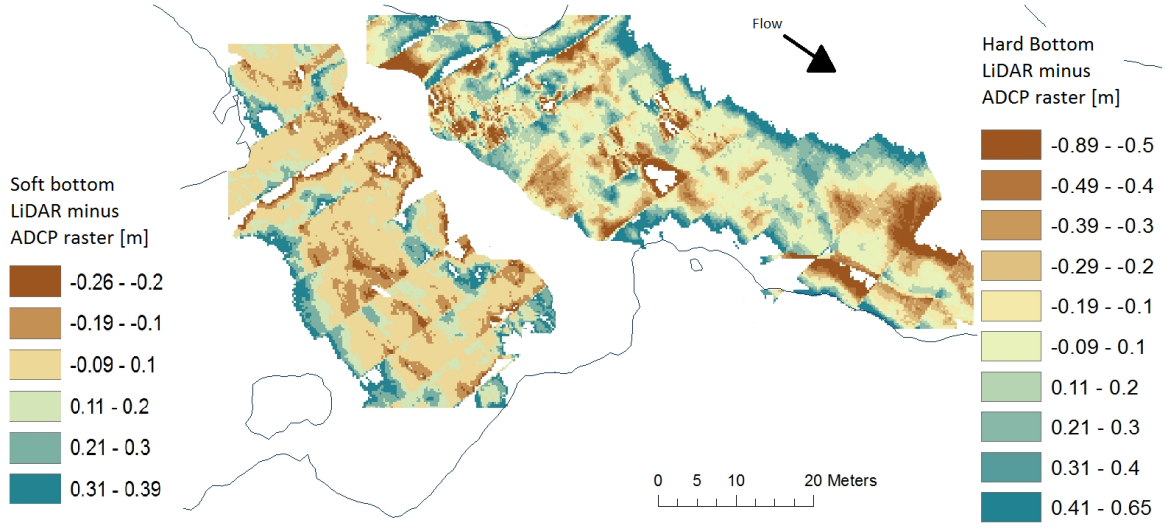

Figure 24: Residual raster from LiDAR DEM minus ADCP DEM for the soft bottom (left) and the hard bottom (right) in Storåne with 0.25 m grid size. The light coloured areas show the lowest errors whereas the darker colour shows higher errors

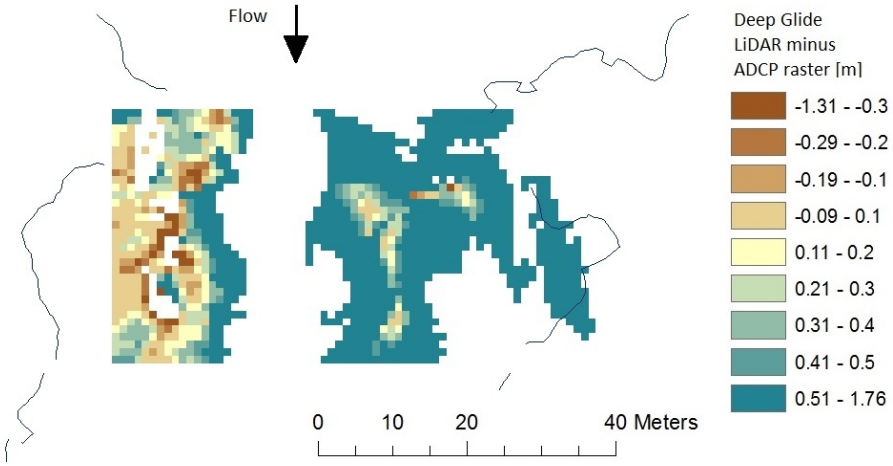

Figure 25: Residual raster from LiDAR DEM minus ADCP DEM for the deep glide in Storåne with 1 m grid size. The light coloured areas show the lowest errors whereas the darker colour shows higher errors

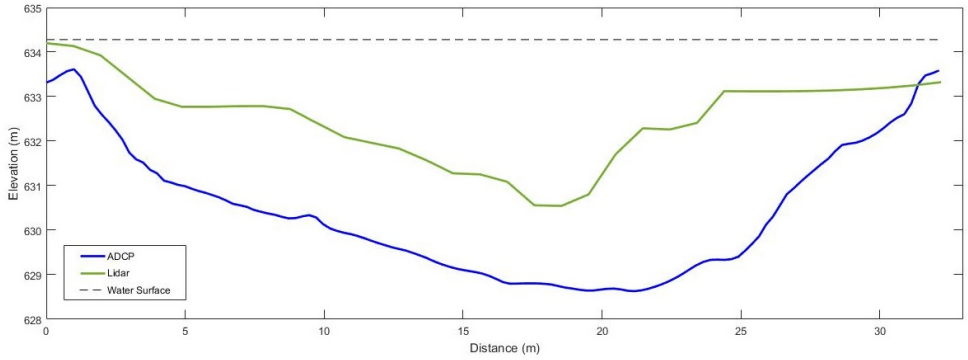

Figure 26: Extracted cross section from the LiDAR DEM (green) and the ADCP DEM (blue) in the deep glide in Storåne with few LiDAR points. Left side has faulty LiDAR points in the shallow areas from 0-5 m. The dashed line is the water surface

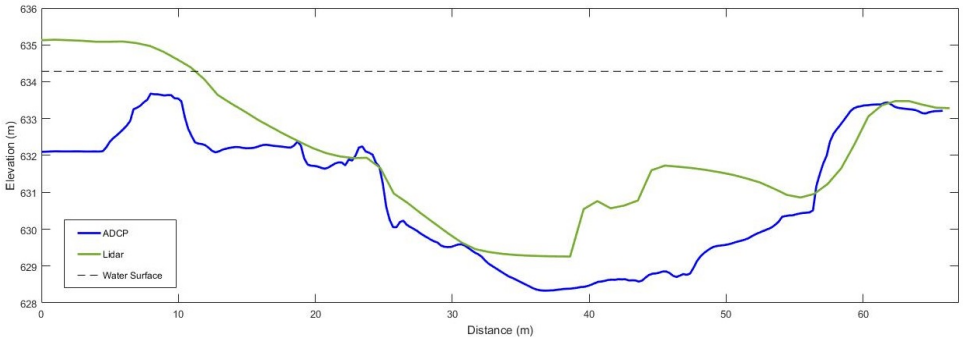

Figure 27: Extracted cross section from the LiDAR DEM (green) and the ADCP DEM (blue) in the deep glide in Storåne. Left side has LiDAR points above the water surface from 0-10 m. Next point is at 22 m. The dashed line is the water surface

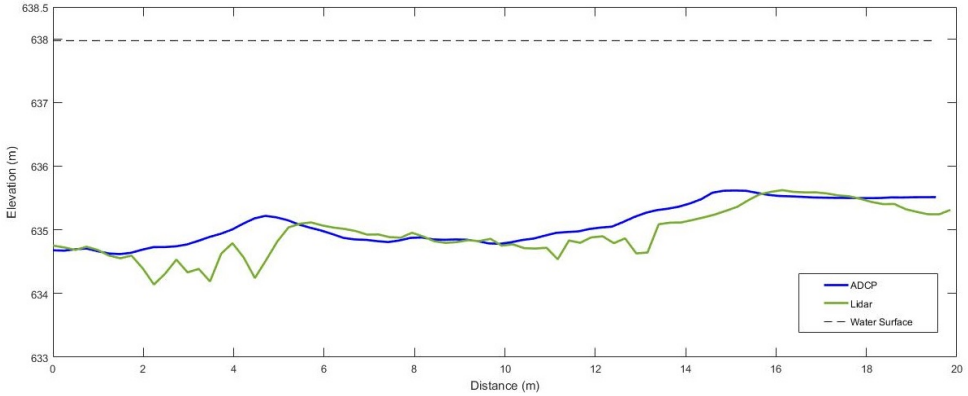

Figure 28: Extracted cross section from the LiDAR DEM (green) and the ADCP DEM (blue) in the hard bottom Storåne. The offsets may be caused by false LiDAR points or missing ADCP measurements. The dashed line is the water surface

4.2 INTERPOLATION IN AREAS WITH MISSING LIDAR DATA

The validation of the LiDAR data showed that large areas without LiDAR range cause high errors in the interpolated DEM which furthermore would cause errors in the hydraulic model. To improve these areas would require additional measurements or finding a method to estimate the cross sections. Figure 29 shows the elevation difference between the original LiDAR DEM and the corrected LiDAR DEM with added ADCP points from the deep sections in Viforsen. The grey areas show the influence of adding only a few points in areas with missing LiDAR data. The points do not cover the entire areas of missing data and would require data from a wider areas. Figure 30 show cross sections from the corrected DEM (red) along with that of the ADCP measurements (blue dashed) and the LiDAR DEM before correction (green dashed). Figure 30a is from the top most area where there is no LiDAR range and the addition of a few points lead to an improvement, but because the added points are not in the deepest section it still misses a large part of the river bed. Figure 30b is from the lower part where there is good LiDAR range on one side but no LiDAR range on the other side of the river. Adding only a few points from the middle section does not adequately cover the river bed as the width of the missing range is in the range of 40 - 150 m and would need more data. The cross sections extracted from the corrected DEMs in Storåne showed a more promising results after adding only a few points to the missing area, figure 32. The width of the missing section between each LiDAR cross section is not more than 20 meters and the added points appeared to have improved almost the entire area. Figure 32 show cross sections extracted from the corrected DEM (red) along with the original LiDAR DEM (green) and ADCP DEM (blue). The corrected DEM shows a higher accuracy where there are more points added,32b, as this ensures that the deepest points are included whereas 32a barely misses the deepest section. The LiDAR has full coverage on both sides of the pool and thus the small missing area is improved by adding points to the middle section. The accuracy is still highly improved in both cases and the interpolation has only minor errors as the missing area is smaller. The error on the left is caused by the faulty LiDAR points adressed in section 4.1.2

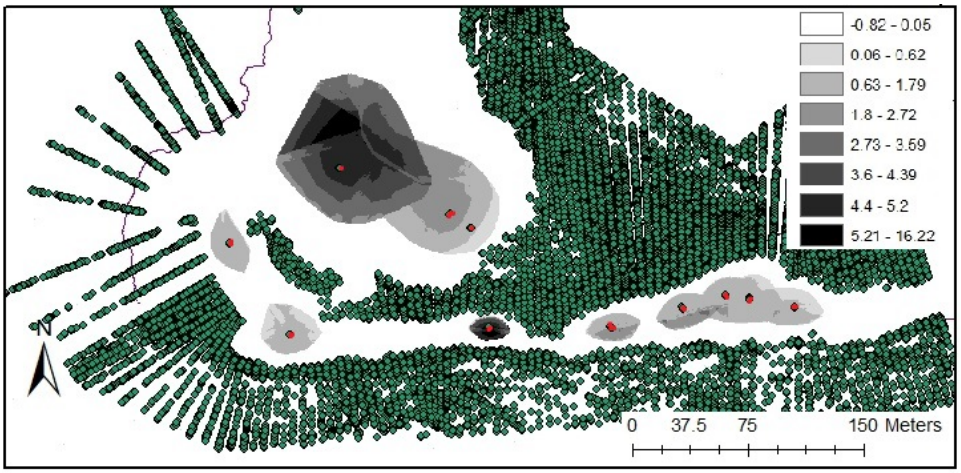

Figure 29: The shaded grey areas are the residual between the initial LiDAR DEM and the corrected LiDAR DEM with added ADCP points in Ljungan. The green dots are the LiDAR points and the red dots are the added ADCP points

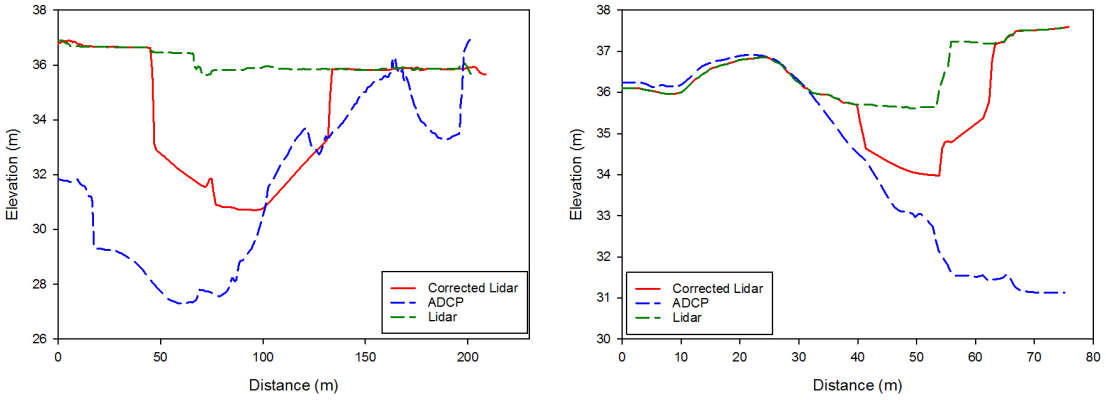

(a) No LiDAR range (b) Partial LiDAR range

Figure 30: Cross sections extracted from the corrected LiDAR DEM (red), initial LiDAR DEM (green dashed) and ADCP DEM (blue dashed) in Viforsen

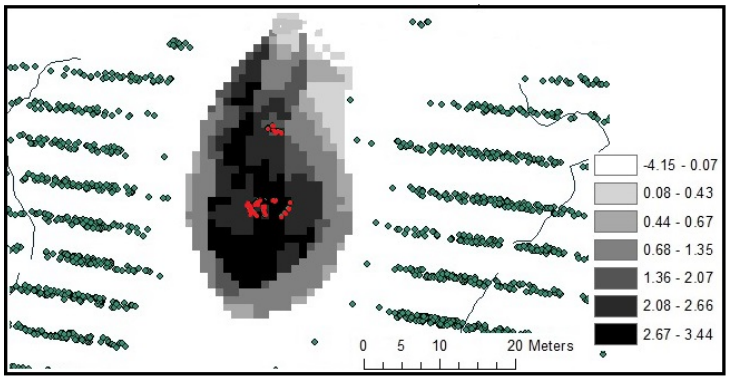

Figure 31: The shaded grey areas are the residual between the initial LiDAR DEM and the corrected LiDAR DEM with added ADCP points in Storåne. The green dots are the LiDAR points and the red dots are the added ADCP points

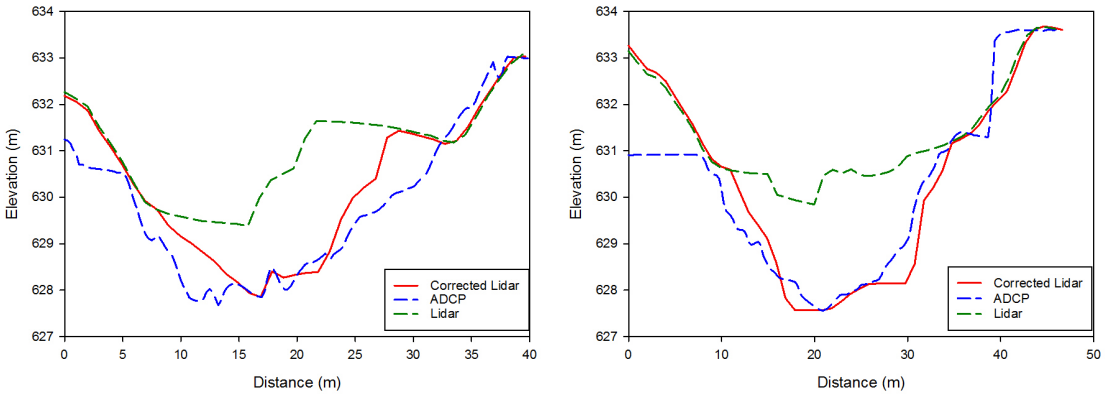

(a) (b)

Figure 32: Cross sections extracted from the corrected LiDAR DEM (red), initial LiDAR DEM (green dashed) and ADCP DEM (blue dashed) in Storåne

The interpolated cross sections based on the slope of the banks showed highly variable results but implied that this method could work for some areas if there are LiDAR points obtained from the side banks. Some of the interpolated cross sections from the deep glides in Ljungan and Storåne are showed in figure 33 - 36 where the green dots are the LiDAR points and the blue triangles are the ADCP points from the manual measurements. The cross section in figure 33 from Ljungan shows the linear trend line from the left bank points based on only 5 LiDAR points measured from the steep bank where only one is placed below the water surface. Despite the few points, the slope appears to be close to the actual bank but there were no ADCP measurements for comparison. The right bank has full LiDAR range of the river bed in the shallow area and the calculated polynomial trend line intersects with the deepest ADCP points although the shape is different. The cross section in 34 from Ljungan also show a reasonable estimated trend line on the left side based on the steep bank with more points from the river bed. The right bank only has LiDAR points from the shallow steep section which resulted in a steep trendline that missed the flattening part of the river bed. Figure 35 showed a reasonable fit with a linear trend line on the left bank and a polynomial trend line on the right bank. However, figure 36 had similar amount of obtained points but the estimated depth is off by 3 m. The polynomial trend line from the left bank is too steep as it misses the flattening part of the bank and the deepest LiDAR points on the right bank appears to be too deep compared to the ADCP points, resulting in a linear trend line that is too steep.

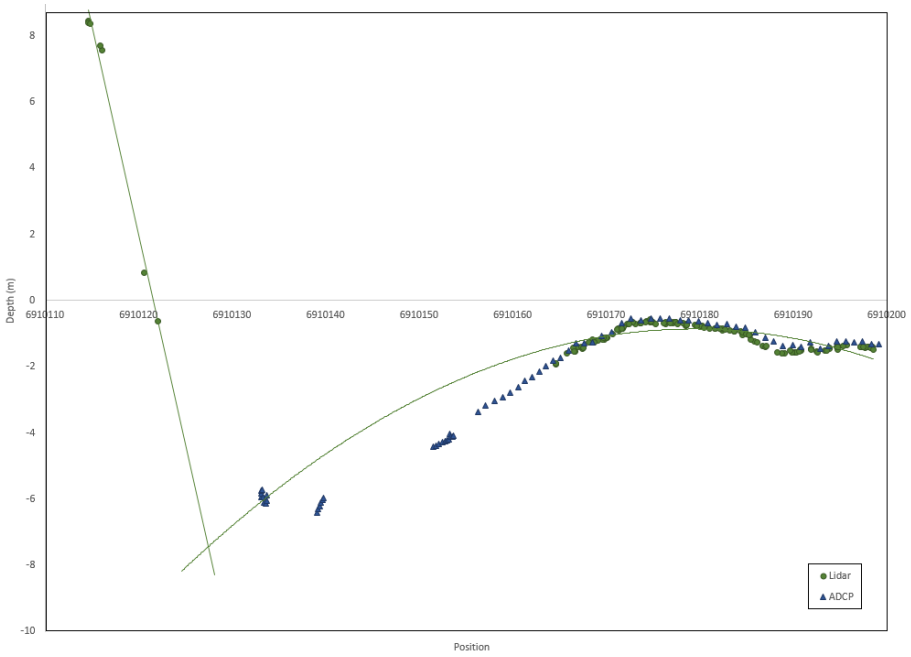

Figure 33: The constructed bank lines from Ljungan in green from the LiDAR points (green) and the ADCP points (blue) indicate the measured river bed

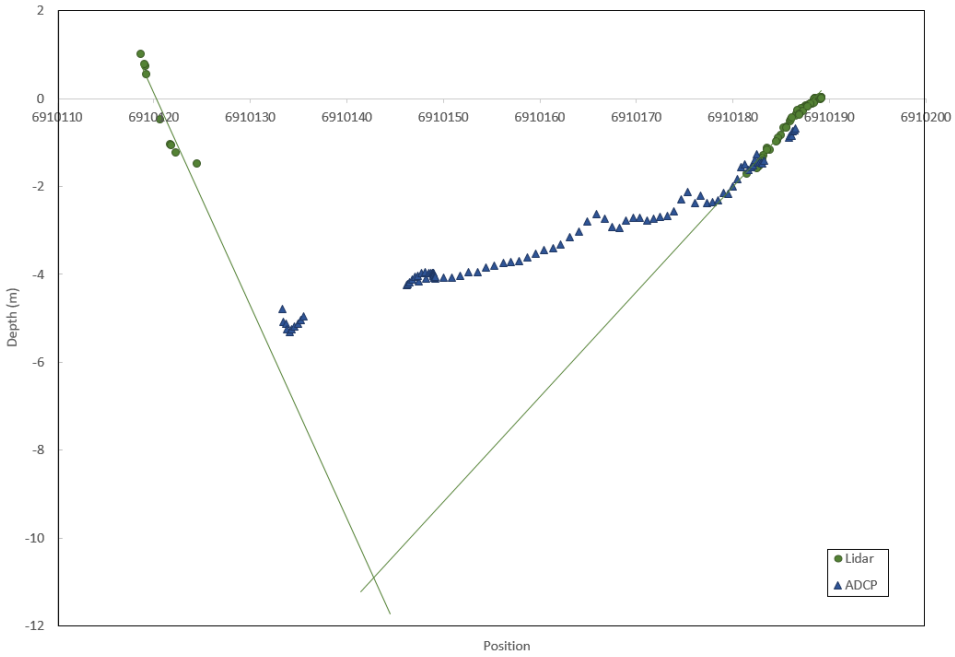

Figure 34: Constructed bank lines from Ljungan in green from the LiDAR points (green) and the ADCP points (blue) indicate the measured river bed

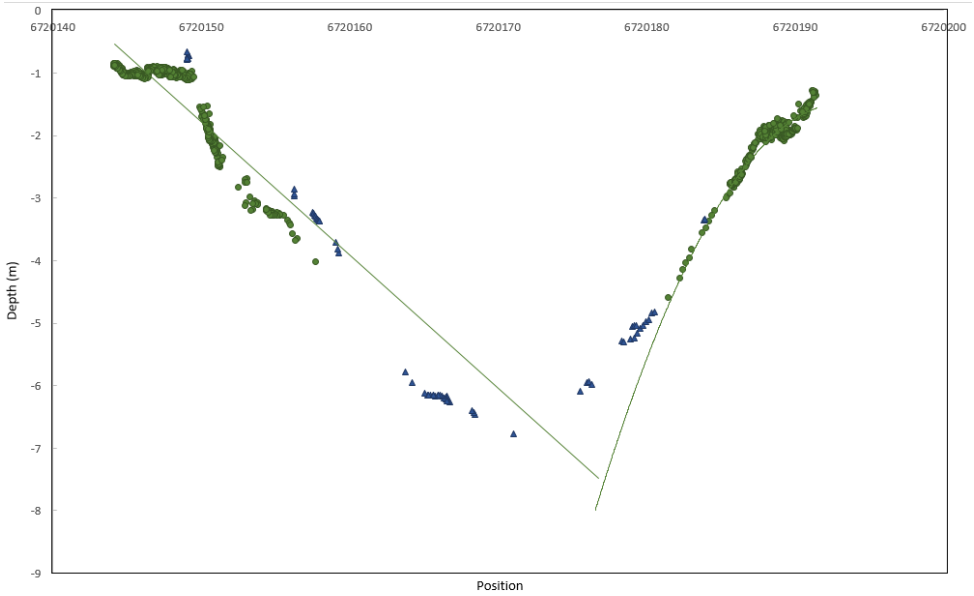

Figure 35: Constructed bank lines from Storåne in green from the LiDAR points (green) and the ADCP points (blue) indicate the measured river bed

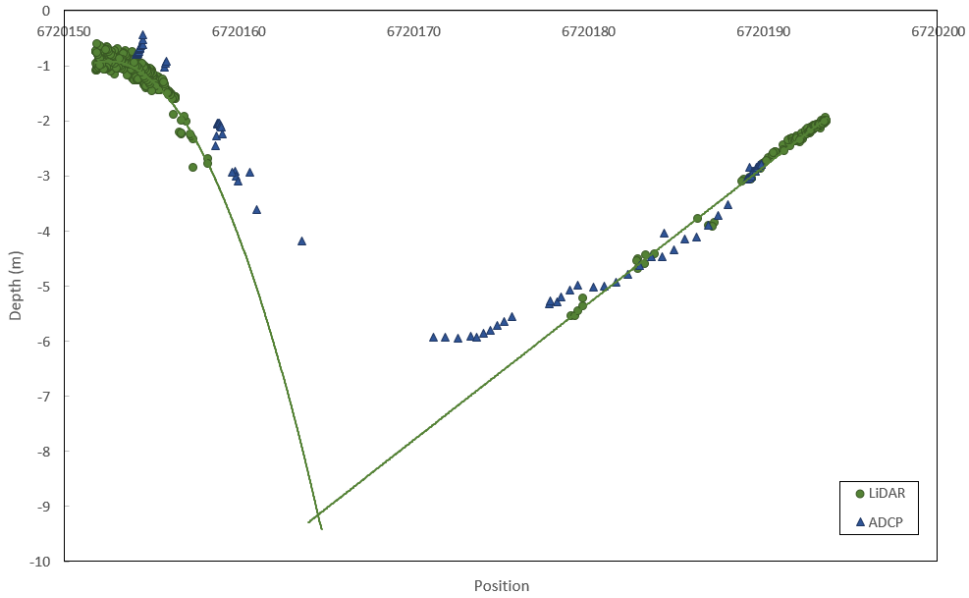

Figure 36: Constructed bank lines from Storåne in green from the LiDAR points (green) and the ADCP points (blue) indicate the measured river bed

4.3 HYDRAULIC MODELING

The model for Ljungan was calibrated with the flow of 58.9 m^3/s, figure 37a, by changing the Mannings n value but errors in the DEM induced by the missing LiDAR data caused the model to have a discontinuous water string, figure 37c. The flood simulation, figure 37b, was less affected by the errors in the DEM but showed that not all the profiles were wide enough to account for the flow area. The water surface elevation lines for the two flow scenarios can be seen in figure 38 where the low flow (red) shows the three steep riffle sections. The gradient of the river bed can be useful to identify potential spawning areas for fish.

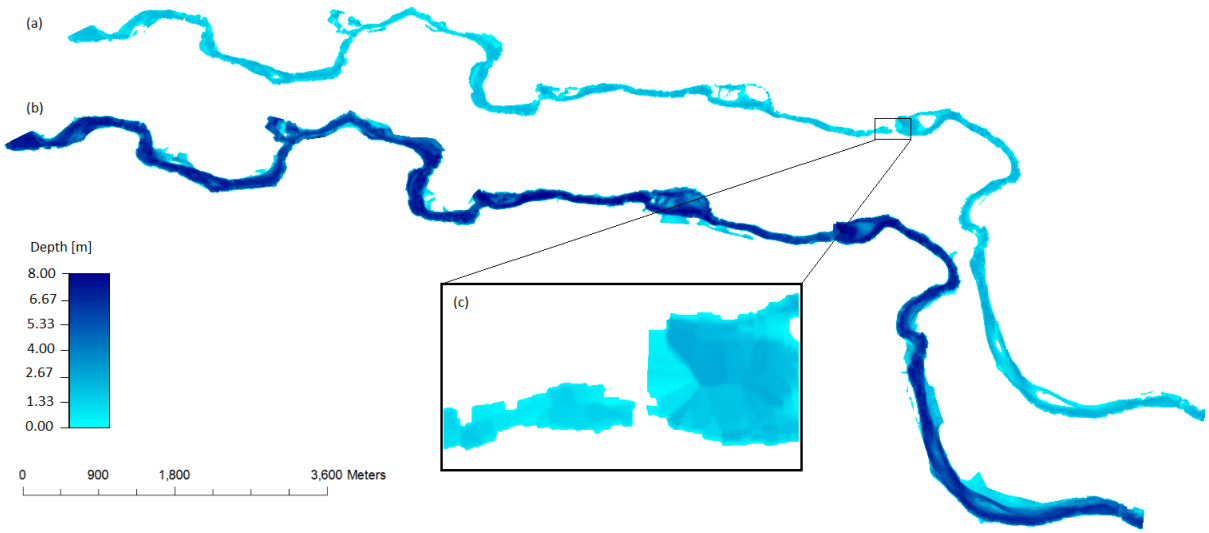

Figure 37: Water depth from the steady simulations in Ljungan **(a)** 58.9 m^3/s from the day of the scan; **(b)** 1059 m^3/s from the highest recorded flood; **(c)** detail of the area where the water stream was broken

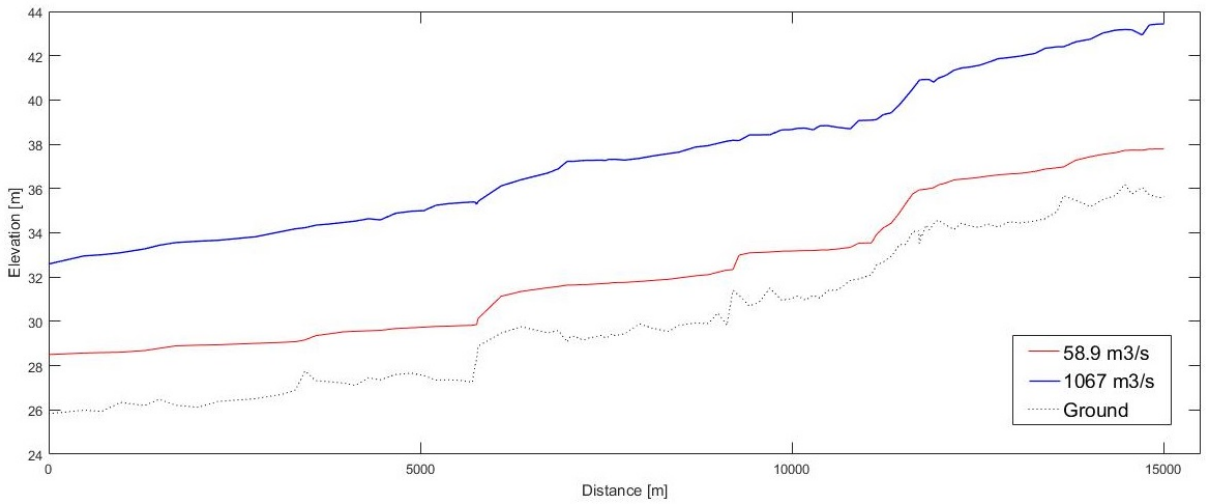

Figure 38: The water surface elevation lines from the two steady simulations from Ljungan along with the ground points. The blue line is the flood (1059 m^3/s), the red line is the scan date (58.9 m^3/s) and the black dotted line is the riverbed

The result from the three different steady flow scenarios that were run for Storåne can be seen in figure 39. When running the model from Storåne it was discovered some cross sections where HEC-RAS had assumed a vertical bank, figure 39d. This was found to be caused by the LiDAR data not extending further than the river bed and thus the DEM that the cross sections were drawn from did not include the river bank. This was fixed manually by correcting the cross sections in HEC-RAS and assuming a slope of the bank to end the cross section. The flood simulation also had this problem as the cross sections did not extend far enough either due to no LiDAR data or the cross sections extracted in GeoRAS were not extended far enough. The water surface edge line for the three flow scenarios in figure 40 show the areas with steep riffles and the location of the deep pools.

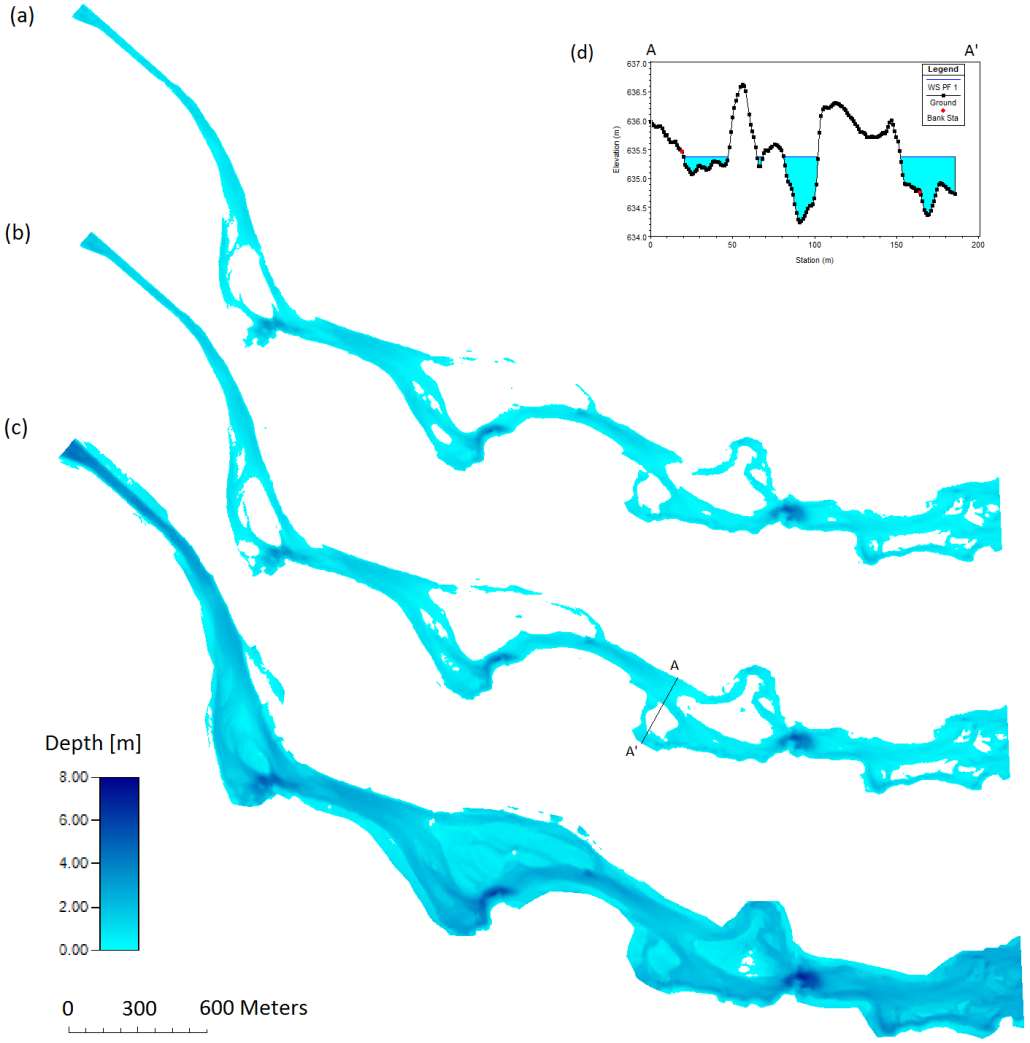

Figure 39: Water depth from the simulations in Storåne with a flow of **(a)** 15.6 m^3/s from the day of the manual measurements; **(b)** 30.72 m^3/s from the day of the scan; **(c)** 217 m^3/s from a recorded flood

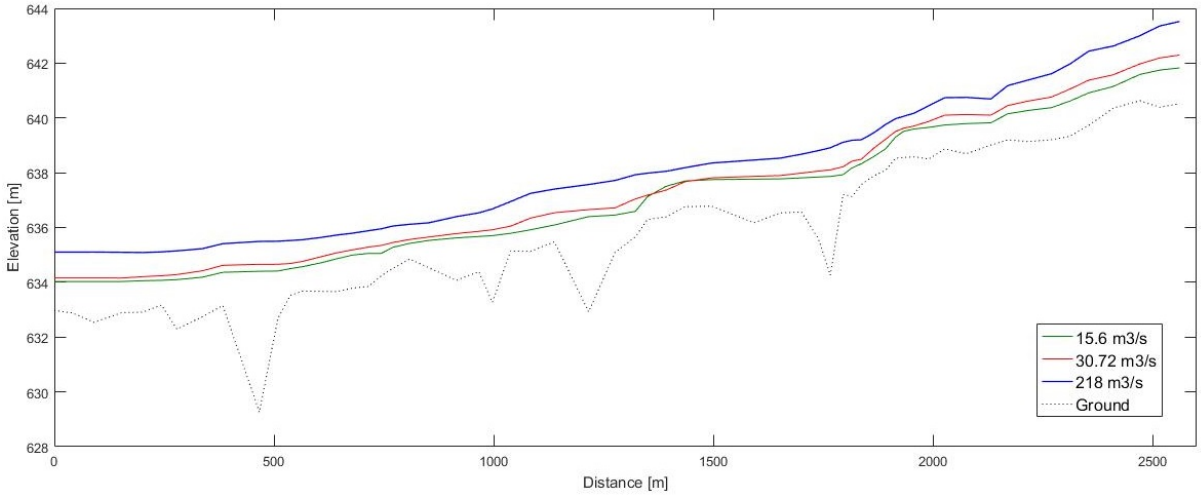

Figure 40: The water surface elevation lines from the two steady simulations from Ljungan along with the ground. The blue line is the flood (1059 m^3/s), the red line is the scan date (58.9 m^3/s), the green line is the low flow (15.6 m^3/s) and the black dotted line is the riverbed

The unsteady simulations provide a basis for evaluating potential stranding areas for fish habitat by combining the information from the calculated water covered area, figure 41 and 43, with the stage at various flows, figure 42 and 44. The water covered area at different flows identifies critical flow changes which is useful for the regulation of the power plants. The input data for the unsteady models used in this study had 12 hour and 24 hour flow input which would not be sufficient for modeling potential stranding of fish.

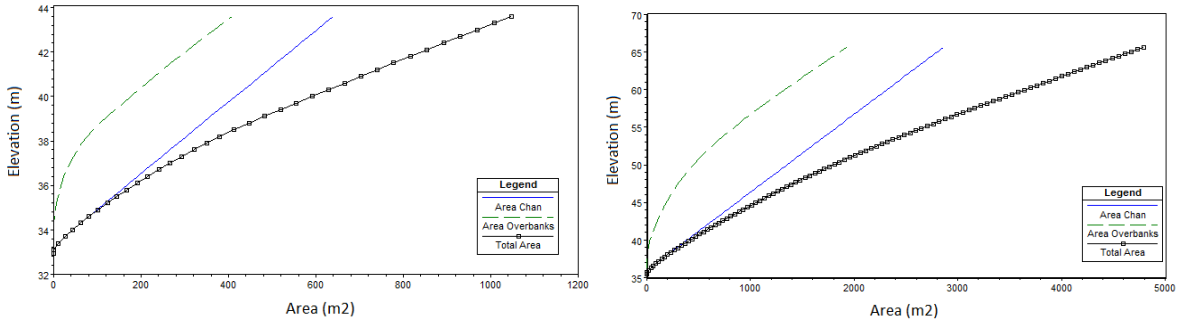

(a) (b)

Figure 41: Calculated stage versus area from two profiles in Ljungan generated in HEC-RAS. The black line is the total area covered at each water surface elevation combined from the area of the channel (blue) and the overbanks (green dashed)

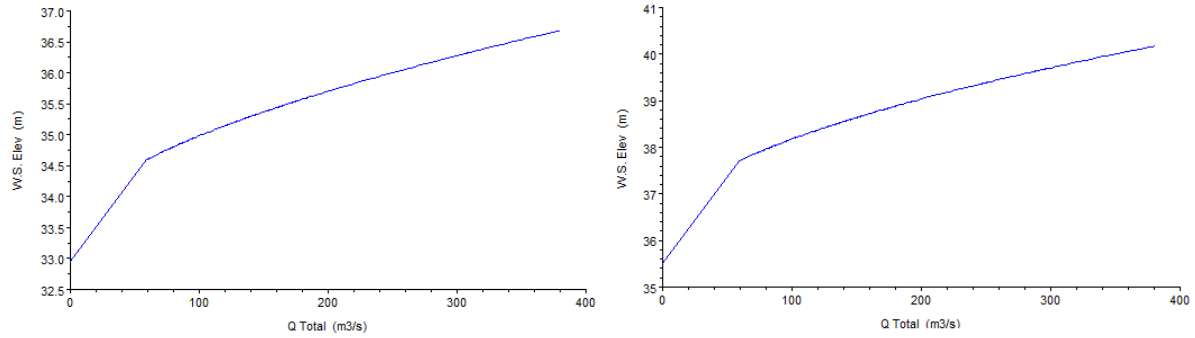

(a) (b)

Figure 42: The surface elevation line (blue) for varying flow generated in HEC-RAS from two profiles in Ljungan

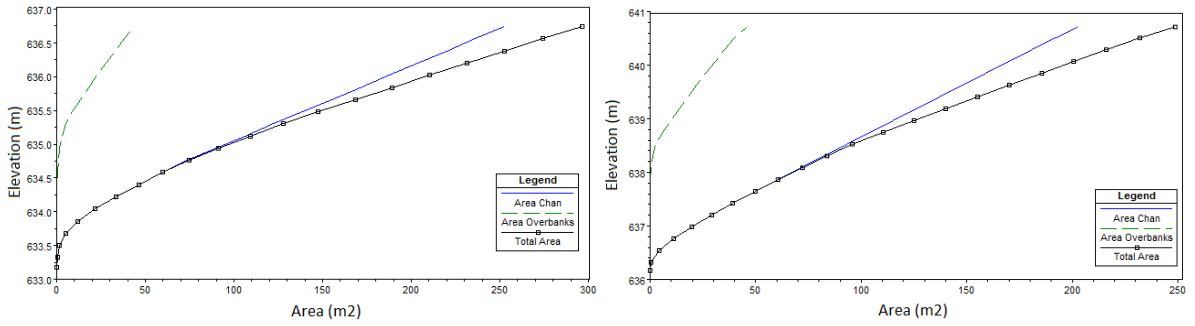

(a) (b)

Figure 43: Calculated stage versus area from two profiles in Ljungan generated in HEC-RAS. The black line is the total area covered at each water surface elevation combined from the area of the channel (blue) and the overbanks (green dashed)

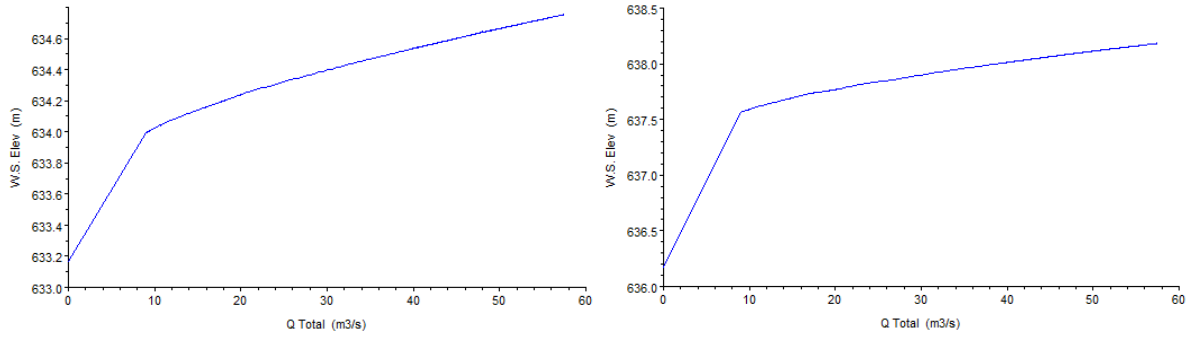

(a) (b)

Figure 44: The surface elevation line (blue) for varying flow generated in HEC-RAS from two profiles in Storåne

5

DISCUSSION

This study has evaluated ALB as a tool for mapping underwater topography in two rivers with different characteristics to asses the potential for applying ALB in Nordic rivers. ALB is an efficient method for data collection and provide a detailed and accurate basis for hydraulic models. The study compared the LiDAR data from a clear, shallow river to the LiDAR data from a dark and deep river to evaluate the impact of environmental conditions on accuracy and density. The study found that the accuracy did not appear to be affected by depth or river characteristics as it showed a high overall accuracy. The water colour and bottom reflectivity did however affect the LiDAR's depth range. The LiDAR data from the clear river reflected points down to 6 meters mapping 99 % of the river bed, whereas the river with dark coloured water had a depth range of less than 3 meters and mapped around 60 % of the river bed. However, the point density was significantly decreased at depths exceeding 3 m and 2.5 m respectively, which indicates that a dark river bed may also influence the range. It may be possible to correct areas with missing LiDAR data by interpolation based on the slope of the river banks but this would require further study as the results were highly variable. With a complete data set, the high density of ALB surveys provide a detailed, seamless map of the river bed and banks. LiDAR data thus have a a wide application such as studying habitat, morphology, sediment, floods and hydraulics. ALB surveys can serve as an important tool for holistic management of rivers and shallow water bodies with the ability to model hydraulics and ecology with an integrative approach.

5.1 VALIDATION OF LIDAR DATA

The comparison of manual measurements and LiDAR measurements demonstrated that ALB is a viable method for mapping rivers with an accuracy similar to conventional methods. The accuracy was assessed in relation to water clarity, depth, mesohabitat and bottom material but no clear correlation was found. The elevation comparison of LiDAR points and measured points from the two study sites showed that the accuracy of the LiDAR data was on centimetre level for both channel and bank areas. The accuracy did not decay with increased depth but the point density was significantly reduced after 2.5 m for Ljungan and 3 m for Storåne. The mean was found to be less than 0.04 m for 100 % of the point elevations whereas the median was less than 0.03 m for 74 % of the point elevations. The standard deviation ranged from 0.09 m to 0.23 m for the majority of the groups, except for the deep glides and alluvial forest. The highest errors were found in the deep glides (0.17 m and 0.11 m) for both rivers with a standard deviation of 0.93 m and 0.18 m which implies that the accuracy is not impacted by

water clarity. These values were higher than what has been measured previously by Mandlburger et al. (2015) during a repeat survey for monitoring sediment transport and bank erosion in a gravel bed river ($Q < 10$ m^3/s) with the RIEGL VQ-880. Their accuracy assessment was conducted on sub centimetre level based on the categories sealed road, river bed, alluvial forest, grassland and gravel bank. The largest vertical errors (median) found by Mandlburger et al. (2015) were for the groups alluvial forest (0.055 m) and grassland (0.031 m) whereas the river bed had an error of 0.006 m.

As the manual measurement devices used in this study had an accuracy of up to 10 cm the assessment was only calculated to centimetre level. There were a number of factors from the manual measurements that could impact the accuracy of the data, such as the measurement of the transducer depth on the ADCP, placement and signal of the GPS, as well as the measured and calculated water surface. The offsets in the deep glide in Storåne were first thought to be caused by a classification problem where the water surface points had been mistaken as river bed points but further investigations showed that it was most likely caused by false returns, explained in section 4.1.2. The water edge line constructed by the supplier was not placed correctly in this area as the ADCP had obtained measurements outside the constructed water edge line. There were few returned LiDAR points in the deep glide, especially in areas deeper than 3 m which demonstrated that the point density was significantly reduced when the depth exceeded 3 m, even for a clear stream like Storåne. This implies that the depth range of the LiDAR may be more affected by a dark bottom than the water clarity. This was also supported by the findings in Ljungan where the Secchi depth in the deep glide was measured to 3 m, which could imply that the depth range of the LiDAR would be down to 4.5 m (1.5 Secchi). However, the deepest intersecting points were found at 3 m with a significant reduction after 2.5 m. This may be caused by dark substrate or vegetation on the river bed that lowered the reflection of the LiDAR points. The comparison still found 60 % of the ADCP points intersecting with LiDAR points, which was mainly distributed between 1 m and 2.5 m depths. The precision (std. dev.) was higher than for Storåne as the errors were evenly distributed with only a few outliers. This could indicate that the overall offset is higher in the deep glide Ljungan but it can not be generalised for the whole river as the data from the pool showed a high accuracy. However, only 12 % of the points measured in the pool in Ljungan were found to intersect with the LiDAR points which is very few compared to the deep glide. The calculated water surface from the pool in Ljungan may have lead to an improvement of the accuracy as the calculated mean offset between the LiDAR and the ADCP points were added to the ADCP data set. It is therefore difficult to conclude whether there is a correlation between the accuracy and the water colour. Soft river bed has previously been a challenge for the LiDAR's detection of the river bed but has now been improved according to the supplier. The findings from this study support this as the measurements from the soft river bed had a higher accuracy than the hard river bed. The hard bottom data had a high maximum error and deviations of 1 m between two LiDAR points intersecting with the same ADCP point which was either caused by sudden drops in the terrain or false echoes. For the grassland, some of the measurements intersected with more than one LiDAR point, some places as many as four or five. This did not appear for any of the alluvial forest points which could imply that the point density is lower in the alluvial forest compared to the open banks. This is to be expected as the LiDAR will receive fewer returns from the ground where there is dense vegetation that prevents the beams from reaching the ground. The accuracy was found to be high in this group

which indicate that the classification and removal of vegetation is accurate. The intersection of multiple LiDAR points per ADCP point was due to the high density of the LiDAR points and the horizontal accuracy of 0.06-0.07 m which was used as XY tolerance to locate the intersecting points. By calculating the average value of the neighbouring LiDAR points, only one point would be compared to each ADCP point which may be better for point comparisons, as done in the accuracy assessment of Mandlburger et al. (2015). The point elevation assessment indicated that there may be some outliers throughout the LiDAR data set with maximum error of 0.3 - 1.86 m but the high point density and stacking of points lead to an overall accuracy.

The comparison of reference points to LiDAR DEM showed that LiDAR cross sections can be applied to interpolate a DEM with a high accuracy for both larger and smaller grid sizes in areas where the LiDAR reaches the full depth of the river. The point to DEM comparison showed an accuracy in the same range as the point comparison for all categories that were within the LiDAR's depth range but both the deep glides and the pool had large areas without LiDAR points and thus high errors (see table 10 and 13). As the depth in these areas exceeded the LiDAR's range, there were no points from the deepest sections. The absence of deep points caused the interpolation to calculate a flat bottom until another point was in the vicinity and thus failed to capture the shape of the channel bottom. The reduced point density below 2.5 m and 3 m for the deep and shallow river, respectively, contributed to a lower accuracy also in areas shallower than the depth range. For the deep, dark waters in Ljungan there were missing areas throughout the river and thus the DEM did not properly represent the features of the channel. In the deep glide in Storåne, the faulty LiDAR points in the shallow areas further increased the error in the DEM interpolation.

The comparison of the ADCP DEM and LiDAR DEM showed high accuracies in the areas with overlapping points except for the faulty points in the deep glide in Storåne which caused higher errors. The residual rasters demonstrated a large variation in the errors but generally appeared to be in the scale of 0.1 m - 0.2 m in areas in close vicinity of the overlapping points. McKean et al. (2009) also found errors in the range of 0.1 m - 0.2 m when conducting a study with the EEARL system on two shallow ($<$ 1 m) rivers in USA using 3 m and 2 m raster cell sizes created by isotropic kriging. Their study found that the largest errors tend to be along the stream banks or in small pools where the large grid size does not capture the abrupt changes over a small spatial scale. The study suggested that EEARL data adequately represents boundary conditions for 1D and 2D numerical modeling (McKean et al., 2009). The raster comparison applied in this study used a smaller grid size (0.25 m, 0.5 m, 1 m) and were conducted over smaller areas which should capture abrupt changes in the topography but may not reflect the overall accuracy of the LiDAR raster. There were no ground points measured in the areas near the ADCP measurements and it was therefore not possible to compare the transition from river bed to ground. Several cross sections measured with the GPS would allow for an interpolation of both terrain and river bed to compare the transition zones. To obtain a full evaluation of the LiDAR DEM one should obtain measurements of the banks as well as the river bed to investigate how well it captures abrupt changes from river to banks. It may be better to use Triangulated Irregular Network (TIN) to create a surface with inconsistent resolution that captures important channel features and abrupt changes in the morphology better than rasters. With a raster size of 1 m and 2 m some features may be lost but the

accuracy is assumed to be adequate for the purpose of this study. The raster surface is considered easier to process and was considered to be sufficient for the application of the LiDAR cross sections with 5 m spacing. The point reduction performed on the LiDAR data prior to the DEM creation presents an uncertainty in the possible degradation of the data quality. As the script would pick out points at a firm interval it should not lose the features of the river bed. However, the accuracy of the DEM is reduced and important features may be lost when there are less points to interpolate between. In areas with an initially low point density such as deep sections or very steep banks the point reduction may degrade the data quality. The supplier stated that the maximum depth reached in Storåne was 6 m but the deepest points were found to be at 5.1 m depth after the point reduction. As the deep glide already had a low density the point reduction may have lead to a removal of the deepest points. If a point reduction is required it may be better to reduce the density proportionally with the number of points in the vicinity to prevent a reduction in critical parts where the initial density is low.

The conversion of the measured reference data from orthometric to ellipsoidal height system imposes an uncertainty on the results from the accuracy assessment. For future reference the data should be measured in the same height system or a geoid height model should be applied to ensure a correct conversion. As the geoid height can vary over small spatial scales, it may induce errors when calculating one common factor for a larger area as was noted in Storåne. This was later discussed with the supplier who confirmed that the spatial variation could be in the range of 0.3 m which was found for Storåne and that the correction for a small area should be within the offset range that already exists between the manual measurements and the LiDAR. It is therefore assumed that the calculated correctional heights were within a range that would not have largely impacted the resulting accuracy.

5.2 CORRECTION OF DATA IN AREAS WITH NO LIDAR RANGE

The extent of the missing LiDAR data from Ljungan raised a question of whether ALB is a suitable tool for mapping deep rivers with turbid water. The validation showed that the point accuracy is not affected by water clarity but the limited depth range imposes a problem as there are large undetected areas. The comparison of measured points and LiDAR DEM demonstrated that it is not sufficient to simply use interpolation tools in large undetected areas as this will induce errors in the DEM. In rivers like Ljungan it will be necessary to conduct manual measurements in addition to the ALB survey to obtain an accurate model. Shallower rivers like Storåne may also need manually measured data if there are deep pools not mapped by the LiDAR. In either case it is recommended to conduct a few manual measurements for validation of the data, as there can be areas with large local errors. The added data may not have to be of the same density as the LiDAR data to improve the DEM but more importantly should cover the deep sections to ensure that the interpolated channel is deep enough. To ensure that the deepest section of the channel is covered, the measurements should be conducted as cross sections covering the entire width of the missing area. However, the addition of manually measured ADCP points to the missing section in Storåne showed a high improvement after only adding a few points to the middle section of the channel. This indicates that it may be sufficient to only measure a few points if there are a high amount of LiDAR points on both sides of the channel and the missing area is relatively small ($<$20 m). It is still important to ensure that the deepest section is covered because the interpolation will not

extend beyond the deepest measured point. If the missing section is very wide as for Ljungan (>>30 m) or there are points from only one side of the channel, it would be necessary to measure a larger area.

If there is sufficient coverage of LiDAR data on both sides of the channel it may be possible to estimate the channel cross section based on the slope of the banks. The attempts to do this for the two rivers demonstrated that this potentially could work for some areas but the results were highly variable and would require further work. The cross sections from Ljungan showed that steep banks could predict a good estimate despite few measured points. It may not work in areas where the slope changes abruptly from the shallow zone to the deep zone. As the estimated trendline will either be polynomial of linear it may not be wise to apply the estimated line directly to the LiDAR cross sections but rather add a few of of the estimated points to the data set. The figures 33 - 36 demonstrate that the results are highly variable and it may not provide a close estimate despite LiDAR data on both sides. It may be possible to develop a method that can provide an estimated guess of the depth or cross section shape to save time by avoiding manual measurements but it may not provide the exact shape of the cross section. If this is to be developed into an algorithm that does automatic corrections it is recommended that the results are checked against manual measurements. The stream type and topography should be known as the result may be off by several meters and it is thus important to be able to identify wrong estimates. It may be possible to apply other correctional measures in combination with the estimated slope. As the water line and flow is measured on the day of the scan it may be possible to provide an estimate of the corresponding flow area for each cross section using the Mannings formula.

To ensure an accurate estimate of the cross sections it would be safer to conduct manual measurements. The scope of the measurements needed to complete the data set would be significantly less for a river like Storåne where there may be nothing more than a few deep pools that are out of the LiDAR's depth range. The scope of the manual measurements for a river like Ljungan would be larger but the point density from the LiDAR data is still superior to what can be achieved from conducting purely ground surveys. The high level of detail can not be achieved by conventional methods over such large areas without spending weeks or months in the field. The cost of conducting ALB with additional measurements may therefore outweigh the cost of conducting purely manual measurements if a high density is required. If the intention of the ALB is a flood survey then it may not be as important to collect data from the missing sections as the channel topography will not affect the simulations as much. For low flow simulations the flow pattern will depend more on the channel topography and therefore require more accurate data.

To achieve optimal results from an ALB survey and limit the need for additional data it is beneficial to consider the environmental factors that can influence the result of the scan. The depth range depends on both water colour and bottom reflectivity but there may be other factors such as turbulence or steep drops that could affect the result. The influence of such factors may be kept at a minimum if the survey is planned well in advance according to the time of year and at a time with lower discharge if the river is deep or higher discharge in shallow rivers to reduce turbulent water. Conducting a survey directly after heavy rainfall or a period of high discharge may reduce the water clarity and thus limit the depth range of the LiDAR.

5.3 LIDAR FOR HYDRAULIC MODELING

The application of LiDAR data proved to be an efficient method for setting up a hydraulic model in HEC-RAS with accurate cross sections and a variable spacing to capture the features of the river in areas with changing geometry. The ability to build a DEM based on the detailed LiDAR data provided an accurate basis for the hydraulic model and would only be possible for a small area if the data was collected by manual measurements. The addition of the DEM in HEC-RAS allowed for adding cross sections directly in the model as the cross sections interpolated by HEC-RAS could be adjusted to the attached DEM. This allowed for simpler and faster modeling without having to export and import data to other programs. The LiDAR data can be used for modeling both smaller or larger areas with a high accuracy which results in a wide application of the LiDAR data. Low flow simulations for mapping potentially dry spawning areas or stranding areas for fish habitat are highly dependent on accurate cross sections from the channel. Flood mapping requires wide cross sections that cover both channel and terrain which often requires two different measurement methods. The hydraulic modeling conducted for this study was only run in one dimension and does not take full advantage of the high density of the LiDAR data. With the increasing use of numerical models it is becoming more important to have efficient methods for collecting accurate and detailed data. Legleiter et al. (2011) found that the topographic uncertainty caused by decreased data density in channels result in a proportional increase in the uncertainty of the two dimensional model predictions of water surface elevations, water velocity and boundary shear stress, which furthermore influenced aquatic habitat suitability indices.

The LiDAR data should be checked to see if the results seem valid as there may be faulty points or missing data which lead to inaccuracies in the DEM as discussed in section 5.1. Classification of the LiDAR data is done automatically with a manual correction afterwards which means that mistakes may not always be discovered during the correction. The errors may not impact the overall result of the modeling if they are only in a small area, like in Storåne, but for rivers like Ljungan the large areas of missing data would cause inaccuracies in the DEM. The water elevation may be fitted to the constructed water line that was used for the calibration by changing the Mannings n values but it may not reflect the actual flow conditions. The water edge line provided by the supplier may not be sufficient to calibrate the model as it showed a high variation between each bank. This may be due to the topography of the river but could also be caused by the wrongful placement of the water edge line, as mentioned in section 4.1.2. To ensure a correct calibration it may be better to measure the water surface manually on the day of the scan. In areas with steep banks a horizontal displacement of the water surface line may affect the corresponding elevation significantly which may have caused the high variation of the left and right bank line in Ljungan. Creating depth plots by interpolating the water surface edge line may therefore be uncertain. It would be better to apply the exported water surface profiles from HEC-RAS to create the depth plots but the spacing between the cross sections should not be as large as they were for Ljungan as this induces uncertainties between the profiles. For future reference it is recommended that water surface points are measured manually on the day of the ALB survey in addition to what is measured by the supplier to further strengthen the calibration.

For complex rivers like Storåne with wide areas and many side streams and islands it is likely that the water surface elevation will vary from one bank to the other. The one dimensional

model in HEC-RAS does not capture the variability in the water surface and the elevation was therefore set to a single value at each profile. For low flow simulations it would be better to use a two dimensional model to include these surface variations in the model. The flood simulations were ideal cases for running the one dimensional model in HEC-RAS which got to apply the full width of the profiles. The simulations showed that not all the profiles extended far enough which caused HEC-RAS to assume a vertical edge. This was mainly due to the width of the GeoRAS profiles but certain areas were not mapped LiDAR, as shown in section 4.3 For modeling of flood prone areas with wide flood plains the necessary extent of the area should be specified to the supplier to ensure that the full width is mapped. Alternatively, the data could be integrated with the terrain models of the public mapping authorities like Kartverket. For the latter it is important to ensure that the data is in the same height system which was not the case for this study, as the data was in ellipsoidal heights and those of Kartverket are in orthometric heights. For studies that require interaction with other elevation data and maps it is beneficial to utilise GIS tools like Arc to process the data and create terrain models. However, the large size of the LiDAR data restricted the use of ArcGIS without reducing the data size. Although it may be sufficient with a lower point density than that of the full LiDAR data, any reduction should be done critically as there may be areas where the initial point density is low and further reductions could cause missing areas, as discussed in section 5.1. If the full density of the data is required it may better to use a different tool than ArcGIS that is more suitable for handling large data. The LiDAR data applied in this study were cross sections extracted from the LiDAR point cloud but it is possible to utilise the full point cloud with the right data tools at hand. The suppliers often have their own software which is possible to purchase or there may be other programs designed for handling large data. It may be possible to order an already processed raster or TIN surface from the supplier, but the size may still restrict the use of programs like ArcGIS.

Rivers like Storåne with many side streams and islands are time consuming to map by manual measurements and may take weeks or even months in order to achieve the same density as the LiDAR. It would require a terrestrial GPS in the shallow zones and the terrain, in addition to ADCP in the deep areas. The many riffles and rocks would challenge the navigation of the ADCP by boat. To map a deep river like Ljungan by manual measurements would be challenging as there are areas with strong currents and riffles that may not be safe to access with a boat or kayak to navigate the ADCP. A high density of the measurements would be difficult to obtain in these areas. To map the terrain would require a topographic LiDAR as the banks are not always accessible by foot. ALB is an efficient method for collecting data and can cover areas of tens of kilometres in a few hours. The post processing is the most time consuming part of the survey and may take several weeks or months, depending on the size. Once the LiDAR data is processed it has a wide application and the end user product can be suited to different purposes. If the intention of the LiDAR survey is flood mapping then this should be communicated to the supplier to ensure that the sufficient width of the area is included. For monitoring of sediment transport and bank erosion it is required to conduct repeat surveys with a high density, which would only be feasible with efficient mapping tools like ALB.

The ability to simultaneously map terrain and channel is one of the great advantages of ALB. The increasing need for flood risk assessments and flood mapping could benefit from using a

single method for mapping both channel and floodplains with a high accuracy and density. With the increased use of multidimensional hydraulic models, the accuracy and resolution of the data describing the channel topography is becoming more important. This requires efficient methods for data collection. The current and future need for monitoring and management of water bodies with consideration to ecosystems, specific habitats, hydropower or other industries would benefit from mapping rivers on a catchment scale to account for upstream and downstream conditions in addition to the area of interest.

6

CONCLUSIONS

This study has compared the LiDAR data from a deep, dark river and a clear, shallow river in terms of accuracy and evaluated the potential influence of various environmental conditions. The accuracy did not appear to be affected by the different river characteristics but the depth range of the LiDAR was limited by water clarity and low reflectivity from the river bed. For deep rivers with a dark river bed and coloured water the ALB survey may not be sufficient to obtain an accurate hydraulic model. Depending on the depth and characteristics of the targeted river it is recommended to conduct manual measurements in addition to the ALB survey, both to compliment the data set if there are missing areas and to validate the LiDAR measurements. The size of the LiDAR data challenges the use of conventional programs like ArcGIS and it is recommended to use other programs optimised for large data if the full point cloud is to be applied. For simpler hydraulic models it may be adequate to reduce the point density of the LiDAR data but as the density varies through the data set any reduction should be conducted with caution. ALB surveys provide a highly detailed data basis that is unmatched by conventional methods over such a large spatial scale. LiDAR data has a wide application such as studying floods, habitat, sediment transport, river morphology and hydraulics. With the increasing focus on monitoring and management of rivers it is beneficial to have holistic tools to allow for an integrated approach of both hydraulics and ecosystem.

The key findings from this study are summed up as the following:

- ALB mapped depths down to 3 meters in a dark river and 6 meters in a clear river but showed a significant reduction in point density when exceeding depths of 2.5 m and 3 m, respectively
- The vertical accuracy of the data was on centimetre level and did not appear to be affected by physical characteristics or depth
- Water clarity seem to have the largest influence on the LiDAR's depth range but dark substrate and vegetation on the river bed also limit the depth range
- ALB surveys on deep ($>$ 3 m) rivers with turbid water and dark bottom may require additional measurements to obtain accurate terrain models
- It may be possible to estimate the cross section shape in some areas with missing LiDAR data by interpolating the slope of the LiDAR points from the shallow areas

6.1 RECOMMENDATIONS FOR FUTURE WORK

- Create algorithms for interpolating cross sections based on the slope of the side banks or other correctional methods to estimate and locate deep sections in areas with missing LiDAR data
- Further investigate the accuracy of corrected LiDAR DEMs based on added measured points and estimate the required density of additional points
- Collect data from the deep sections in Ljungan to obtain a complete data set and an accurate hydraulic model to simulate future measures for habitat improvement
- Compare the results from the flood simulation in Ljungan to the previously conducted flood mapping that was based on topographic LiDAR and cross sectional data
- Set up a two dimensional model for Storåne to simulate low flow scenarios with a variable water surface

REFERENCES

AHAB (2015). *AHAB Datasheet Leica HawkEye-III*. URL: http://www.airbornehydro.com/sites/default/files/Leica%20AHAB%20HawkEye%20DS.pdf (visited on 02/24/2016).

AHAB (2014). *Leica AHAB Chiroptera II Topographic & Bathymetric LiDAR System*. URL: http://www.airbornehydro.com/chiroptera-ii (visited on 02/24/2016).

AHM (2015). "Gewässervermessung aus der Luft - High resolution topo-bathymetric survey". In: Innsbruck: AHM.

Bendiksby, Lars (2013). *Fiskeundersøkelser i forbindelse med revisjon av Holsreguleringen*. Tech. rep. Norconsult AS.

E-CO Energi (2014). *Konsesjonssøknad og konsekvensutredning - Hol 1 Stolsvatn kraftverk*. Tech. rep. URL: http://webfileservice.nve.no/API/PublishedFiles/Download/201002426/1125809.

European Environment Agency (2011). *Disasters in Europe: more frequent and causing more damage*. URL: http://www.eea.europa.eu/highlights/natural-hazards-and-technological-accidents (visited on 03/16/2016).

Fernandez-Diaz, Juan Carlos, Craig L. Glennie, William E. Carter, Ramesh L. Shrestha, Michael P. Sartori, Abhinav Singhania, Carl J. Legleiter, and Brandon T. Overstreet (2014). "Early results of simultaneous terrain and shallow water bathymetry mapping using a single-wavelength airborne LiDAR sensor". In: *IEEE Journal of Selected Topics in Applied Earth Observations and Remote Sensing* 7.2, pp. 623–635. ISSN: 19391404. DOI: 10.1109/JSTARS.2013.2265255.

Flener, Claude and Peggy Zinke (2013). "Experience from the use of Unmanned Aerial Vehicles (UAV) for River Bathymetry Modelling in Norway". In:

Fugro LADS Corporation (2011). *Fugro LADS Mk 3 ALB System*. URL: http://www.fugrolads.com/download/datasheets/Fugro-LADS-Mk3 (visited on 02/24/2016).

Halleraker, Jo Hallvard, Jan Sørensen, Martine Bjørnhaug, Roy Malvin Langåker, Odd Kristian Selboe, Eilif Brodtkorb, Ingrid Haug, and Jakob Fjellanger (2013). *Vannkraftkonsesjoner som kan revideres innen 2022*. Tech. rep. Norges vassdrags- og energidirektorat (NVE). URL: http://www.miljodirektoratet.no/Documents/publikasjoner/M49/M49.pdf.

Hammeren, Ragnhild and Ingrid Alne (2015). "The Process and Performance of Bathymetric LiDAR Survey". Student Thesis. Norwegian University of Science and Technology.

IPCC (2007). *Climate Change 2007: Synthesis Report*. URL: https://www.ipcc.ch/publications%7B%5C_%7Dand%7B%5C_%7Ddata/ar4/syr/en/spms2.html (visited on 06/15/2016).

Irish, Jennifer L. and W.Jeff Lillycrop (1999). "Scanning laser mapping of the coastal zone: the SHOALS system". In: *ISPRS Journal of Photogrammetry and Remote Sensing* 54.2-3, pp. 123–129. ISSN: 09242716. URL: http://www.sciencedirect.com/science/article/pii/S0924271699000039.

Kartverket (2014). *TopoBaty 2014: Eit pilotprosjekt om datainnsamling med grøn laser i kystsona*. Tech. rep. URL: http://www.kartverket.no/globalassets/kart/topobaty-2014/rapport-topobaty2014.pdf.

Kinzel, Paul J., Carl J. Legleiter, and Jonathan M. Nelson (2013). "Mapping River Bathymetry With a Small Footprint Green LiDAR: Applications and Challenges". In: *Journal of the American Water Resources Association* 49.1, pp. 183–204. ISSN: 1093474X. DOI: 10.1111/jawr.12008.

Kristofers, Johan (2014). "Kartläggning av fysiska faktorer som begränsar laxbeståndet i Ljungan nedströms Viforsens kraftverk". Master Thesis. Norwegian University of Science and Technology. URL: http://brage.bibsys.no/xmlui/handle/11250/2350485.

Legleiter, Carl J., Phaedon C. Kyriakidis, Richard R. McDonald, and Jonathan M. Nelson (2011). "Effects of uncertain topographic input data on two-dimensional flow modeling in a gravel-bed river". In: *Water Resources Research* 47.3, pp. 1–24. ISSN: 00431397. DOI: 10.1029/2010WR009618.

Maddock, Ian, Atle Harby, and Paul Kemp (2013). *EcoHydraulics: An Integrated Approach*. Wiley_Blackwell. ISBN: 9781118526545.

Mandlburger, Gottfried, Christoph Hauer, Martin Wieser, and Norbert Pfeifer (2015). "Topo-bathymetric LiDAR for monitoring river morphodynamics and instream habitats-A case study at the Pielach River". In: *Remote Sensing* 7.5, pp. 6160–6195. ISSN: 20724292. DOI: 10.3390/rs70506160.

Mandlburger, Gottfried, Martin Pfennigbauer, and Norbert Pfeifer (2013). "Analyzing near water surface penetration in laser bathymetry - A case study at the River Pielach". In: *ISPRS Annals of the Photogrammetry, Remote Sensing and Spatial Information Sciences* II-5/W2.November, pp. 175–180. ISSN: 2194-9050. DOI: 10.5194/isprsannals-II-5-W2-175-2013.

McKean, Jim, Dave Nagel, Daniele Tonina, Philip Bailey, Charles Wayne Wright, Carolyn Bohn, and Amar Nayegandhi (2009). "Remote sensing of channels and riparian zones with a narrow-beam aquatic-terrestrial LIDAR". In: *Remote Sensing* 1.4, pp. 1065–1096. ISSN: 20724292. DOI: 10.3390/rs1041065.

McKean, Jim, Daniele Tonina, Carolyn Bohn, and Charles Wayne Wright (2014). "Journal of Geophysical Research Earth Surface". In: *Journal of Geophysical Resarch: Earth Science* 119, pp. 644–664. DOI: 10.1002/2013JF002897.Received.

Optech (2016). *SHOALS_3000 Specification/Deliverables*. URL: http://www.geo3d.hr/download/shoals/SHOALS%7B%5C_%7D3000.pdf (visited on 02/24/2016).

Optech NOVA (2016). *Bathymetric Airborne Lidar Sheet Specification*. URL: http://www.teledyneoptech.com/wp-content/uploads/CZMIL-Nova-Specsheet-150626-WEB.pdf (visited on 02/24/2016).

RIEGL (2016). *RIEGL VQ-880-G*. URL: http://www.riegl.com/uploads/tx_pxpriegldownloads/VQ-880-G_at_a_glance_2015-09-01.pdf (visited on 02/24/2016).

Rosgen, Dave (1996). *Applied River Morphology*. Wildland Hydrology, 5–20:5–24. ISBN: 0-9653289-0-2.

Shrestha, Kristofer Y., K. Clint Slatton, William E. Carter, and Tristan K. Cossio (2010). "Performance metrics for single-photon laser ranging". In: *IEEE Geoscience and Remote Sensing Letters* 7.2, pp. 338–342. ISSN: 1545598X. DOI: 10.1109/LGRS.2009.2035133.

SMHI (2002). *Län och hovudavrinnigsområden i Sverige*. URL: http://www.smhi.se/sgn0102/n0205/lan%7B%5C_%7Dharo%7B%5C_%7Dhuvud.pdf (visited on 10/26/2015).

SMHI (2003). *Vattendragsregistret*. URL: http://web.archive.org/web/20060721130302/http://www.smhi.se/sgn0102/n0204/vdragreg.pdf (visited on 10/26/2015).

Sontek (2016). *RiverSurveyor Specifications*. URL: http://www.quantum-hydrometrie.de/RiverSurveyor-S5-M9.pdf (visited on 04/16/2016).

Statkraft (2009). "Vannkraft". In: URL: http://www.statkraft.no/globalassets/old-contains-the-old-folder-structure/documents/no/vannkraft-09-no%7B%5C_%7Dtcm10-4585.pdf.

Statkraft Sweden (2015). *Ljungan*. URL: http://statkraft.se/globalassets/old-contains-the-old-folder-structure/documents/se/vattenkraftverk/statkraft_ljungan_111005_orig_tcm11-17989.pdf (visited on 10/26/2015).

The EU Floods Directive (2016). *The EU Floods Directive - A Communication on Flood risk management; Flood prevention, protection and mitigation*. URL: http://ec.europa.eu/environment/water/flood%7B%5C_%7Drisk/com.htm (visited on 02/08/2016).

The EU Floods Directive (2015). *The EU Floods Directive - Flood Risk Management*. URL: http://ec.europa.eu/environment/water/flood%7B%5C_%7Drisk/ (visited on 03/16/2016).

USACE (2010). *HEC-RAS River Analysis System : User's Manual Version 4.1*. Tech. rep. Davis, California: Hydrological Engineering Center.

World Energy Council (2016). *Energy Resources: Hydropower*. URL: https://www.worldenergy.org/data/resources/resource/hydropower/ (visited on 05/18/2016).

APPENDICES

Appendix A:	Photos from the study sites
Appendix B:	DEMs from Ljungan and Storåne
Appendix C:	HEC-RAS models for Ljungan and Storåne
Appendix D:	Calibration values
Appendix E:	Flow hydrograph from the unsteady simulations
Appendix F:	Location of intersecting points for the DEM comparisons
Appendix G:	Source code for point reduction
Appendix H:	Depth plots from Ljungan
Appendix I:	Map for additional data collection in Ljungan

Photos from Ljungan at Allsta (top) and Viforsen (bottom) where the manual measurements were conducted

Photos from the lower part of Storåne where the manual measurements were conducted

Photos of the upper part of Storåne where the manual measurements were conducted

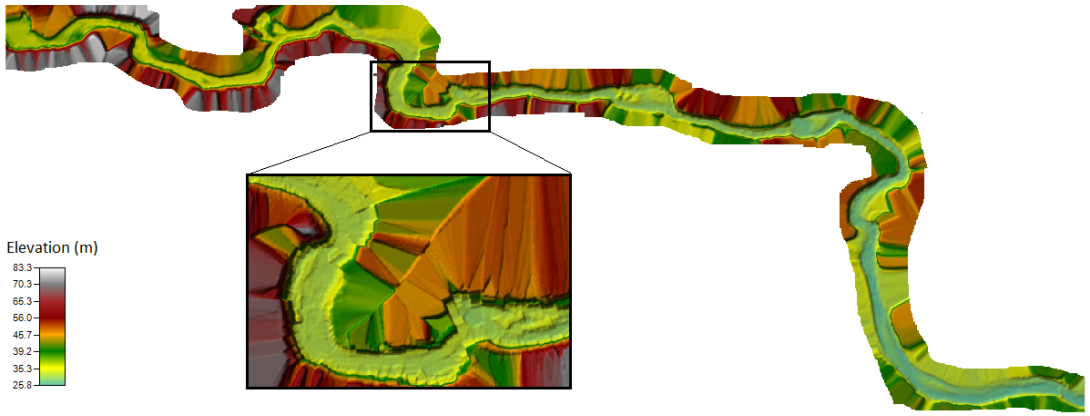

The LiDAR DEM from Ljungan created with 2 m grid size and 25 m cross section spacing

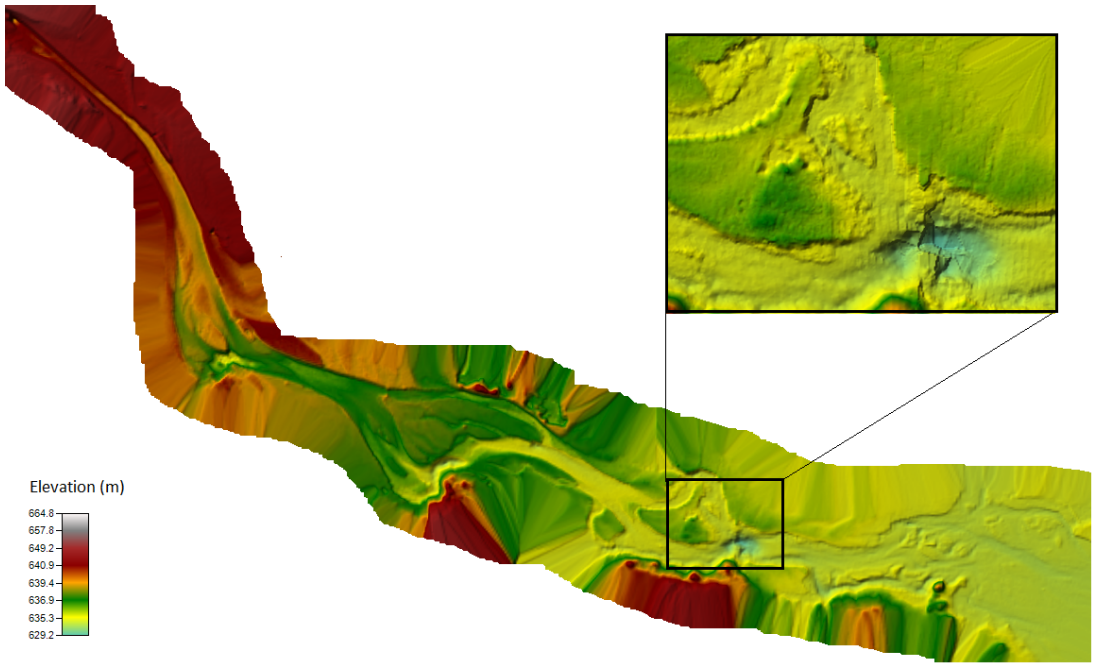

The LiDAR DEM from Storåne created with 1 m grid size and 5 m cross section spacing

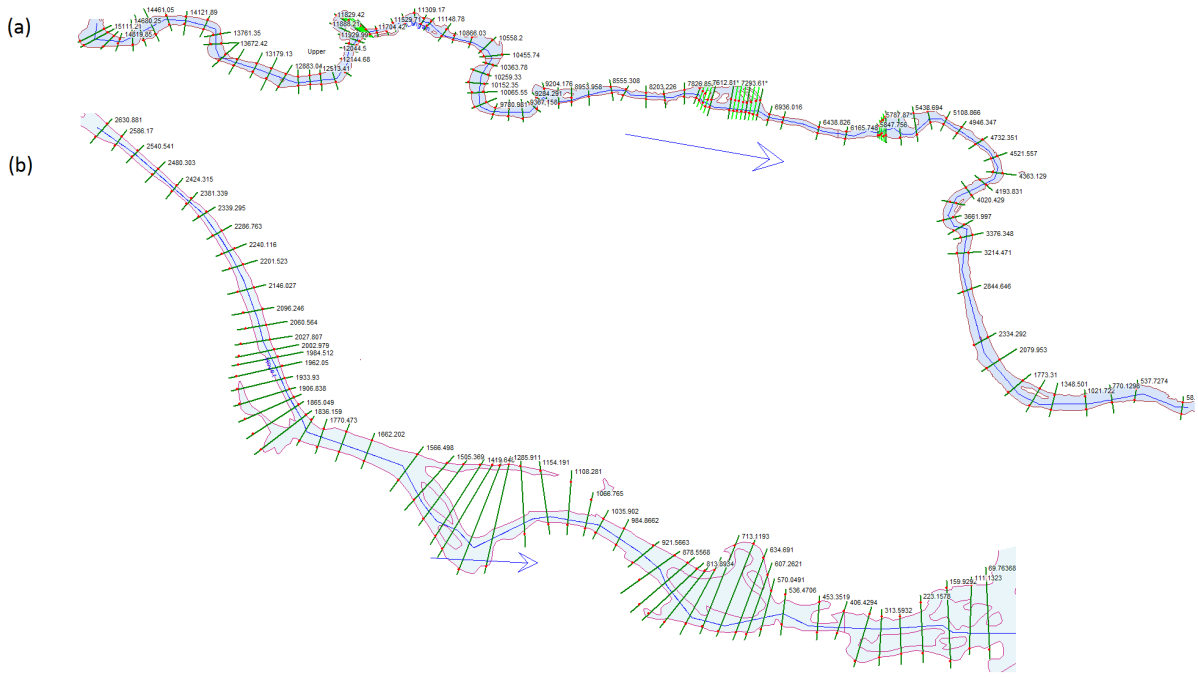

The two models set up in HEC-RAS with cross sections and water course for (a) Ljungan; (b) Storåne

Calibration values for the channel from the scan date flow in Ljungan

River Station	Mannings n	River Station	Mannings n	River Station	Mannings n
15111.21	0.02	11309.17	0.04	7134.99*	0.04
15050.69	0.02	11219.62	0.07	7094.92*	0.04
14914.12	0.02	11148.78	0.06	7054.855	0.04
14819.85	0.02	10977.92	0.02	6936.016	0.04
14680.25	0.02	10866.03	0.03	6795.54	0.04
14583.42	0.06	10698.25	0.04	6438.826	0.04
14461.05	0.06	10558.2	0.04	6165.748	0.06
14293.41	0.06	10455.74	0.04	5847.756	0.09
14121.89	0.06	10363.78	0.04	5827.80*	0.09
13924.01	0.06	10259.33	0.04	5807.83*	0.08
13761.35	0.06	10152.35	0.04	5787.87*	0.08
13672.42	0.06	10065.55	0.04	5767.913	0.08
13510.38	0.06	9941.865	0.04	5617.063	0.08
13374.15	0.06	9780.981	0.04	5438.694	0.04
13179.13	0.06	9639.751	0.04	5268.687	0.04
13031.99	0.06	9507.487	0.06	5108.866	0.04
12883.04	0.06	9367.158	0.06	4946.347	0.04
12733.5	0.06	9284.291	0.07	4732.351	0.04
12618.75	0.06	9204.176	0.08	4521.557	0.04
12513.41	0.06	9081.509	0.04	4363.129	0.04
12377.24	0.06	8953.958	0.04	4193.831	0.04
12261.25	0.06	8782.572	0.04	4020.429	0.04
12144.68	0.06	8555.308	0.04	3832.353	0.04
12044.5	0.06	8419.155	0.04	3661.997	0.04
11983.51	0.06	8203.226	0.04	3522.193	0.06
11929.99	0.06	8027.094	0.04	3376.348	0.07
11888.21	0.06	7826.858	0.04	3214.471	0.07
11829.42	0.06	7699.022	0.04	2844.646	0.06
11820.5*	0.06	7655.92*	0.04	2334.292	0.04
11811.6*	0.06	7612.81*	0.04	2079.953	0.04
11802.7*	0.06	7569.71*	0.04	1773.31	0.06
11793.8*	0.06	7526.607	0.04	1550.479	0.08
11784.94	0.06	7333.133	0.04	1348.501	0.08
11704.42	0.09	7293.61*	0.04	1021.722	0.04
11612.94	0.12	7254.09*	0.04	770.1298	0.03
11529.71	0.09	7214.57*	0.04	537.7274	0.06
11416.96	0.08	7175.05	0.04	58.12875	0.08

Calibration values for the channel from the scan date flow in Storåne

River Station	Mannings n	River Station	Mannings n	River Station	Mannings n
2630.881	0.07	1865.049	0.2	878.5568	0.03
2586.17	0.06	1836.159	0.3	840.7979	0.04
2540.541	0.04	1808.774	0.055	813.8934	0.065
2480.303	0.045	1770.473	0.055	785.2667	0.06
2424.315	0.038	1721.485	0.055	753.1144	0.05
2381.339	0.07	1662.202	0.04	713.1193	0.065
2339.295	0.052	1566.498	0.043	676.1507	0.065
2286.763	0.044	1505.369	0.045	634.691	0.055
2240.116	0.06	1462.145	0.05	607.2621	0.055
2201.523	0.05	1419.648	0.04	570.0491	0.06
2146.027	0.015	1392.411	0.1	536.4706	0.065
2096.246	0.07	1345.901	0.15	453.3519	0.065
2060.564	0.07	1285.911	0.18	406.4294	0.08
2027.807	0.043	1207.978	0.05	348.6489	0.085
2002.979	0.045	1154.191	0.04	313.5932	0.005
1984.512	0.05	1108.281	0.12	270.6689	0.04
1962.05	0.055	1066.765	0.06	223.1578	0.02
1933.93	0.06	1035.902	0.035	159.9292	0.01
1906.838	0.045	984.8662	0.075	111.1323	0.01
1885.369	0.025	921.5663	0.045	69.76368	0.05

Calibration values for the channel from the low flow simulation in Storåne

River Station	Mannings n	River Station	Mannings n	River Station	Mannings n
2630.881	0.07	1865.049	0.13	878.5568	0.04
2586.17	0.06	1836.159	0.35	840.7979	0.2
2540.541	0.04	1808.774	0.055	813.8934	0.3
2480.303	0.045	1770.473	0.055	785.2667	0.04
2424.315	0.038	1721.485	0.055	753.1144	0.05
2381.339	0.07	1662.202	0.04	713.1193	0.065
2339.295	0.052	1566.498	0.043	676.1507	0.065
2286.763	0.044	1505.369	0.09	634.691	0.055
2240.116	0.06	1462.145	0.11	607.2621	0.055
2201.523	0.05	1419.648	0.17	570.0491	0.2
2146.027	0.025	1392.411	0.09	536.4706	0.15
2096.246	0.05	1345.901	0.1	453.3519	0.07
2060.564	0.04	1285.911	0.4	406.4294	0.08
2027.807	0.05	1207.978	0.4	348.6489	0.085
2002.979	0.09	1154.191	0.02	313.5932	0.005
1984.512	0.06	1108.281	0.19	270.6689	0.04
1962.05	0.045	1066.765	0.075	223.1578	0.02
1933.93	0.045	1035.902	0.045	159.9292	0.01
1906.838	0.05	984.8662	0.08	111.1323	0.01
1885.369	0.03	921.5663	0.07	69.76368	0.05

APPENDIX E: FLOW HYDROGRAPHS

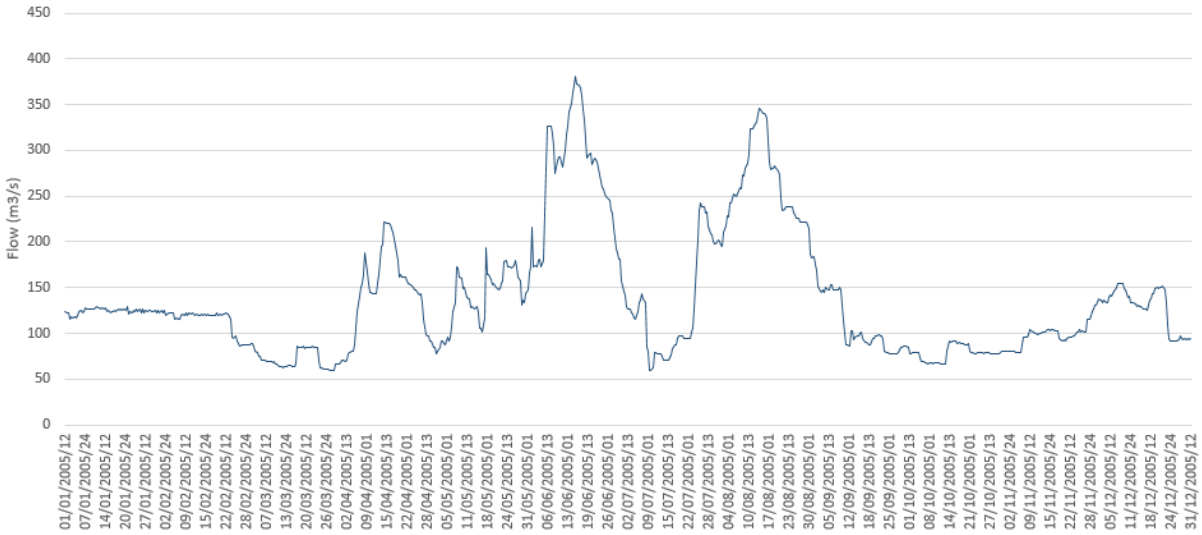

Hydrograph from Ljungan from the unsteady simulation

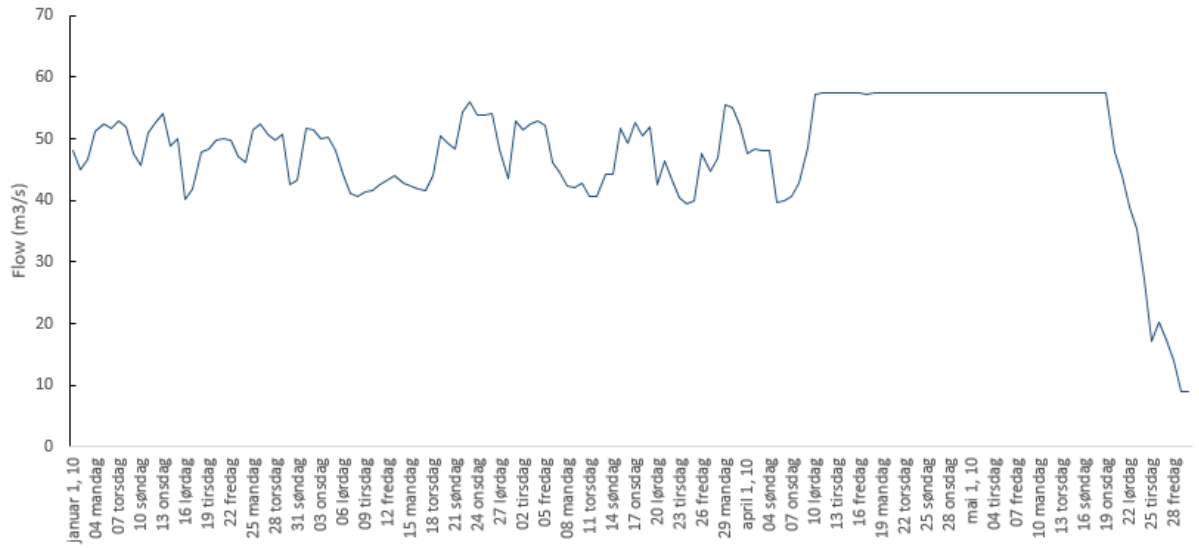

Hydrograph from Storåne from the unsteady simulation

APPENDIX F: LOCATION OF INTERSECTING ADCP AND LIDAR POINTS

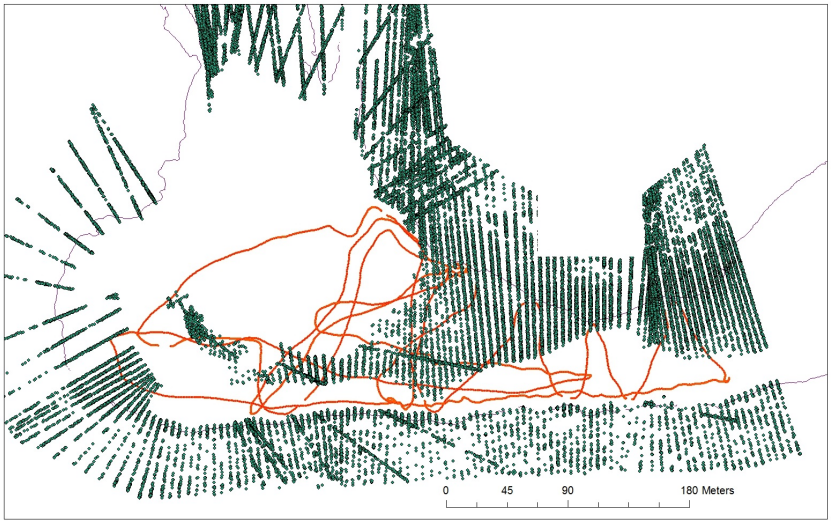

ADCP points (red) and LiDAR points (green) in the deep glide in Ljungan

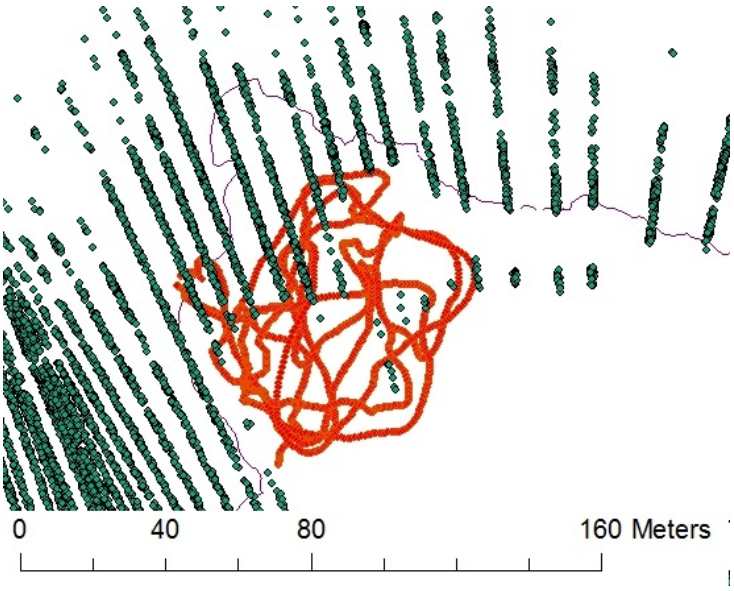

ADCP points (red) and LiDAR points (green) in the pool in Ljungan

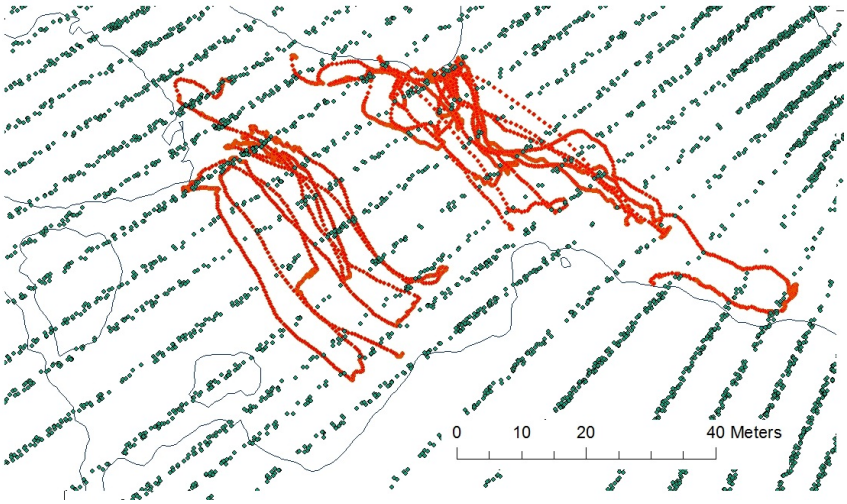

ADCP points (red) and LiDAR points (green) in the soft bottom (left) and hard bottom (right) in Storåne

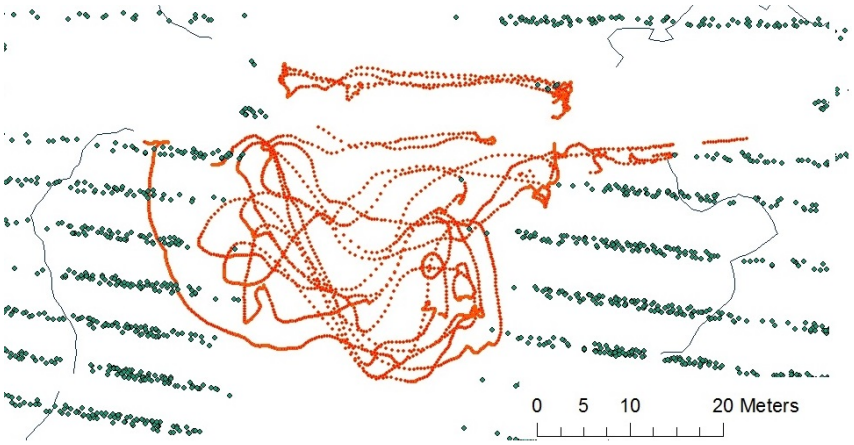

ADCP points (red) and LiDAR points (green) in the deep glide in Storåne

APPENDIX G: SOURCE CODE FOR REDUCTION OF POINT DENSITY IN R

```
filedir <- "."
fl <- list.files(filedir, pattern="\\.txt$", full.name=TRUE)
#

#
for (i in 1:length(fl)){
    ahm <- read.csv(fl[i], header=FALSE)

  ahm2 <- ahm[seq(1,NROW(ahm),by=length(ahm$V1)/500),]


  write.table(ahm2,file=paste("r_",basename(fl[i]),sep=""), row.names=FALSE, col.names = FALSE, quote=FALSE)
}
```

APPENDIX H: DEPTH PLOTS FOR LJUNGAN

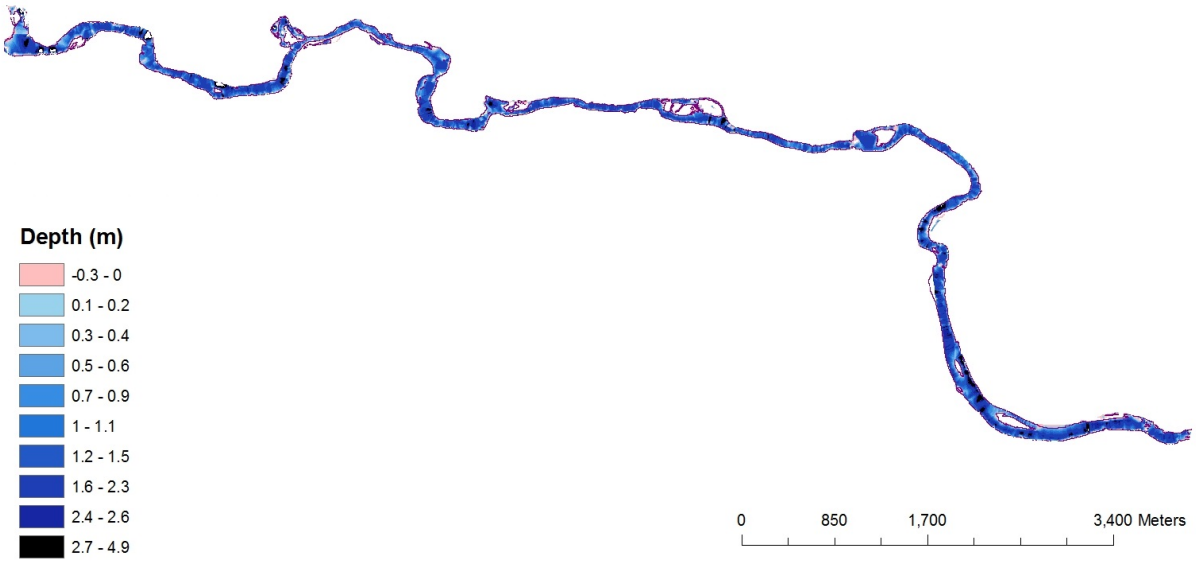

The depth plot from the interpolated water surface edge line for Ljungan

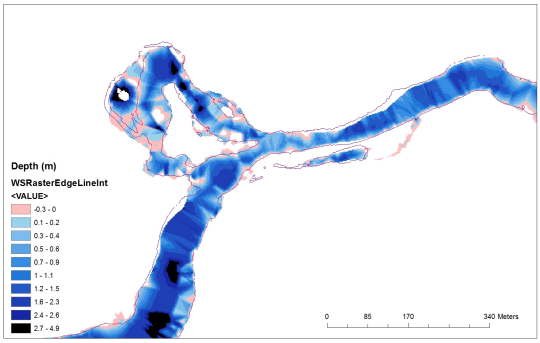

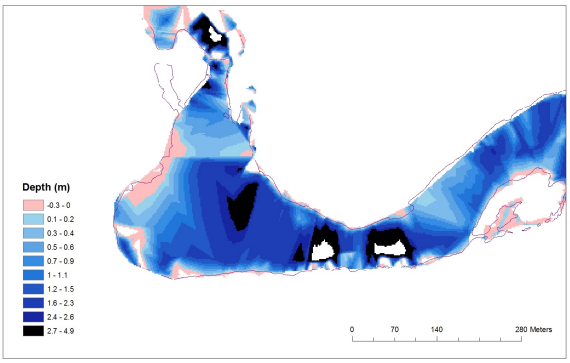

Depth plots based on the interpolation of the constructed water surface edge line

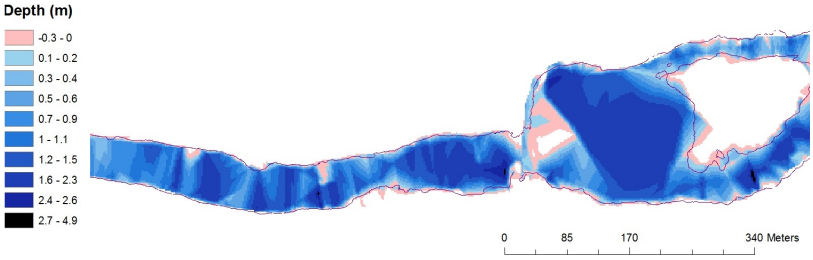

Depth plots based on the interpolation of the constructed water surface edge line

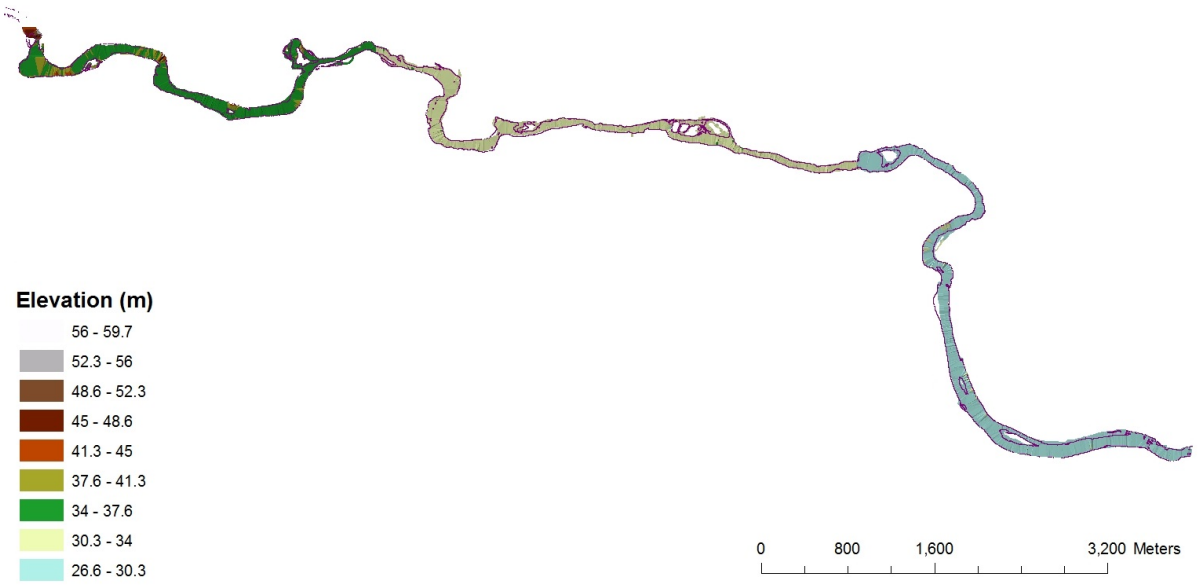

The water surface TIN created from the HEC-RAS water surface profiles for Ljungan

APPENDIX I: MAP FOR ADDITIONAL DATA COLLECTION FOR LJUNGAN

The upper part of Ljungan indicating areas in need of additional data collection

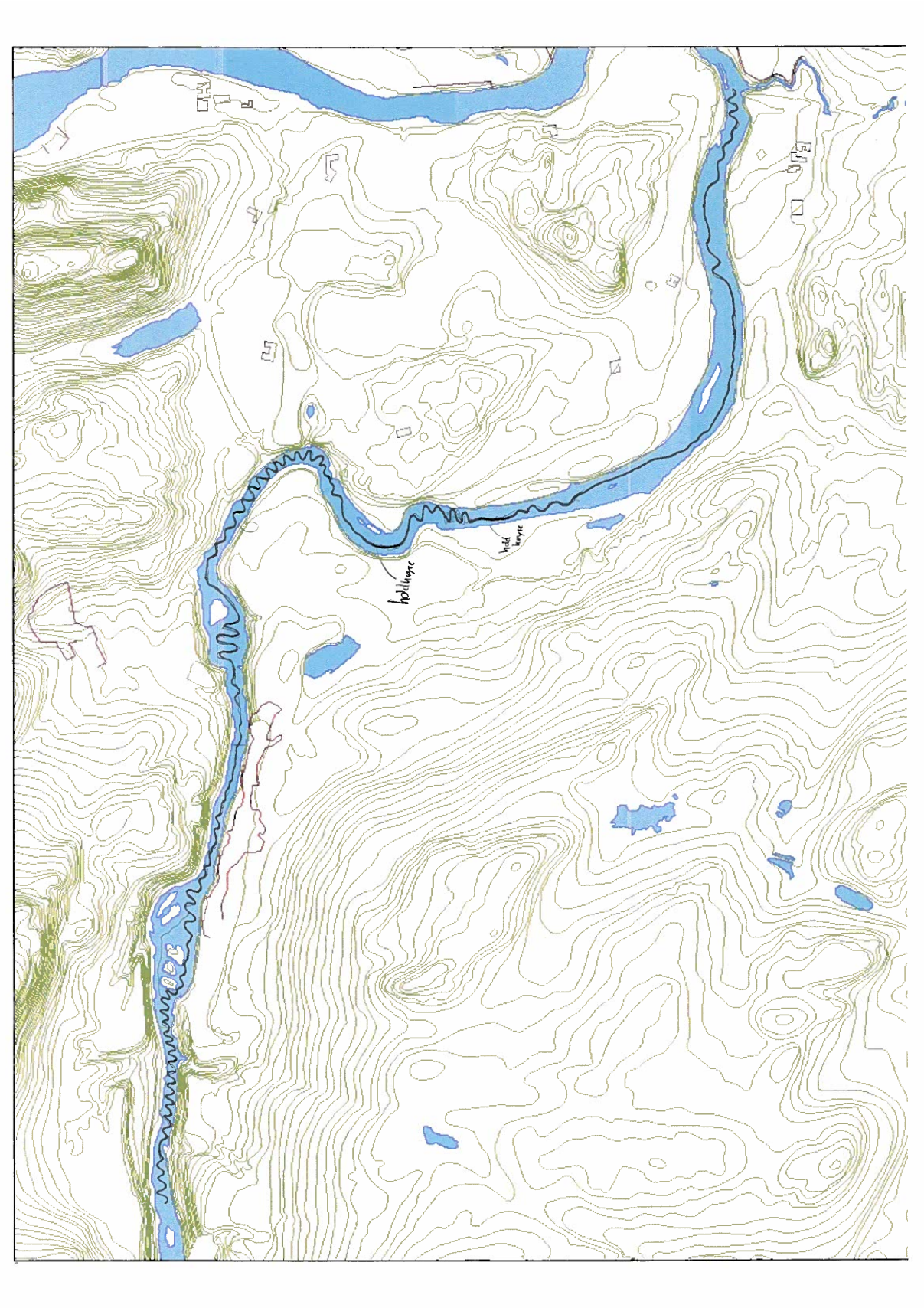

The lower part of Ljungan indicating areas in need of additional data collection